Regulation von intrazellulären Transportwegen in *Arabidopsis*

Dissertation

der Mathematisch-Naturwissenschaftlichen Fakultät
der Eberhard Karls Universität Tübingen

zur Erlangung des Grades eines
Doktors der Naturwissenschaften
(Dr. rer. nat.)

vorgelegt von
Hauke Beckmann
aus Bünde/Westfalen

Tübingen
2015

Gedruckt mit Genehmigung der Mathematisch-Naturwissenschaftlichen Fakultät der Eberhard Karls Universität Tübingen.

Tag der mündlichen Qualifikation:	27. März 2015
Dekan:	Prof. Dr. Wolfgang Rosenstiel
1. Berichterstatter:	Prof. Dr. Gerd Jürgens
2. Berichterstatter:	Prof. Dr. Klaus Harter

Meinen Eltern

Antje und Paul Werner Beckmann

Danksagung

An erster Stelle möchte ich mich bei Prof. Dr. Gerd Jürgens für die tolle Betreuung meiner Doktorarbeit bedanken. Durch die Gestaltungsfreiheit, die Du den Mitgliedern Deiner Arbeitsgruppe gewährst, habe ich gelernt, wissenschaftliche Fragestellungen und Probleme zu lösen. Schwierigere, scheinbar unlösbare Probleme wurden nach einem Gespräch mit Dir zu interessanten Ausgangspunkten für neue Experimente.

Prof. Dr. Klaus Harter danke ich für die Begutachtung dieser Arbeit.

Großen Dank meinen Laborkolleginnen und –kollegen: Manoj, Marika, Misoon, Sandra und Tamara: Mit eurer Erfahrung und durch viele Diskussionen habt ihr mir bei praktischen und theoretischen Problemen sehr geholfen. Besonders danke ich in dieser Hinsicht Manoj, der meine oft abstrusen Ideen nicht sofort abgeschmettert hat, sondern erst nach Verweis auf mehrere Publikationen und Fakten, und Sandra für ihren klaren Blick auf zielführende Experimente. Richie danke ich für die kompromisslose Verbreitung guter Laune. Mit meinen Mitdoktoranden Kerstin, Matthias und Sabine konnte ich mein experimentelles Leid teilen. Außerdem haben wir, unterstützt von den „Müllers“ Doro, Elli und Arvid und den „Pimpls“ Fabi und Simone, viele lustige Abende in der Tübinger Altstadt verbracht. An dieser Stelle möchte ich auch Nilles lobend erwähnen, der den Schwierigkeitsgrad dieser Abende (und der folgenden Tage) deutlich erhöht hat. Ich danke euch allen für die gute Zusammenarbeit und dafür, dass ihr meine Launen ertragen habt.

Last but not least möchte ich meinen Eltern danken. Danke für eure Liebe und Unterstützung, auch wenn ich nicht immer den geraden Weg gegangen bin. Ich habe von euch mindestens so viel über das Leben gelernt wie durch das Studium der Biologie.

Inhaltsverzeichnis

1 Zusammenfassung

Das trans-Golgi-Netzwerk (TGN) stellt eine bedeutende Sortierungsstation im Rahmen des intrazellulären Vesikeltransports dar. In Pflanzenzellen wird an diesem Kompartiment der Transport von Frachtmolekülen zu verschiedenen Zielorten organisiert. Neusynthetisierte Proteine, die über das endoplasmatische Reticulum (ER) und den Golgi-Apparat hier angeliefert werden, werden zum Beispiel zur Plasmamembran (PM) weitertransportiert (Sekretion); abzubauende Moleküle gelangen über multivesikuläre Körper (multi-vesicular bodies, MVBs) genannte Kompartimente zur Vakuole; und endocytierte Plasmamembranproteine, wie zum Beispiel Rezeptoren, werden entweder zur PM rezykliert oder ebenfalls dem Abbau in der Vakuole zugeführt. Während der Cytokinese wird außerdem die neuentstehende Zellwandplatte zwischen den Tochterzellen vom TGN aus mit Material versorgt. Diese unterschiedlichen Transportprozesse unterliegen der Regulation durch spezifische ARF-Guanin-Nukleotid-Austauschfaktoren (ARF-guanine-nucleotide exchange factors, ARF-GEFs), Enzyme, die über die Aktivierung von GTPasen der ARF-Familie die Vesikelbildung koordinieren. Im Zuge dieser Arbeit konnte gezeigt werden, dass die ARF-GEFs BIG1-4 Regulatoren des post-Golgi-Vesikeltransports sind: Sie sind essentiell für die Funktion der sekretorischen und vakuolären Transportwege, während die Rezyklierung endocytierter Proteine zur PM durch den ARF-GEF GNOM vermittelt wird. Interessanterweise steuern BIG1-4 aber in der Zellteilungsphase den Transport von endocytierter Fracht zur Zellplatte und „konkurrieren“ dabei mit der GNOM-abhängigen Rezyklierung. Diese Verschiebung von Material von der PM zur Zellteilungsebene stellt möglicherweise den schnellen und effizienten Ablauf der Cytokinese sicher.

Zusätzlich zu dem Ergebnis, dass der vakuoläre Transport von BIG1-4 abhängig ist, wurden im Rahmen dieser Arbeit weitere Aspekte der Regulation dieses Transportwegs aufgeklärt. Nach gängiger Vorstellung entstehen die als Zwischenstationen auf dem Weg zur Vakuole dienenden MVBs durch Abknospung von definierten Bereichen des TGNs und verschmelzen schließlich mit der Vakuole, wobei zwei Unterfamilien von RAB-GTPasen, 5/F und 7/G, die verschiedenen Stadien des Reifungsprozesses markieren. In nichtpflanzlichen Organismen, wie zum Beispiel Hefe, geht die Bildung der MVBs mit dem Austausch von RAB5/F durch RAB7/G an der Membran einher. Im Gegensatz dazu deuten unsere Ergebnisse

darauf hin, dass dieser Prozess in Pflanzen nicht für die Abknospung der MVBs, sondern für ihre Fusion mit der Vakuole notwendig ist. Wie wir zeigen konnten, ist der Vorgang der RAB-Auswechslung selbst aber in den verschiedenen Organismen konserviert: Aktives (GTP-gebundenes) RAB5/F rekrutiert ein Heterodimer aus den Proteinen SAND und CCZ1, das einerseits die Inaktivierung und damit den Membranabfall von RAB5/F bewirkt, und andererseits RAB7/G aktiviert und an der MVB-Membran stabilisiert.

Der dritte Teil dieser Arbeit behandelt die Rolle von Proteindomänen in der Regulation von ARF-GEFs. Die Gruppe der großen ARF-GEFs besitzt eine konservierte Domänenstruktur: Die zentrale katalytische SEC7-Domäne wird von nicht-katalytischen Domänen flankiert, deren Funktion erst in Ansätzen untersucht ist. Unsere Ergebnisse ergaben keine Hinweise darauf, dass die SEC7-Domäne an der korrekten Membranlokalisation der ARF-GEFs beteiligt ist, da der Austausch dieser Domäne zwischen zwei unterschiedlich lokalisierten ARF-GEFs nicht zum Funktionsverlust führte. Für eine weitere, in dieser Hinsicht bisher nicht charakterisierte Domäne konnten wir hingegen eine Mitwirkung in einer speziellen Proteinkonformation demonstrieren, die für die Membranassoziation essentiell ist: Hierbei interagieren N- und C-terminal der SEC7 –Domäne gelegene Bereiche miteinander und scheinen so eine schützende Struktur über dem katalytischen Zentrum zu bilden, die eine Aktivität des ARF-GEFs zur falschen Zeit und am falschen Ort verhindern könnte.

2 Summary

The trans-Golgi network (TGN) constitutes a major sorting hub in the context of intracellular vesicle trafficking. In plant cells, the transport of cargo molecules to different destinations is coordinated at this compartment. Newly synthesized proteins delivered here via the endoplasmic reticulum (ER) and Golgi apparatus are, for instance, transported onward to the plasma membrane (PM); molecules destined for degradation are sent to the vacuole via so-called multi-vesicular bodies (MVBs); and endocytosed plasma membrane proteins, such as receptors, are either recycled to the PM or also delivered to the vacuole for degradation. Additionally, during cytokinesis the developing cell plate between the daughter cells is supplied with material from the TGN. These diverse transport processes are regulated by specific ARF guanine-nucleotide exchange factors (ARF-GEFs), enzymes that coordinate vesicle formation through activation of GTPases of the ARF family. In the course of this study it could be demonstrated that ARF-GEFs BIG1-4 are regulators of post-Golgi vesicle traffic: They are essential for proper function of the secretory and vacuolar pathways, whereas recycling of endocytosed proteins to the PM is governed by the ARF-GEF GNOM. Interestingly, though, during cytokinesis BIG1-4 mediate the transport of endocytosed cargo to the cell plate, thereby “competing” with GNOM-dependent recycling. This shift of material from the PM to the plane of cell division potentially ensures fast and efficient progression of cytokinesis.

In addition to the results revealing dependence of vacuolar transport on BIG1-4, further aspects of the regulation of this pathway have been elucidated in this study. According to current understanding, MVBs, which serve as way stations on the route to the vacuole, are formed through budding from defined areas of the TGN and finally fuse with the vacuole. Two subfamilies of RAB GTPases, 5/F and 7/G, mark the different stages of this maturation process. In non-plant organisms like yeast, formation of MVBs is accompanied by an exchange of RAB5/F for RAB7/G at the membrane. In contrast to that, our results indicate that in plants this process is not required for budding of MVBs, but for their fusion with the vacuole. However, we could show that the mechanism of RAB conversion itself is conserved between the different kingdoms: Active (GTP-bound) RAB5/F recruits a heterodimer composed of the proteins SAND and CCZ1, which on the one hand mediates inactivation and

subsequent membrane dissociation of RAB5/F, and on the other hand activates RAB7/G, thereby stabilizing it at the membrane.

The third part of this work addresses the role of protein domains in the regulation of ARF-GEFs. The group of large ARF-GEFs shares a conserved domain structure: The central catalytic SEC7 domain is flanked by non-catalytic domains, whose function has only begun to be elucidated. Our results did not provide any indications that the SEC7 domain affects membrane localization of ARF-GEFs, since exchange of this domain between two differently localized ARF-GEFs did not cause loss of function. By contrast, we could demonstrate that another domain, which had until now not been characterized in this respect, participates in a special protein conformation essential for membrane association. In this conformation, regions situated N- and C-terminally of the SEC7 domain interact with each other, thereby apparently forming a protective structure over the catalytic center which might prohibit inadvertent ARF-GEF activity.

3 Einleitung

3.1 Vesikeltransport

Eukaryotische Zellen besitzen funktionell unterschiedliche, membranumhüllte Kompartimente, die zusammen das Endomembransystem bilden (Abb.1, Jürgens 2004). Für essentielle Funktionen der Zelle wie Ernährung, Kommunikation und Umweltanpassung ist eine dynamische Verteilung von Lipiden, Proteinen und anderen Makromolekülen zwischen diesen Kompartimenten erforderlich. Auf dem exocytischen Transportweg werden neusynthetisierte Proteine vom Endoplasmatischen Reticulum (ER) über den Golgi-Apparat und das trans-Golgi-Netzwerk (TGN) zur Plasmamembran (PM) oder aus der Zelle heraus transportiert. Über den endocytischen Weg werden von außerhalb der Zelle aufgenommene Moleküle oder Plasmamembran-Proteine an ein als frühes Endosom bezeichnetes Kompartiment geliefert. Von hier aus werden sie über Rezyklierungs-Endosomen (RE) dem polaren Rücktransport zur PM oder über späte Endosomen (auch *multi-vesicular bodies*, MVBs oder *prevacuolar compartments*, PVCs) dem Abbau in Lysosomen beziehungsweise Vakuolen zugeführt. Auch nicht-endocytierte Moleküle wie zum Beispiel Protein abbauende Enzyme können auf dieser Degradationsroute zu den lytischen Kompartimenten transportiert werden. Als „Sortierungsstation“ und Schnittstelle zwischen den verschiedenen Routen dient das TGN, das in Pflanzen auch die Funktion eines frühen Endosoms innehat (Duden 2006, Viotti et al. 2010).

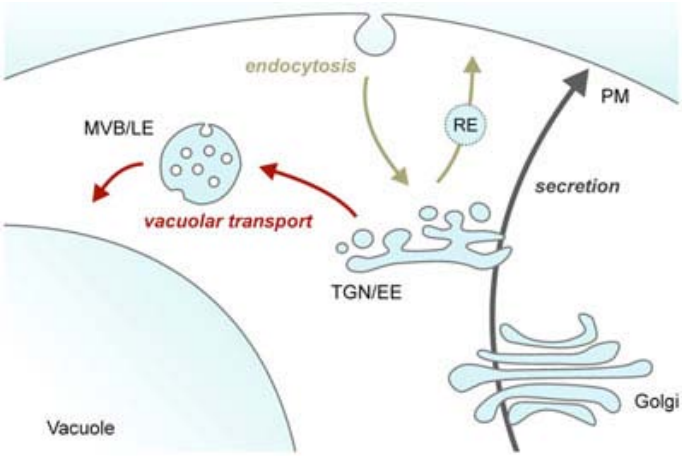

Abb. 1: Das pflanzliche Endomembransystem mit dem TGN als Schnittstelle der Vesikeltransportwege (Scheuring und Robinson. Kapitel: Trans Golgi Network, Web-Ressource *http://illuminatedcell.com: The Illuminated Plant Cell*. 2008. Ed. J. Mathur)**.**

Der Transport der Frachtproteine (*Cargo*) erfolgt mithilfe von membranumhüllten Vesikeln, die von der Donormembran abknospen, entlang des Cytoskeletts zum Zielort wandern und dort mit der Akzeptormembran verschmelzen. Ihre Bildung unterliegt der Regulation durch ADP-Ribosylierungsfaktoren (ARFs), einer Unterfamilie der Ras-GTPasen. Die Bezeichnung ARF stammt von der Fähigkeit dieser Proteine, als Cofaktoren des Cholera-Toxins bei der ADP-Ribosylierung der α-Untereinheit heterotrimerer G-Proteine zu agieren (Moss und Vaughan 1998). Von größerer Bedeutung im Kontext des Vesikeltransports ist jedoch ihre Rolle als „molekulare Schalter“: Wie andere GTPasen wechseln ARFs zwischen einem Guanosindiphoshat (GDP)-gebundenen inaktiven und einem Guanosintriphosphat (GTP)-gebundenen aktiven Zustand. Die Aktivierung durch den Austausch von GDP durch GTP wird von ARF-Guanin-Nukleotid-Austauschfaktoren (ARF-GEFs) vermittelt, die Inaktivierung durch die intrinsische Fähigkeit der GTPasen, GTP zu GDP+Pi zu hydrolysieren, oder durch Interaktion mit GTPase-aktivierenden Proteinen (GAPs) (Randazzo und Hirsch 2004, Casanova 2007). GDP-gebundenes, inaktives ARF liegt cytosolisch oder nur schwach membranassoziiert vor, während die aktive GTP-gebundene Form eine starke Bindung mit Membranen eingeht und Hüllproteine für die Vesikelknospung rekrutiert (Abb. 2, Liu et al. 2010).

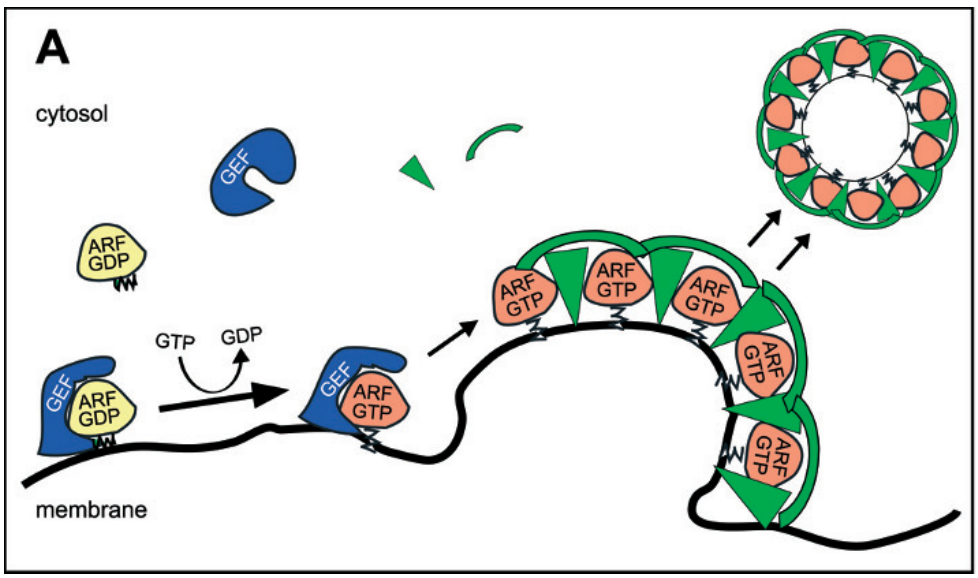

Abb.2: Vesikelbildung. Von ARF-GEFs aktivierte ARFs rekrutieren Hüllproteine, die die Abknospung des Vesikels auslösen (aus Anders und Jürgens 2008).

3.2 Aktivierung von ARFs durch Austauschfaktoren

Das katalytische Zentrum der ARF-GEFs liegt in der ca. 200 Aminosäuren großen SEC7-Domäne, benannt nach dem zuerst identifizierten ARF-GEF Sec7p der Bäckerhefe. Diese interagiert mit den *Switch 1*- und *Switch 2*-Regionen des ARF-Proteins. Durch einen konservierten Glutamat-Rest in der SEC7-Domäne wird über sterische und elektrostatische Abstoßung die Dissoziation des GDPs von ARF ausgelöst (Goldberg 1998). Dies ermöglicht die Bindung von GTP und damit eine Konformationsänderung der *Interswitch*-Region, die ARF zur Rekrutierung von Effektorproteinen befähigt. Zusätzlich zu diesem allen GTPasen gemeinen Mechanismus tritt bei ARF-GTPasen nach erfolgter Aktivierung eine Exposition des myristoylierten N-Terminus auf, die eine verstärkte Membranbindung zur Folge hat (Antonny et al. 1997).

Das Pilzgift Brefeldin A (BFA) hemmt den Vesikeltransport durch eine Stabilisierung des ARF•ARF-GEF-Komplexes in einem GDP-gebundenen, also inaktiven, Übergangsstadium. Strukturbiologische Untersuchungen zeigen, dass BFA an der Berührungsfläche zwischen den Proteinen bindet und die für den Nukleotidaustausch nötigen Konformationsänderungen von ARF verhindert (Mossessova et al. 2003, Renault et al. 2003). Spezifische Aminosäurereste in der SEC7-Domäne beeinflussen die Wirkung von BFA auf den jeweiligen ARF-GEF (Peyroche et al. 1999, Robineau et al. 2000). Bei pflanzlichen ARF-GEFs bewirkt das Vorhandensein eines Leucinrestes in der ARF-Bindestelle BFA-Resistenz, während Methionin an derselben Position Sensitivität bedingt (Geldner et al. 2003).

3.3 Klassifikation von ARF-GEFs

Ihrer Größe entsprechend werden ARF-GEFs als klein (~40-80kD), mittelgroß (~100-120kD) und groß (~150-220kD) klassifiziert. Pflanzen besitzen weder kleine noch mittelgroße ARF-GEFs. Das Genom von *Arabidopsis thaliana* codiert für acht große ARF-GEFs, die sich in zwei Unterfamilien einordnen lassen: GNOM und zwei GNOM-ähnliche (*GNOM-like*, GNL) Proteine GNL1 und GNL2, die mit dem menschlichen GBF1 verwandt sind, sowie BIG1-5, die eine phylogenetische Nähe zu menschlichem BIG1 aufweisen (Abb. 3, Cox et al. 2004, Mouratou et al. 2005).

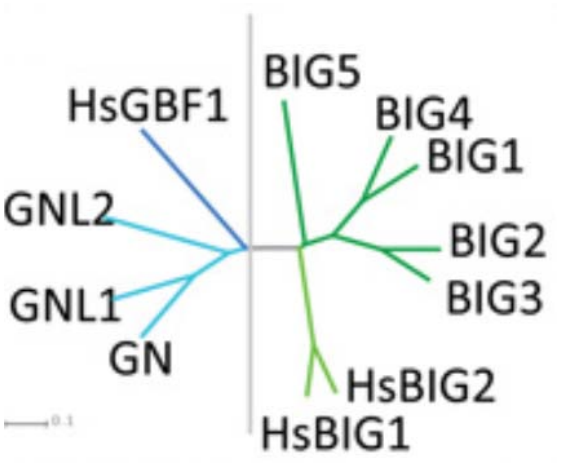

Abb. 3: Phylogenetischer Stammbaum von pflanzlichen und menschlichen großen ARF-GEFs (ZMBP-Homepage, 2/2014).

GBF1 lokalisiert am Golgi-Apparat und reguliert dort den retrograden Vesikeltransport zum ER (Zhao et al. 2006). In Pflanzen erfüllen sowohl GNOM als auch GNL1 diese Aufgabe (Richter et al. 2007). GNOM spielt außerdem eine Rolle bei der endosomalen Rezyklierung; insbesondere ist es essentiell für den polaren Transport des Auxin-Efflux-Carriers PIN1 zur basalen Plasmamembran in vaskulären Zellen und damit für die Ausbildung des Auxingradienten und der apikal-basalen Polaritätsachse in der Embryonalentwicklung von *Arabidopsis* (Steinmann et al. 1999, Geldner et al. 2001, Geldner et al. 2003). GNL2 wird pollenspezifisch exprimiert und ist dort bei Keimung und Pollenschlauchwachstum involviert (Anders und Jürgens 2008, Richter et al. 2012). Säugetier-BIG1 und 2 wurden am TGN nachgewiesen und regulieren den post-Golgi-Vesikeltransport (Zhao et al. 2002, Charych et al. 2004).

3.4 Struktur von ARF-GEFs

Die Domänenarchitektur von großen ARF-GEFs ist hochkonserviert (Abb. 4). N- und C-terminal der katalytischen SEC7-Domäne liegen wenig charakterisierte homologe Bereiche (HUS und HDS1-3, *homology upstream/downstream of SEC7*). Die N-terminale DCB-Domäne (*Dimerization and Cyclophilin Binding*) vermittelt inter- und intramolekulare Interaktionen (Grebe 2005, Anders et al. 2008).

Abb. 4: Domänenstruktur von großen ARF-GEFs (nach Mouratou et al., 2005)**.**

3.5 Regulation von ARF-GEFs

Es wurde gezeigt, dass die DCB-Domäne nicht nur mit anderen DCB-Domänen homotypisch interagiert, sondern auch heterotypisch mit dem Rest des Proteins. Insbesondere Bereiche in der HUS- und SEC7-Domäne wurden durch Punktmutationsstudien an GNOM als wichtig für diese Interaktion identifiziert. Die Rückfaltung der DCB-Domäne ist essentiell für die Fähigkeit des ARF-GEFs, an Membranen zu binden (Anders et al. 2008). Große ARF-GEFs besitzen keine klassische Membranbindungsdomäne wie die Pleckstrin-Homologie (PH)-Domäne der kleinen und mittleren ARF-GEFs (Blomberg et al. 1999, Gillingham und Munro 2007), obwohl der von ihnen vermittelte Nukleotidaustausch an Membranen stattfindet. Für eine räumlich und zeitlich kontrollierte Aktivierung ihrer ARF-Substrate ist zudem eine reversible Membranassoziation der ARF-GEFs erforderlich. Eine solche Regulation ist möglicherweise durch den Wechsel zwischen einer im Cytosol vorliegenden geschlossenen Konformation, in der die DCB-Domäne auf den Rest des Proteins rückfaltet, und einer offenen, katalytisch aktiven, membranassoziierten Form gegeben (Abb. 5, Anders et al. 2008). Für ARF-GEFs der BIG-Familie wurde bei *Saccharomyces cerevisiae* und Säugetieren eine Rekrutierung an die TGN-Membran durch aktivierte ARF- und RAB-GTPasen nachgewiesen (Christis und Munro 2012, Richardson et al. 2012, Lowery et al. 2013, McDonold und Fromme 2014).

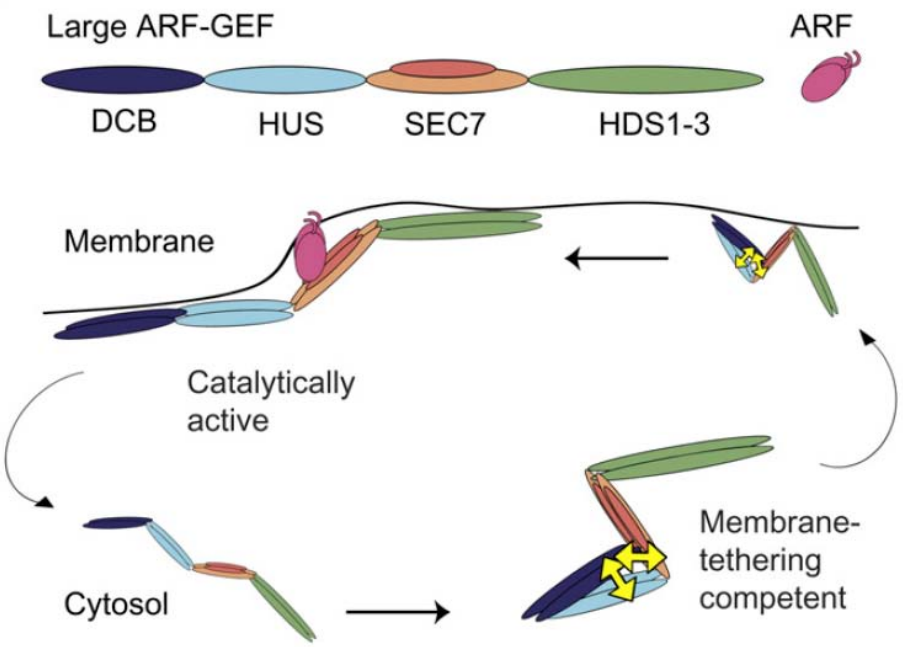

Abb. 5: Regulation von großen ARF-GEFs durch Konformationswechsel zwischen einer geschlossenen cytosolischen Form und einer membranassoziierten offenen Form, die katalytisch aktiv ist (aus Anders et al., 2008)**.**

3.6 Klassifikation von ARFs

Den acht ARF-GEFs stehen in *Arabidopsis* 19 ARF- und ARF-ähnliche (*ARF-like*, ARL) Proteine gegenüber (Vernoud et al. 2003), die oft Redundanz in Funktion und Lokalisation aufweisen. Das Zusammenspiel zwischen den einzelnen ARFs und ihren jeweiligen Austauschfaktoren ist noch nicht im Detail bekannt. Die Unterscheidung zwischen ARF und ARL beruht auf Sequenzähnlichkeit und funktionalen Kriterien; so weisen ARF-Proteine zum Beispiel eine höhere Effizienz als Cofaktoren des Cholera-Toxins sowie bei der Rettung von *arf*-Mutationen in *Saccharomyces cerevisiae* auf als ARLs (Van Valkenburgh et al. 2001). Sechs der *Arabidopsis*-ARF-Isoformen entsprechen aufgrund von Aminosäuresequenz, Phylogenie und Genstruktur den Klasse I-ARFs der Säugetiere. Drei weitere werden den pflanzenspezifischen Klassen A und B zugeordnet (Abb. 6, Jürgens und Geldner 2002, Gebbie et al. 2005). Pflanzliches ARF1 findet sich wie Säugetier-ARF1 am Golgi-Apparat und am TGN (Xu und Scheres 2005, Stierhof und El Kasmi 2010), während ARF B Plasmamembran-lokalisiert ist (Matheson et al. 2008).

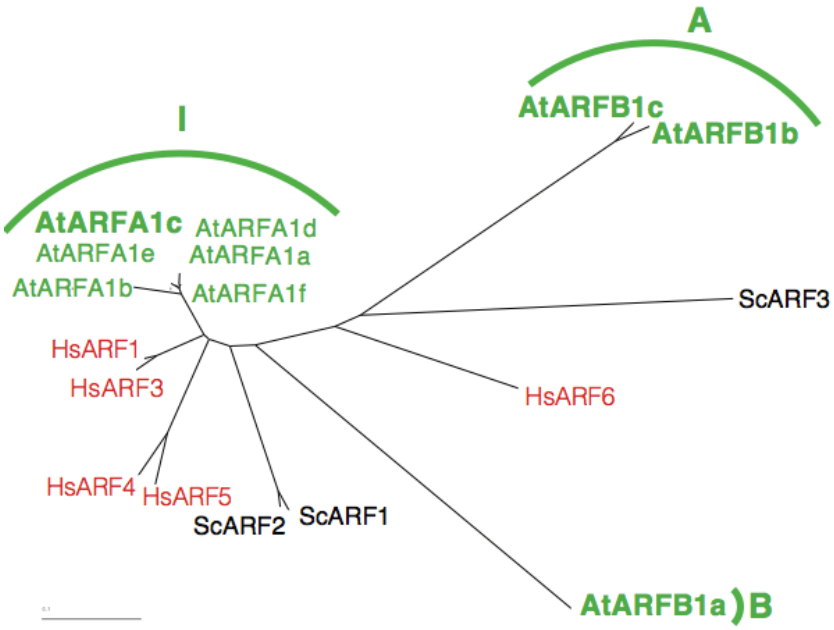

Abb. 6: Phylogenetischer Stammbaum von ARF-GTPasen aus *S. cerevisiae*, *H. sapiens* und *A. thaliana* (Sandra Richter)**.**

3.7 ARFs als Regulatoren der Vesikelbildung

ARF-GTPasen modifizieren Membranoberflächen, indem sie lipidmodifizierende Enzyme aktivieren und cytosolische Hüllproteine zum Ort der Vesikelknospung rekrutieren, die der Sammlung von Cargo, der Krümmung der Membran zu einer Knospe und der Koordination der Vesikelabspaltung dienen. Es sind drei Arten von Proteinhüllen von Transportvesikeln bekannt: COP-I, COP-II und Clathrin-Hüllen (Kirchhausen 2000). ARF-GTPasen rekrutieren COP-I- und Clathrin-Hüllen, während Sar1p-GTPasen, eine Unterfamilie der ARF-GTPasen, COP-II-Hüllen rekrutieren. Eine COP-I-Hülle besteht aus ARF und den sieben Untereinheiten (α -, β-, β‘-, γ-, δ-, ε- und ζ-COP) des Proteinkomplexes Coatomer (Rothman und Warren 1994). Die Bildung von COP-I-Vesikeln kann in drei Schritte unterteilt werden (Abb. 7):

(1.) GTP-abhängige Bindung von ARF an die Donormembran, (2.) Knospenbildung und gleichzeitige Hüllenzusammensetzung durch die Rekrutierung von Coatomer, (3.) Abtrennung des neugebildeten COP-I-umhüllten Vesikels (Nickel und Wieland 1997).

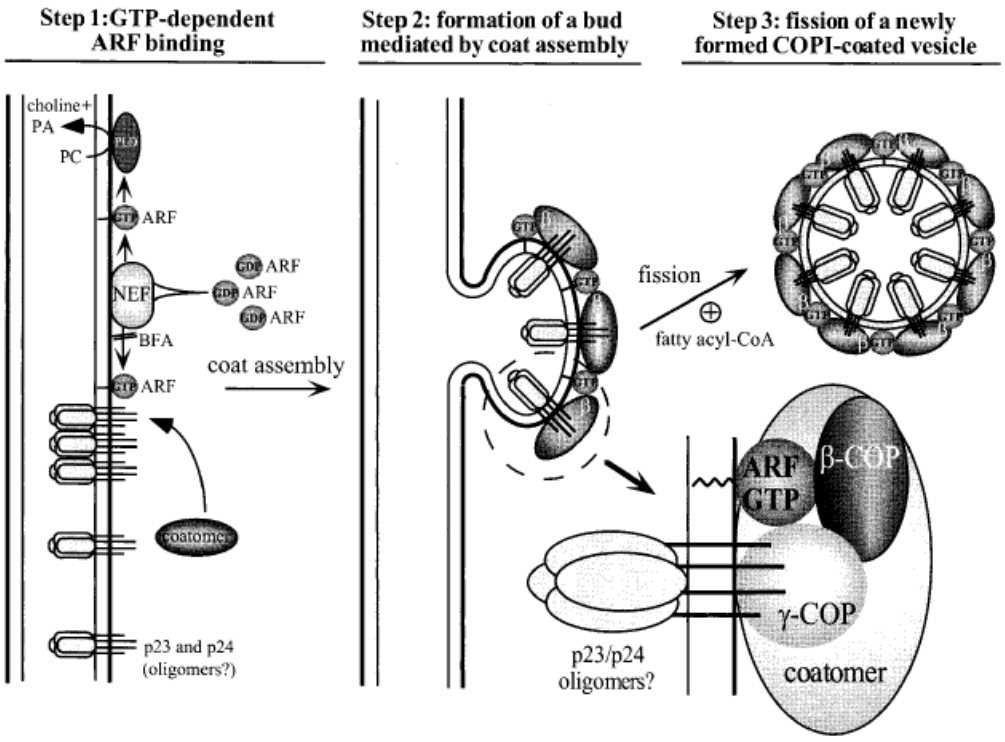

Abb. 7: Modell der Biogenese von COP-I-Vesikeln (aus Nickel und Wieland, 1997).

Die Auflösung der Vesikelhülle beginnt durch die von ARF-GAP katalysierte Hydrolyse des ARF-gebundenen GTPs zu GDP. Dieser Prozess wird möglicherweise durch im Vesikel enthaltene Cargomoleküle, die mit Cargorezeptoren in der Vesikelmembran oder -hülle interagieren, ausgelöst (Springer et al. 1999, Zhu et al. 1999, Goldberg 2000). Das somit inaktivierte ARF löst sich von der Membran, gefolgt von den Coatomer-Proteinen. Das „nackte“ Vesikel kann nun, vermittelt von SNARE (*soluble N-ethylmaleimide-sensitive-factor attachment receptor*)-Proteinkomplexen, mit der Akzeptormembran verschmelzen (Bassham und Blatt 2008).

Die Bildung der COP-II- und Clathrin-umhüllten Vesikel (*clathrin coated vesicles*, CCVs) folgt ähnlichen Prinzipien. Eine Clathrin-Hülle besteht aus zwei separaten Komplexen, einem Adaptorkomplex und dem Clathrin-„Käfig“. An den verschiedenen intrazellulären Membranen finden sich unterschiedliche Adaptorkomplexe, die von den heterotetrameren Adaptoren AP1-5 bis zu den monomeren GGA-Proteinen reichen (Bonifacino 2004, Faini et al. 2013). Sie sind über spezielle Domänen in der Lage, Membran, Membranproteine und die Käfigkomponenten zu verbinden. GGA-Adaptoren wurden in Pflanzen bis jetzt nicht nachgewiesen (Hwang 2008).

COP-I-Vesikel sind Träger des Transports innerhalb des Golgi-Apparates und des retrograden Golgi-ER-Transports, während der anterograde ER-Golgi-Transport von

COP-II-Vesikeln geleistet wird. Clathrin-umhüllte Vesikel sind im späten sekretorischen (post-TGN) und im endocytischen Transportweg involviert (Abb. 8, Kirchhausen 2000).

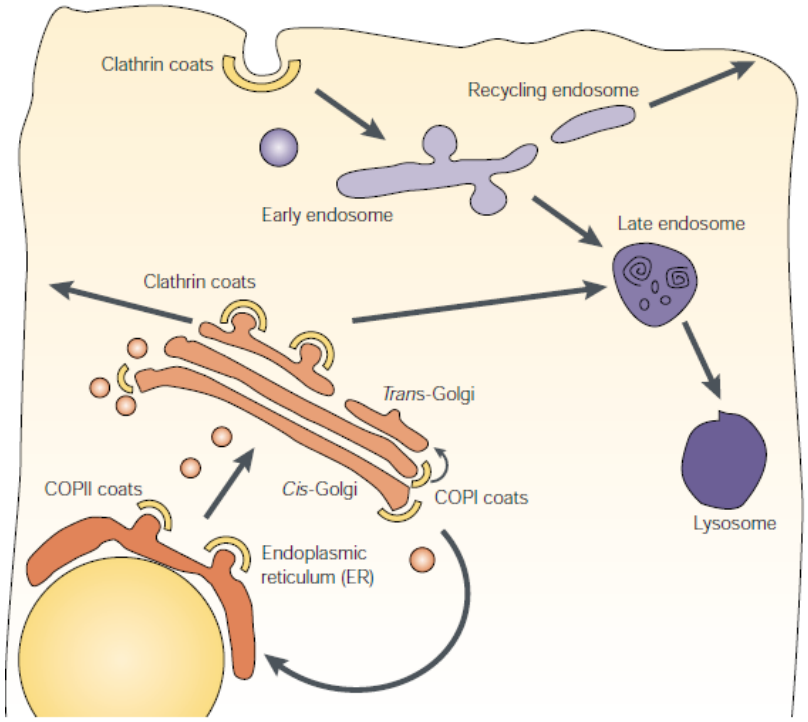

Abb. 8: Hüllproteine in Vesikeltransportwegen am Beispiel einer tierischen Zelle. In Pflanzenzellen fungiert das TGN als frühes Endosom (aus Kirchhausen, 2000)**.**

3.8 RAB-GTPasen

Neben der Vesikelbildungs-Maschinerie mit ARFs, ARF-GEFs und Hüllproteinen sind GTPasen der RAB (*Ras-related in brain*)-Familie wichtige Regulatoren des intrazellulären Transports. Sie werden als bestimmende Faktoren der Membranidentität angesehen und regulieren Membranerkennungsprozesse, die der SNARE-vermittelten Membranfusion vorangehen (Novick und Brennwald 1993, Saito und Ueda 2009). Außerdem impliziert die Identifikation von bestimmten RAB-Effektoren eine Beteiligung an der Vesikelbildung (McDonold und Fromme 2014) und der Rekrutierung von Motorproteinen des Cytoskeletts (Echard et al. 1998, Nielsen et al. 1999, Hoepfner et al. 2005). Wie ARFs werden RABs nukleotidabhängig aktiviert und inaktiviert. Im Unterschied zu der N-terminalen Myristoylierung der ARFs weisen

RABs eine Prenylierung von C-terminalen Cystein-Resten auf, die hier im inaktiven Zustand eine Membranverankerung vermittelt (Desnoyers et al. 1996). Ein RAB-GEF aktiviert das membraninserierte inaktive RAB, das daraufhin für den jeweiligen Transportprozess spezifische Effektorproteine rekrutiert. Nach der Inaktivierung durch RAB-GAP-unterstützte Hydrolyse des gebundenen GTPs wird RAB durch GDP-Dissoziations-Inhibitoren (GDIs) aus der Membran extrahiert und in der GDP-gebundenen Form im Cytosol stabilisiert (Ullrich et al. 1993, Wu et al. 1996).

3.9 Klassifikation von RABs

Die 57 vom *Arabidopsis*-Genom codierten RABs werden aufgrund von Sequenzähnlichkeit untereinander sowie mit Homologen aus Hefe und Säugetieren in die acht Unterfamilien A-H eingeordnet (Pereira-Leal und Seabra 2001). Ebenso ist eine numerische Nomenklatur in Anlehnung an die Säuger-RABs gebräuchlich (Nielsen et al. 2008). Die RAB-Unterfamilien 5/F und 7/G sind im Rahmen dieser Arbeit von besonderer Bedeutung (Abb. 9).

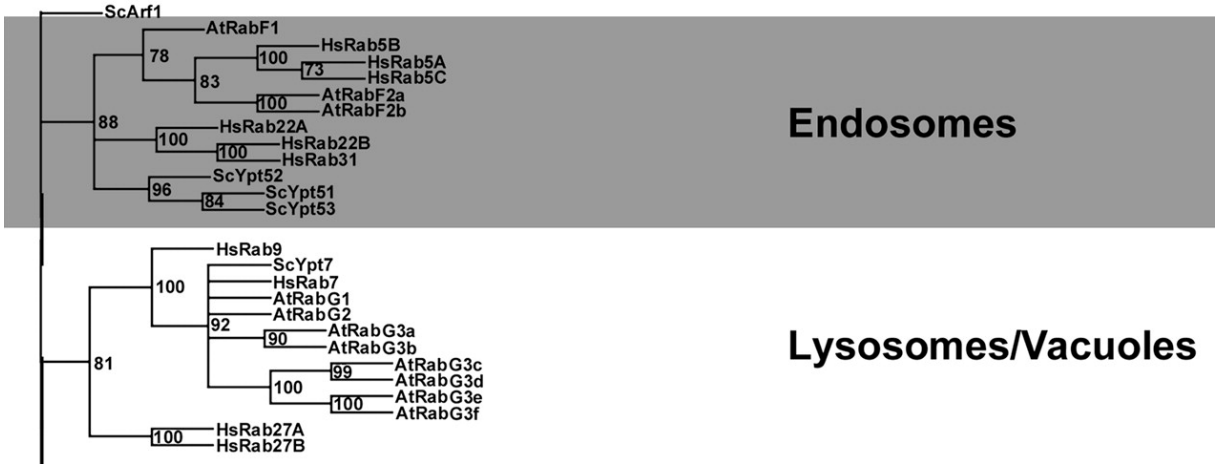

Abb. 9: Phylogenetischer Stammbaum von RAB-GTPasen der Untergruppen 5/F und 7/G aus *S. cerevisiae*, *H. sapiens* und *A. thaliana* (aus Vernoud et al. 2003)**.**

Für Mitglieder der Untergruppe 5/F wurde bei Säugetieren eine regulatorische Funktion bei Membranfusionsereignissen in endosomalen und endocytischen Transportschritten demonstriert (Gorvel et al. 1991, Bucci et al. 1992). Im *Arabidopsis*-Genom finden sich drei RAB5-Homologe: RABF1/ARA6, RABF2a/RHA1

und RABF2b/ARA7 (Ueda et al. 2001). Die beiden RABF2-Proteine lokalisieren an MVBs und spielen eine Rolle im vakuolären Transportweg (Sohn et al. 2003, Kotzer et al. 2004, Lee et al. 2004). RABF1 scheint trotz der Homologie zu den RAB5-Proteinen anderer Organismen ein pflanzenspezifischer Sonderfall zu sein. So besitzt es anstelle des C-terminalen Cysteinmotivs N-terminale Erkennungsbereiche für Myristoylierung und Palmitoylierung, die für eine korrekte Membranlokalisation wichtig sind. RABF1 wurde ebenfalls an MVBs nachgewiesen, colokalisiert jedoch nur teilweise mit RABF2b/ARA7 (Ueda et al. 2001, Haas et al. 2007, Ebine et al. 2011). Dies deutet auf die Existenz unterschiedlicher Populationen von MVBs hin. RABF1 wurde außerdem gelegentlich an der PM detektiert und könnte daher bei unterschiedlichen Transportprozessen aktiv sein, unter anderem bei pflanzenspezifischen, die die Anpassung an Umwelteinflüsse regulieren (Ebine et al. 2011).

In Säugetieren und Hefen reguliert RAB7/G die Membranfusion an späten Endosomen beziehungsweise die Fusion von Vakuolen (Nielsen et al. 2008). *Arabidopsis*-RAB7/G findet sich größtenteils an der vakuolären Membran (Saito et al. 2002).

3.10 Der vakuoläre Weg: MVB-Reifung statt Vesikeltransport

Bei den Transportwegen von endocytierten und neusynthetisierten Proteinen zu den lytischen Kompartimenten offenbaren sich Unterschiede zwischen Pflanzen und Nichtpflanzen, wie zum Beispiel Säugetieren. Bei letzteren werden abzubauende PM-Proteine nach ihrer Internalisierung und Ubiquitinierung zunächst an ein frühes Endosom (*early endosome*, EE) geliefert und dort durch Proteine der ESCRT-Maschinerie in intraluminale Vesikel (ILVs) verpackt (Polo et al. 2002, Jovic et al. 2010). Begleitet von einem Austausch von RAB 5/F durch RAB 7/G an der endosomalen Membran reift das frühe zu einem späten Endosom (*late endosome*, LE). Die RAB-Konversion wird durch den heterodimeren RAB-GEF SAND/CCZ1 reguliert (Nordmann et al. 2010, Poteryaev et al. 2010, Huotari und Helenius 2011). Das LE fusioniert schließlich mit dem Lysosom und entlässt dabei die ILVs in dessen Inneres (Luzio et al. 2009). Neusynthetisierte lösliche vakuoläre Cargo-Proteine, zum Beispiel lytische Enzyme, werden am TGN in Clathrin-umhüllte Vesikel (CCVs) sortiert und zum EE transportiert (Braulke und Bonifacino 2009).

Pflanzenzellen besitzen kein separates EE, stattdessen übernimmt das TGN damit assoziierte Funktionen (Viotti et al. 2010). In Analogie zu den Säugetiermodellen wurde lange angenommen, dass lösliche vakuoläre Fracht über CCVs vom TGN/EE zum LE, in Pflanzen auch MVB (*multi-vesicular body*) genannt, transportiert wird (Foresti et al. 2010, Zouhar et al. 2010). Es gibt jedoch Hinweise darauf, dass CCVs auf dieser Route keine Rolle spielen (Scheuring et al. 2011). Stattdessen wird eine Abknospung der MVBs aus Subdomänen des TGN vorgeschlagen, ähnlich der Reifung des EEs zum LE bei Säugetieren, gefolgt von der Fusion mit der Vakuole (Abb. 10, Scheuring et al. 2011).

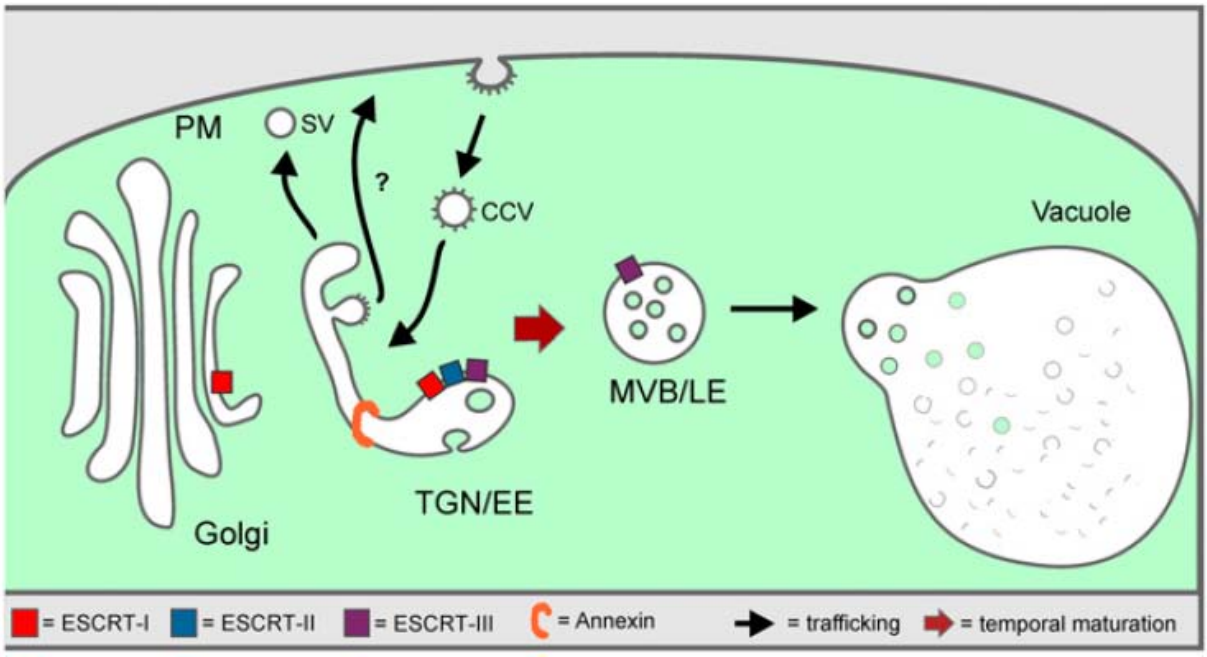

Abb. 10: Modell der Reifung von MVBs aus dem TGN. Eine Subdomäne des TGN durchläuft schrittweise Änderungen, wie zum Beispiel die Erzeugung von ILVs durch die ESCRT-Maschinerie, die schließlich zur Abknospung des MVBs führen (aus Scheuring et al., 2011)**.**

4 Zielsetzung

Große ARF-GEFs sind bedeutende Regulatoren des intrazellulären Vesikeltransports. Während die Rolle der GBF1-verwandten ARF-GEFs GNOM, GNL1 und GNL2 in der Koordination des retrograden Golgi-ER-Transports und der Rezyklierung von Plasmamembranproteinen gut untersucht ist (Geldner et al. 2003; Richter et al. 2007; Richter et al. 2012), wurden die BIG1-verwandten ARF-GEFs BIG1-4 in *Arabidopsis* bisher nicht analysiert. Ein Ziel dieser Arbeit war die Charakterisierung dieser Proteine in Bezug auf ihre Funktion und subzelluläre Lokalisation, um dadurch die von ihnen regulierte Vesikeltransportroute aufzuklären.

Große ARF-GEFs besitzen eine konservierte Domänenstruktur (Mouratou et al. 2005). Die einzelnen Domänen haben unterschiedliche Funktionen, wie zum Beispiel Katalyse des Nukleotidaustauschs bei ARF-Substraten und die Vermittlung von inter- und intramolekularen Interaktionen (Grebe et al. 2000; Anders et al. 2008). Als Teil dieser Arbeit sollte der Beitrag einzelner Domänen bei der Erzeugung von Membran- und Substratspezifität untersucht werden. Außerdem ist eine spezielle Proteinkonformation, bei der die DCB-Domäne auf den Rest des Proteins zurückfaltet, für die Membranassoziation von GNOM von Bedeutung (Anders et al. 2008). Die Beteiligung bestimmter Proteindomänen an diesem Mechanismus sollte durch Interaktionsstudien im Detail geklärt werden.

Für den vakuolären Transportweg in Pflanzenzellen wurde, in Analogie zu Säugetier- und Hefemodellen, eine Reifung des MVBs aus definierten Bereichen des TGNs vorgeschlagen, gefolgt von der Fusion des MVBs mit der lytischen Vakuole (Scheuring et al. 2011). In tierischen und Hefezellen ist dabei eine durch SAND/MON1 vermittelte RAB-Konversion von Bedeutung (Poteryaev et al. 2010), während das SAND-Homolog in *Arabidopsis* bisher nicht charakterisiert wurde. Im Rahmen dieser Arbeit sollte die mögliche konservierte Rolle von SAND in dem vorgeschlagenen endosomalen Reifungsprozess analysiert werden.

5 Publikationen

5.1 Richter et al., 2014

Delivery of endocytosed proteins to the cell–division plane requires change of pathway from recycling to secretion

Sandra Richter, Marika Kientz, Sabine Brumm, Mads Eggert Nielsen, Misoon Park, Richard Gavidia, Cornelia Krause, Ute Voss, Hauke Beckmann, Ulrike Mayer, York-Dieter Stierhof, Gerd Jürgens

eLife 2014;3:e02131

eLIFE elifesciences.org

RESEARCH ARTICLE

Delivery of endocytosed proteins to the cell–division plane requires change of pathway from recycling to secretion

Sandra Richter[1], Marika Kientz[1], Sabine Brumm[1], Mads Eggert Nielsen[1†], Misoon Park[1], Richard Gavidia[1], Cornelia Krause[1], Ute Voss[1‡], Hauke Beckmann[1], Ulrike Mayer[2], York-Dieter Stierhof[2], Gerd Jürgens[1]*

[1]Department of Developmental Genetics, The Center for Plant Molecular Biology (ZMBP), University of Tübingen, Tübingen, Germany; [2]Microscopy, The Center for Plant Molecular Biology (ZMBP), University of Tübingen, Tübingen, Germany

Abstract Membrane trafficking is essential to fundamental processes in eukaryotic life, including cell growth and division. In plant cytokinesis, post-Golgi trafficking mediates a massive flow of vesicles that form the partitioning membrane but its regulation remains poorly understood. Here, we identify functionally redundant Arabidopsis ARF guanine-nucleotide exchange factors (ARF-GEFs) BIG1–BIG4 as regulators of post-Golgi trafficking, mediating late secretion from the trans-Golgi network but not recycling of endocytosed proteins to the plasma membrane, although the TGN also functions as an early endosome in plants. In contrast, BIG1-4 are absolutely required for trafficking of both endocytosed and newly synthesized proteins to the cell–division plane during cytokinesis, counteracting recycling to the plasma membrane. This change from recycling to secretory trafficking pathway mediated by ARF-GEFs confers specificity of cargo delivery to the division plane and might thus ensure that the partitioning membrane is completed on time in the absence of a cytokinesis-interphase checkpoint.
DOI: 10.7554/eLife.02131.001

***For correspondence:** gerd.juergens@zmbp.uni-tuebingen.de

Present address: †Department of Plant and Environmental Sciences, University of Copenhagen, Copenhagen, Denmark; ‡Plant Sciences Division, School of Biosciences, University of Nottingham, Nottingham, United Kingdom

Competing interests: The authors declare that no competing interests exist.

Funding: See page 14

Received: 19 December 2013
Accepted: 27 February 2014
Published: 08 April 2014

Reviewing editor: Christian S Hardtke, University of Lausanne, Switzerland

Introduction

In post-Golgi membrane trafficking, cargo proteins are dynamically distributed between trans-Golgi network (TGN), various endosomes, lysosome/vacuole and plasma membrane (***Surpin and Raikhel, 2004***). In contrast to animals, the TGN also functions as an early endosome in plants and is a major trafficking hub where secretory, endocytic, recycling and vacuolar pathways intersect (***Viotti et al., 2010***; ***Reyes et al., 2011***). Therefore, it has been notoriously difficult to functionally delineate the recycling vs secretory pathways in plants. Sorting of cargo proteins occurs during the formation of transport vesicles, involving activation of small ARF GTPases by ARF guanine-nucleotide exchange factors (ARF-GEFs) and recruitment of specific coat proteins (***Casanova, 2007***). Arabidopsis ARF-GEFs are related to human large ARF-GEFs, GBF1 or BIG1. Whereas the three GBF1-related members GNOM, GNL1 and GNL2 have been characterised in detail (***Geldner et al., 2003***; ***Richter et al., 2007***, ***2012***), of the 5 BIG1-related ARF-GEFs only BIG5 has been analysed so far and implicated in pathogen response (MIN7) and endocytic traffic (BEN1) (***Nomura et al., 2006***, ***2011***; ***Tanaka et al., 2009***; ***Tanaka et al., 2013***). Here, we show that ARF-GEFs BIG1-4 play a crucial role in post-Golgi traffic, which enables us to dissect the regulation of secretory and recycling pathways in interphase and cytokinesis.

eLife digest Cells are surrounded by a plasma membrane, and when a cell divides to create two new cells, it must grow a new membrane to keep the two new cells apart. Animal cells and plant cells tackle this challenge in different ways: in animal cells the new membrane grows inwards from the surface of the cell, whereas the new membrane grows outwards from the centre of the cell in plant cells.

The materials needed to make the plasma membrane are delivered in packages called vesicles: most of these materials arrive from a structure within the cell called the trans-Golgi network, but some materials are recycled from the existing plasma membrane. In plants the formation of the new cell membrane is orchestrated by scaffold-like structure that forms in the plant cell called the 'phragmoplast'. It is widely thought that this structure guides the vesicles bringing materials from the trans-Golgi network, but the details of this process are not fully understood.

Now, Richter et al. have discovered four proteins, called BIG1 to BIG4, that control the formation of the new cell membrane in the flowering plant *Arabidopsis thaliana*, a species that is routinely studied by plant biologists. These four proteins belong to a larger family of proteins that control the trafficking of vesicles within a cell. Richter et al show that a plant cell can lose up to three of these four proteins and still divide, as the plant can still grow and develop as normal. Thus, BIG1 to BIG4 appear to perform essentially the same role in the plant.

Richter et al. also show that, when a plant cell is not dividing, these proteins are involved in controlling the delivery of new materials to surface membrane, and not the recycling of material. However, when a cell is dividing, these proteins switch to regulate both processes, but direct all the material to a new destination—the newly forming membrane, instead of the established surface membrane. Richter et al. suggest that this switch is important to stop any recycling to the plasma membrane that might move material away from the new membrane. The next challenge will be to identify the molecular signals and mechanisms that enable the proteins BIG1 to BIG4 to re-route the recycling of membrane material during cell division.

DOI: 10.7554/eLife.02131.002

Results

ARF-GEFs BIG1 to BIG4 are redundantly required in development

Up to three of ARF-GEFs BIG1 to BIG4 (BIG1-4) were knocked out without recognisable phenotypic effect except for *big1,2,3*, which was retarded in growth because BIG4 is predominantly expressed in root and pollen (***Figure 1A***, ***Figure 1—figure supplement 1A***). Other triple mutants were growth-retarded only if the activity of the respective fourth gene was reduced to 50%. No quadruple mutants were recovered because BIG1-4 were essential in male reproduction, sustaining pollen tube growth (***Figure 1B***, ***Figure 1—figure supplement 1B***). BIG1-4 functional redundancy would be consistent with the occurrence of *BIG1-4*-like single-copy or closely related sister genes in lower plants (***Figure 1—figure supplement 1C***). Although large ARF-GEFs are often inhibited by the fungal toxin brefeldin A (BFA), the SEC7 domain of BIG3 (At1g01960; formerly named BIG2 in ***Nielsen et al., 2006***; see nomenclature used by ***Cox et al., 2004***) displayed BFA-insensitive GDP/GTP exchange activity in vitro (***Nielsen et al., 2006***). BFA treatment of *big3* mutants impaired seed germination and seedling root growth, in contrast to wild-type (***Figure 1D,E***). We engineered a BFA-resistant variant of the naturally BFA-sensitive ARF-GEF BIG4 by replacing amino acid residue methionine at position 695 with leucine, as previously described for the recycling ARF-GEF GNOM (***Geldner et al., 2003***). Engineered BFA-resistant BIG4-YFP rescued BFA-inhibited seed germination of *big3* (***Figure 1F***). The rescue activity of BFA-resistant BIG4 was comparable to that of BIG3 when both were expressed from the ubiquitin 10 (*UBQ10*) promoter whereas BFA-sensitive BIG4 did not at all rescue BFA-inhibited primary root growth of *big3* mutant seedlings (***Figure 1—figure supplement 1D,E***). Thus, BFA treatment of *big3* single mutants effectively causes conditional inactivation of BIG1-4 ARF-GEF function, providing us with a unique tool for studying BIG1-4-dependent trafficking in an organismic context.

BIG1 to BIG4 regulate membrane trafficking at the TGN

BIG4-YFP co-localized with TGN markers vacuolar H^+-ATPase (VHA) subunit a1 and ARF1 GTPase (***Figure 1I–L***, ***Figure 1—figure supplement 2O–R***; ***Dettmer et al., 2006***; ***Stierhof and El Kasmi,***

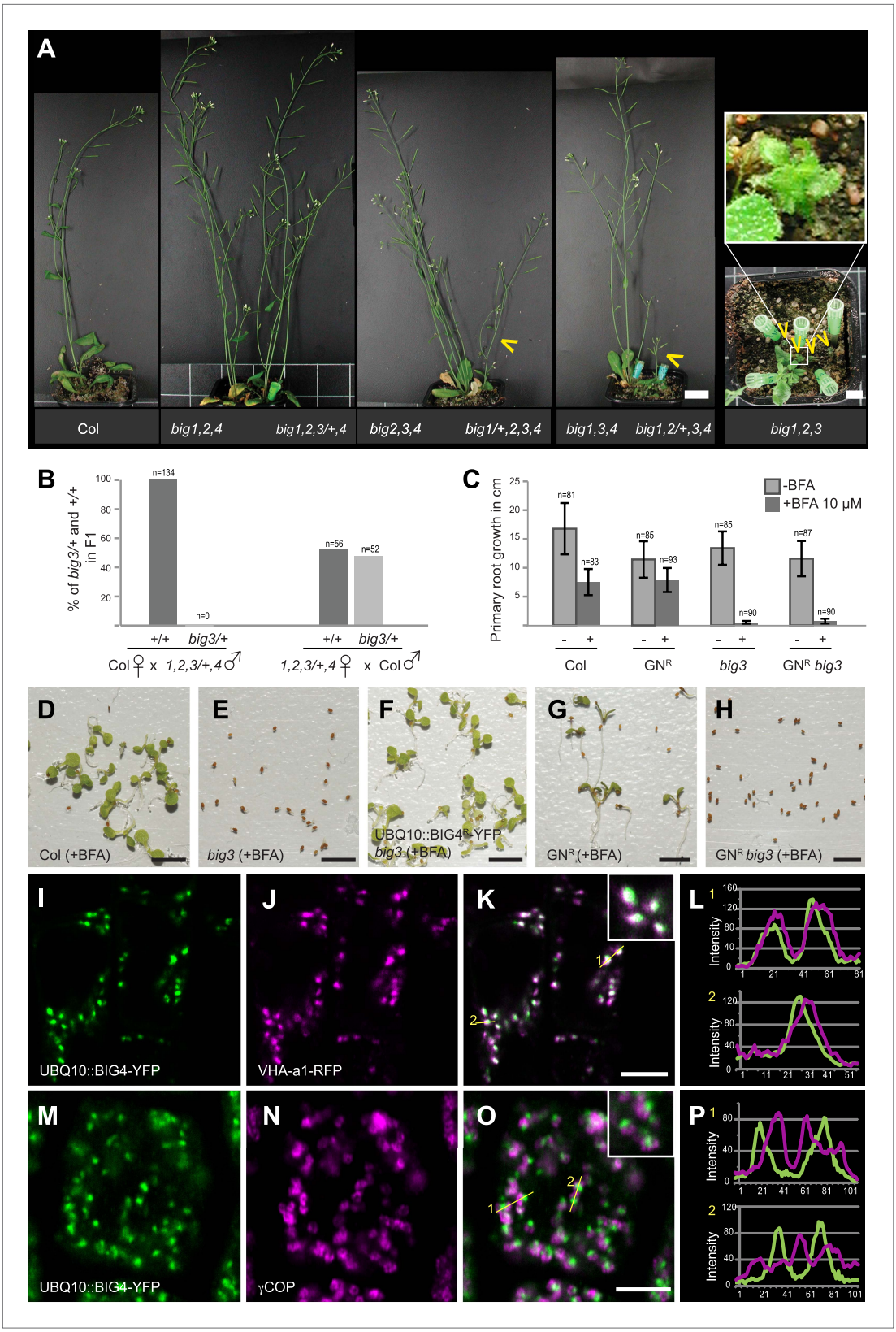

Figure 1. BIG1 – BIG4 act redundantly at TGN and are involved in several physiological processes. (**A**) *big1,2,4 (big1 big2 big4), big2,3,4 (big2 big3 big4), big1,3,4 (big1 big3 big4)* and *big1,2,3/+,4 (big1 big2 big3/BIG3 big4)* mutant plants without obvious phenotype but *big1/+,2,3,4 (big1/BIG1 big2*

Figure 1. Continued on next page

Figure 1. Continued

big3 big4), big1,2/+,3,4 (big1 big2/BIG2 big3 big4) and *big1,2,3 (big1 big2 big3)* were dwarfed (yellow arrowheads). Scale bar, 2 cm. (**B**) F1 of reciprocal crosses between wild-type (Col) and *big1 big2 big3/BIG3 big4* (*1,2,3/+,4*) mutants: 0% or 48% *big3* heterozygous seedlings derived from mutant male or female gamete, respectively. (**C**) BFA inhibited primary root growth of *big3* mutant seedlings with or without BFA-resistant GNOM (GN^R *big3*). Numbers of analysed seedlings are indicated (**B** and **C**). (**D**-**H**) BFA treatment did not prevent seed germination in wild-type (Col; **D**) and BFA-resistant GN (GN^R; **G**) but did so in *big3* mutants without (**E**) or with BFA-resistant GNOM (GN^R *big3*; **H**). This defect was suppressed by BFA-resistant BIG4 (UBQ10::BIG4R-YFP *big3*; **F**). Scale bar, 5 mm. (**I**-**L**) Live imaging of BIG4-YFP (**I**) and TGN marker VHA-a1-RFP (**J**) revealed co- localization (**K**; **L**, intensity–line profile). (**M**–**P**) Immunolocalization of BIG4 (UBQ10::BIG4-YFP; M) and Golgi-marker γCOP (**N**) indicated no co-localization (**O**; **P**, intensity–line profile). (**I**–**K**, **M**–**O**) Scale bar, 5 μm.

DOI: 10.7554/eLife.02131.003

The following figure supplements are available for figure 1:

Figure supplement 1. Expression and phylogeny of BIG ARF-GEFs.

DOI: 10.7554/eLife.02131.004

Figure supplement 2. BIG3 and BIG4 localize at the TGN.

DOI: 10.7554/eLife.02131.005

Figure supplement 3. Ultrastructural localization of BIG4-YFP and ultrastructural abnormalities in BFA-treated *big3* mutant seedling root cells.

DOI: 10.7554/eLife.02131.006

2010) but not with Golgi marker COPI subunit γCOP (***Figure 1M–P***; ***Movafeghi et al., 1999***). TGN localization of BIG4-YFP was confirmed by immunogold labeling on EM sections (***Figure 1—figure supplement 3A,B***). BIG3-YFP and BIG4-YFP co-localized with endocytic tracer FM4-64, labeling TGN after brief uptake (***Figure 1—figure supplement 2A–H***; ***Ueda et al., 2001***; ***Dettmer et al., 2006***). BIG3 and BIG4 also accumulated together with FM4-64 in BFA-induced post-Golgi membrane vesicle aggregates ('BFA compartments'), consistent with ultrastructural abnormalities in these aggregates and Golgi stacks in BFA-treated *big3* mutant (***Figure 1—figure supplement 2I–N, 3C–F***). Together, these data suggest a role for BIG1-4 in post-Golgi membrane trafficking.

Secretory and vacuolar trafficking depend on BIG1 to BIG4 function

To identify trafficking routes regulated by BIG1-4, pathway-specific soluble and membrane-associated cargo proteins were analysed in BFA-treated wild-type and *big3* mutant seedlings (for a list of markers used, see ***Supplementary file 1***; ***Figure 2—figure supplement 1S,T***). Secretory GFP (secGFP) (***Viotti et al., 2010***), which is normally secreted from the cell, and plasma membrane (PM)-targeted syntaxin SYP132 were trapped in BFA compartments and did not reach the plasma membrane of *big3* seedlings, in contrast to wild-type, suggesting a role for BIG1-4 in late secretory traffic, that is from the TGN to the plasma membrane (***Figure 2A–D***). There was a slight retention of SYP132 in the BFA compartments of wild-type seedling roots, which probably reflects slowed-down passage of newly-synthesized proteins through the TGN. This becomes apparent upon BFA treatment because of TGN aggregation into BFA compartments, as has been reported earlier for *HS::secGFP* (***Viotti et al., 2010***). Vacuolar cargo proteins also pass through the TGN via multivesicular bodies (MVBs) to the vacuole (***Reyes et al., 2011***). Soluble RFP fused to phaseolin vacuolar sorting sequence AFVY accumulated in BFA compartments in *big3* mutant, in contrast to wild-type (***Scheuring et al., 2011***; ***Figure 2E–J***, ***Figure 2—figure supplement 1A–F***). Endocytosed PM proteins are delivered to the vacuole for degradation, for example boron transporter BOR1 in response to high external boron concentration (***Takano et al., 2005***; ***Figure 2K–N***). BFA treatment prevented boron-induced trafficking of BOR1 to the vacuole in *big3* mutant, but not in wild-type (***Figure 2L,N***). BOR1 was rapidly turned over in the vacuole of wild-type, leaving no trace of GFP (***Figure 2L***). As expected, ARF-GEF BIG4 and its putative cargo BOR1 co-localized in BFA compartments (***Figure 2—figure supplement 1G–I***). Thus, BIG1-4 mediate both late secretory and vacuolar trafficking from the TGN.

Recruitment of clathrin adaptor complex AP-1 to the TGN requires BIG1 to BIG4 function

ARF-GEFs activate ARF GTPases, resulting in recruitment of vesicular coat proteins to the respective endomembrane compartment, such as COPI complex to Golgi stacks or adaptor protein (AP) complexes to post-Golgi compartments (***Robinson, 2004***). Like BIG1-4, AP-1 complex subunit muB2-adaptin (AP1M2) localizes to SYP61-labeled TGN and is required for late secretory and vacuolar trafficking (***Park et al., 2013***; ***Teh et al., 2013***; ***Wang et al., 2013***; ***Figure 2—figure supplement 1P–R***).

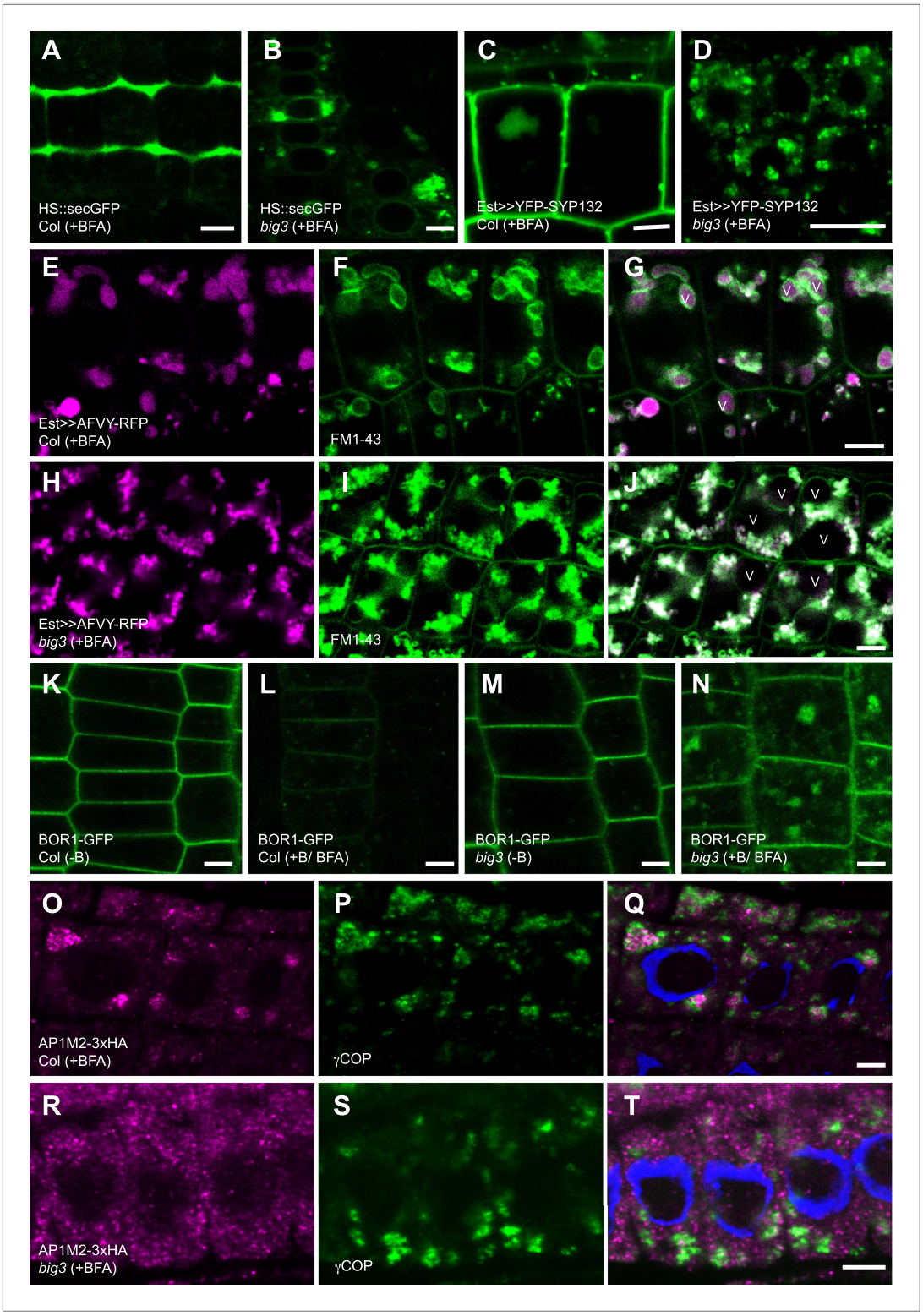

Figure 2. BIG1 – BIG4 regulate secretory and vacuolar trafficking by recruiting AP-1 adaptor complex. (**A** and **B**) BFA inhibited secretion of heat shock (HS)-induced secGFP in *big3* mutants (**B**) but not in wild-type (Col; **A**). (**C** and **D**) BFA inhibited trafficking of estradiol (Est)-induced YFP-SYP132 to the plasma membrane in *big3* mutants (**D**) but not in wild-type (Col; **C**). (**E**–**J**) BFA inhibited trafficking of soluble cargo AFVY-RFP to the vacuole (v), labeled by FM1-43 (**F** and **I**), in *big3* mutants (**H**–**J**) but not in wild-type (Col, **E**–**G**). (**K**–**N**) Live imaging of BOR1-GFP

Figure 2. Continued on next page

Figure 2. Continued

localization. Without boron (−B), BOR1-GFP localized at the plasma membrane in wild-type (**K**) and *big3* mutants (**M**). After BFA and boron treatment (+B), BOR1-GFP was degraded in the vacuole of wild-type (**L**) but accumulated in BFA compartments of *big3* mutants (**N**). (**O**–**T**) Immunostaining of 3xHA-tagged muB2 subunit of AP-1 complex (AP1M2; **O**, **R**) and COPI subunit γCOP (**P** and **S**) in BFA-treated seedlings. AP1M2 accumulated in BFA compartments surrounded by γCOP in wild-type (Col; **Q**). In *big3* mutants, γCOP was still recruited to Golgi membranes whereas AP1M2 was cytosolic (**R**–**T**). Blue, DAPI-stained nuclei. Scale bars, 5 μm.

DOI: 10.7554/eLife.02131.007

The following figure supplements are available for figure 2:

Figure supplement 1. BIG1 – BIG4 regulate trafficking of secretory and vacuolar cargo by recruiting AP-1 complex.

DOI: 10.7554/eLife.02131.008

AP1M2 also co-localized with TGN marker SYP61 in BFA compartments (***Figure 2—figure supplement 1J–L***). In BFA-treated *big3* mutant, however, AP1M2 was cytosolic whereas SYP61 was still TGN-associated (***Figure 2O,R***; ***Figure 2—figure supplement 1J–O***). In contrast to AP1M2, Golgi association of COPI subunit γCOP, which is mediated by BFA-resistant ARF-GEF GNL1 (***Richter et al., 2007***), was not affected in BFA-treated *big3* mutant (***Figure 2O–T***). Thus, BIG1-4 specifically mediate AP-1 recruitment to the TGN.

Secretion and recycling to the plasma membrane are independently regulated trafficking pathways

Another ARF-GEF in post-Golgi traffic, GNOM regulates polar recycling of auxin-efflux carrier PIN1 to the basal plasma membrane (***Geldner et al., 2003***). BFA treatment of wild-type and *big3* mutant seedlings inhibited recycling of PIN1, which accumulated in BFA compartments, and this defect was suppressed by engineered BFA-resistant GNOM (***Figure 3A–D***). Thus, BIG1-4 did not play any obvious role in PIN1 recycling. PIN1 is a stable protein such that most protein detectable at the plasma membrane is delivered via the recycling but not the secretory pathway (***Geldner et al., 2001***). In order to analyse the behavior of newly-synthesized PIN1 protein, we generated transgenic plants expressing estradiol-inducible PIN1. In contrast to recycling PIN1, newly-synthesized PIN1 protein was trapped in BFA compartments of *big3* mutant, regardless of BFA-resistant GNOM (***Figure 3E–H***). In conclusion, secretory ARF-GEFs BIG1-4 and recycling ARF-GEF GNOM regulate different post-Golgi trafficking pathways to the plasma membrane that function independently of each other.

Gravitropic growth response of the seedling root relies on GNOM-mediated PIN1 recycling (***Geldner et al., 2003***). We tested whether BIG1-4 are also required, using *DR5::NLS-3xGFP* expression to visualise auxin response (***Weijers et al., 2006***). BFA-induced inhibition of auxin response in wild-type and *big3* mutant was overcome by BFA-resistant GNOM, suggesting that BIG1-4 mediated secretion plays no role in gravitropic growth response (***Figure 4A–D***). GNOM-dependent PIN1 recycling is also required for lateral root initiation (***Geldner et al., 2003***). Surprisingly, BFA-resistant GNOM failed to initiate lateral root primordia in BFA-treated *big3* mutant in spite of stimulation by NAA, in contrast to seedlings that expressed both BIG3 and BFA-resistant GNOM (***Figure 4E–L***). *big3* mutants displayed binucleate cells, suggesting an essential role for secretory traffic in cytokinesis required for lateral root initiation (***Figure 4M–T***). For comparison, the BFA-induced defects in seed germination and primary root growth of *big3* were not rescued by engineered BFA-resistant GNOM, thus depending on secretory traffic rather than recycling (***Figure 1C,E,H***).

Trafficking of both endocytosed and newly-synthesized proteins to the plane of cell division is regulated by secretory ARF-GEFs BIG1 to BIG4

In plant cytokinesis, which is assisted by a dynamic microtubule array named phragmoplast, both newly-synthesized and endocytosed proteins traffic to the plane of cell division on post-Golgi membrane vesicles that fuse with one another to form the partitioning cell plate (***Samuels et al., 1995***). This raises the problem of coordinating different trafficking routes in the brief period of mitotic division (***Reichardt et al., 2011***). Cell-plate formation requires cytokinesis-specific syntaxin KNOLLE, newly synthesized during late G2/M phase (***Lauber et al., 1997***; ***Reichardt et al., 2007***). In contrast to wild-type, KNOLLE targeting to the division plane was inhibited in BFA-treated *big3* mutants, with KNOLLE accumulating in BFA compartments together with BIG4-YFP (***Figure 5A–F***, ***Figure 5—figure supplement 1A–D***). Cell-plate formation was disrupted, resulting in binucleate cells, which sometimes

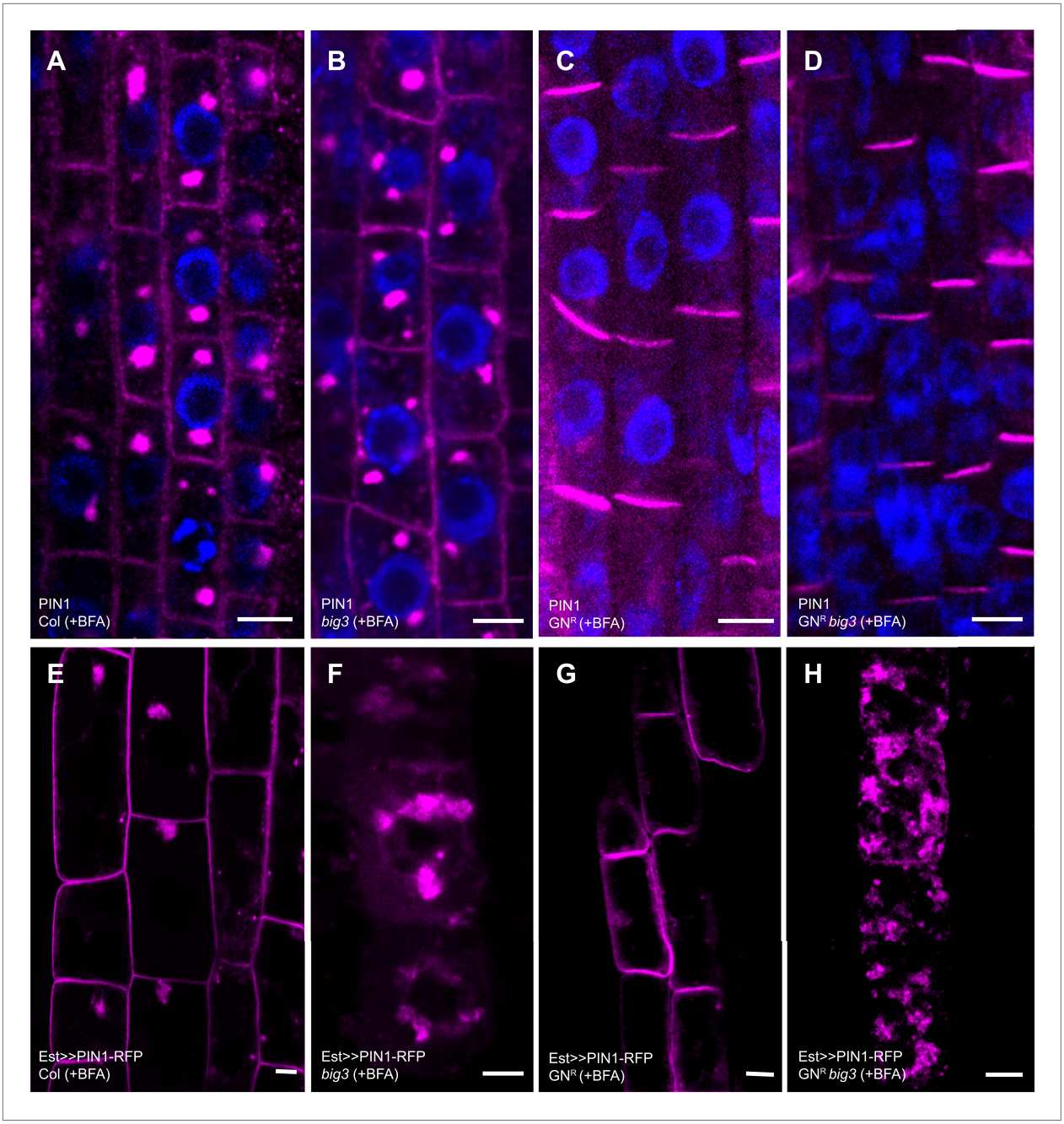

Figure 3. Secretion and recycling to the plasma membrane are regulated by different ARF-GEFs. (**A**–**D**) PIN1 localization in interphase cells of BFA-treated seedlings; apolar at the plasma membrane (PM) and in BFA compartments in wild-type (Col; **A**) and *big3* mutants (**B**); at the basal PM in BFA-resistant GN in wild-type (GN^R, **C**) or *big3* mutant background (GN^R *big3*, **D**). Blue, DAPI-stained nuclei. (**E**–**H**) After BFA treatment, estradiol (Est)-induced PIN1-RFP was trafficked to the PM in wild-type (**E**) and BFA-resistant GN seedlings (GN^R, **G**) but not in *big3* mutants without (**F**) or with expression of BFA-resistant GN (GN^R *big3*; **H**). Scale bars, 5 μm.

DOI: 10.7554/eLife.02131.009

displayed cell-wall stubs (***Figure 5—figure supplement 2A–C***). We used the non-cycling plasma-membrane syntaxin SYP132 expressed from the strong mitosis-specific *KN* promoter as another secretory marker for trafficking to the cell–division plane (***Reichardt et al., 2011***). SYP132 also accumulated, together with KN, in BFA compartments of BFA-treated *big3* mutants, in contrast to BFA-treated wild-type (***Figure 5—figure supplement 1E–J***). We also analysed endocytosed plasma-membrane proteins PEN1 and PIN1 for BFA-sensitive trafficking to the cell plate in *big3* mutants. PEN1 syntaxin involved

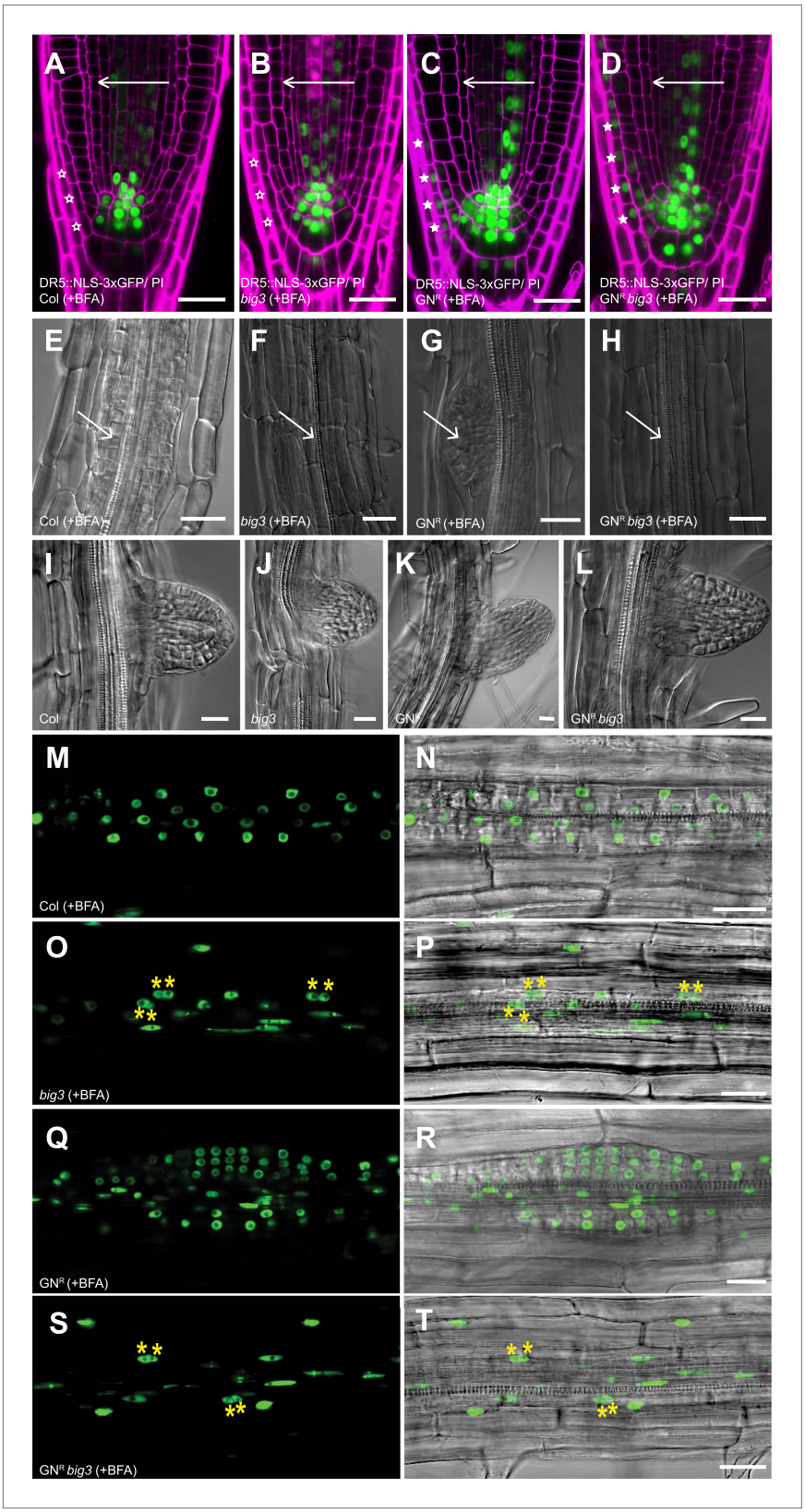

Figure 4. BIG1-4 in response to auxin application. (**A**–**D**) Visualization of auxin distribution by DR5::NLS-3xGFP (green) in BFA-treated seedlings after gravistimulation. Arrows, gravity vector. Cell walls were stained by propidium iodide (PI; magenta). Wild-type (**A**) and *big3* mutant seedling roots (**B**) did not respond to gravity (open asterisks),

Figure 4. Continued on next page

Figure 4. Continued

in contrast to BFA-resistant GN either in wild-type (GN^R, **C**) or *big3* mutant background (GN^R *big3*, **D**). Asterisks, auxin response in epidermal cell layer on lower side (**C** and **D**). (**E**–**H**) NAA and BFA treatment led to proliferation of pericycle cells (arrows) in wild-type (**E**) but not *big3* mutants without (**F**) or with BFA-resistant GN (**H**). Normal lateral root primordia only formed in BFA-resistant GN (GN^R, **G**). Scale bars, 25 μm. (**I**–**L**) Bright-field microcopy of developing lateral root primordia in NAA-treated seedlings; genotypes: wild-type (Col; **I**), *big3* (**J**), BFA-resistant GN (GN^R; **K**) and BFA-resistant GN in *big3* mutant background (GN^R *big3*; **L**). (**M**–**T**) Live imaging of DR5::NLS-3xGFP of seedling roots after NAA and BFA treatment. DR5::NLS-3xGFP signals (left panels **M**, **O**, **Q**, **S**) overlaid with Nomarski images (right panels **N**, **P**, **R**, **T**). Pericycle cells proliferated in wild-type (**M** and **N**) but became binucleate (asterisks) in *big3* (**O** and **P**) and GN^R *big3* (**S** and **T**) mutants. Normal lateral root primordia were only formed in BFA-resistant GN (GN^R; **Q**, **R**) mutant. Scale bars, 25 μm.

DOI: 10.7554/eLife.02131.010

in non-host immunity accumulates at the pathogen entry site by GNOM-dependent relocation following endocytosis from other regions of the plasma membrane (***Collins et al., 2003***; ***Nielsen et al., 2012***). PEN1 continually cycles between plasma membrane and endosomes in interphase and accumulates at the cell plate in cytokinesis (***Reichardt et al., 2011***). To make sure that we were only looking at endocytosed PEN1, PEN1 was expressed from a histone H4 expression cassette that limits protein synthesis to S phase (***Reichardt et al., 2011***). In wild-type, BFA treatment inhibited PEN1 recycling to the plasma membrane but not its trafficking to the cell plate (***Reichardt et al., 2011***; ***Figure 5G–I***). In contrast, in BFA-treated *big3* mutants, endocytosed PEN1 was not trafficked to the cell division plane but accumulated, together with KNOLLE, in BFA compartments (***Figure 5J–L***, asterisks). Endocytosed PIN1 trafficked, like KNOLLE, to the cell plate in BFA-treated wild-type but both PIN1 and KNOLLE were trapped in BFA compartments of *big3* mutants (***Figure 5M–R***). Expression of engineered BFA-resistant GNOM did not overcome the trafficking block to the division plane but rather diverted PIN1 to the basal plasma membrane (***Figure 5S–X***; compare ***Figure 5X*** with ***Figure 5R***). Careful analysis of mitotic cells revealed polar accumulation of PIN1 at the plasma membrane of BFA-resistant GNOM seedling roots throughout mitosis while additional PIN1 accumulates at the forming and expanding cell plate, suggesting that trafficking to the plane of division and polar recycling to the plasma membrane occur simultaneously (***Figure 5—figure supplement 3***). Thus, both endocytosed and newly-synthesized plasma-membrane proteins require secretory ARF-GEF function BIG1-4 for trafficking to the plane of cell division.

Discussion

It is a particularity of Arabidopsis and some other flowering-plant species that the secretory pathway of membrane traffic is comparatively insensitive to BFA treatment whereas endosomal recycling of endocytosed plasma-membrane proteins is rather sensitive (***Geldner et al., 2001***, ***2003***; ***Teh and Moore, 2007***; ***Richter et al., 2007***). The BFA insensitivity of the secretory pathway depends on the BFA resistance of ARF-GEF GNL1, which mediates COPI-vesicle formation in retrograde Golgi-ER traffic (***Teh and Moore, 2007***; ***Richter et al., 2007***), and also requires another BFA-resistant ARF-GEF acting in post-Golgi traffic to the plasma membrane. Here we show that ARF-GEFs BIG1-4 act at the TGN to mediate secretion of newly synthesized proteins to the plasma membrane in interphase but not recycling of endocytosed plasma-membrane proteins, and that BIG3 is BFA-resistant, unlike GNOM involved in recycling to the plasma membrane. Thus, there are two distinct trafficking pathways from the TGN to the plasma membrane in interphase. This is best illustrated by the trafficking of auxin-efflux carrier PIN1 - whereas newly synthesized PIN1 requires BIG1-4 on the late secretory pathway for non-polar delivery to the plasma membrane, polar PIN1 recycling to the basal plasma membrane solely depends on ARF-GEF GNOM (see model in ***Figure 5—figure supplement 4***).

Like newly synthesized proteins, endocytosed proteins are targeted to the division plane during cytokinesis (***Reichardt et al., 2011***). Proteins that cycle between endosomes and the plasma membrane in interphase accumulate, preferentially or even exclusively, at the cell plate (***Reichardt et al., 2011***). In general, recycling to the plasma membrane appears to be switched off during cytokinesis. Here we show that secretory ARF-GEFs BIG1-4 are essential for protein trafficking to the plane of cell division, regardless of proteins being newly synthesized or endocytosed from the plasma membrane (see model in ***Figure 5—figure supplement 4***).

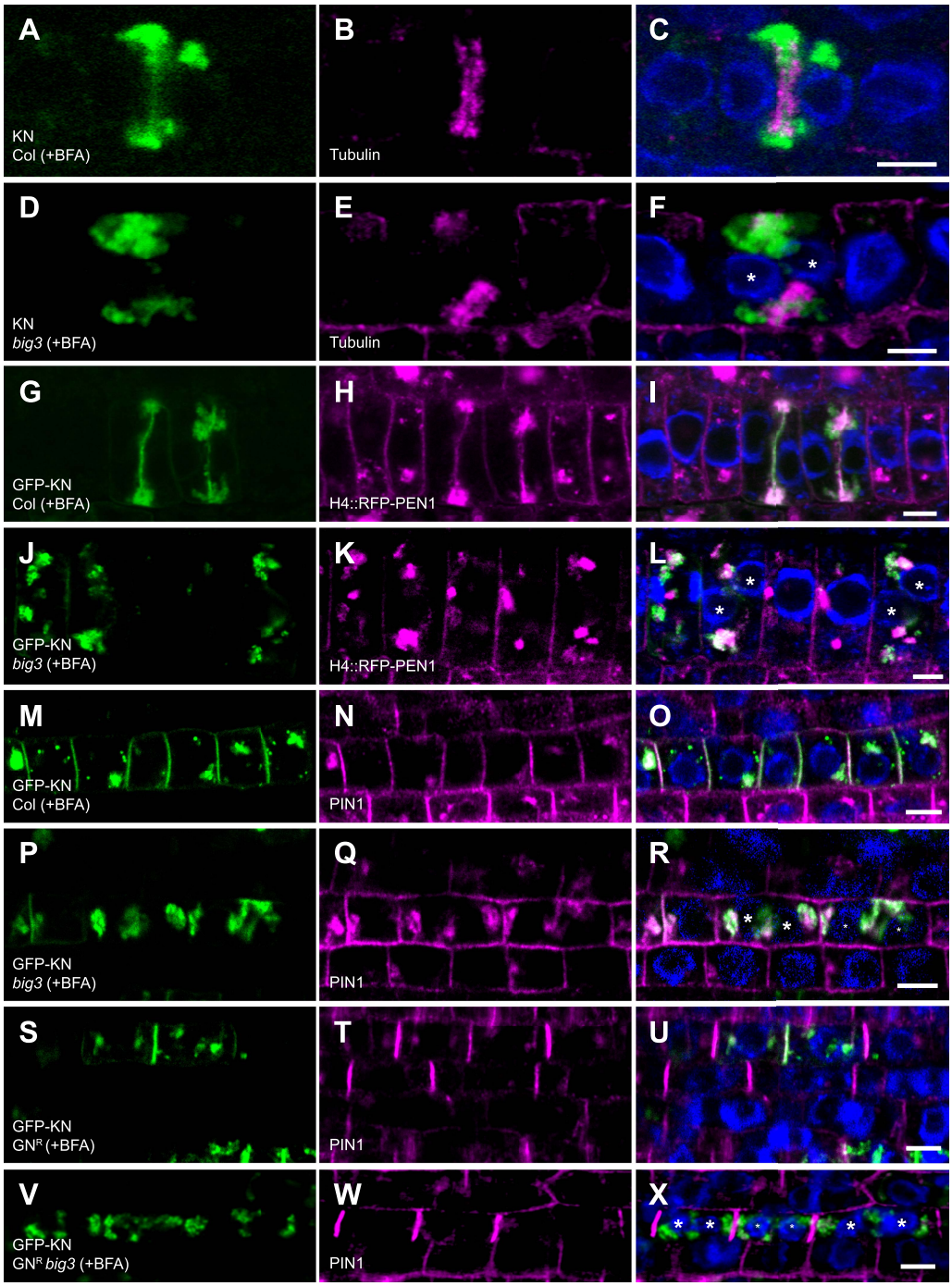

Figure 5. Trafficking to the plane of cell division is mediated by BIG1 – BIG4. (**A**–**F**) Immunolocalization of KNOLLE (KN; **A**, **D**) and tubulin (**B** and **E**) in cytokinetic root cells of BFA-treated seedlings (50 μM for 3 hr). (**A**–**C**) KN was located at the cell plate (**A**) flanked by tubulin-positive phragmoplast (**B**) in wild-type. (**D**–**F**) In *big3* mutants, KN accumulated in BFA compartments separated from tubulin-positive phragmoplast, resulting in a binucleate cell. (**G**–**L**) Co-localization of GFP-tagged KN and endocytosed RFP-PEN1 (H4::RFP-PEN1) in BFA-treated seedlings. KN and PEN1 co-localized at the cell plate and in BFA compartments of wild-type (**G**–**I**) but only in BFA compartments in *big3* mutants (**J**–**L**). (**M**–**X**) Immunostaining of GFP-KN and PIN1 in cytokinetic root cells of BFA-treated seedlings. (**M**–**R**) PIN1 localized apolarly at the plasma membrane (PM) and co-localized with KN in BFA compartments and at the cell plate in wild-type (**M**–**O**) but only in BFA-compartments in *big3* mutants (**P**–**R**). (**S**–**U**) In GN^R, PIN1 localized

Figure 5. Continued on next page

Figure 5. Continued

polarly at the plasma membrane (**T**) and co-localized with KN (**S**) at the cell plate (**U**). (**V**–**X**) Although PIN1 localized polarly at the PM (**W**) in GN^R *big3*, neither PIN1 (**W**) nor KN (**V**) was located at the cell plate. Blue, DAPI-stained nuclei. Asterisks label nuclei of binucleate cells (**F**, **L**, **R**, **X**). Scale bars, 5 μm.

DOI: 10.7554/eLife.02131.011

The following figure supplements are available for figure 5:

Figure supplement 1. BIG4 and cargo proteins trapped in BFA compartments of dividing cells in BFA-treated *big3* mutant seedlings.

DOI: 10.7554/eLife.02131.012

Figure supplement 2. Ultrastructural appearance of cryofixed, freeze-substituted and resin-embedded *big3* seedling root tips treated with BFA.

DOI: 10.7554/eLife.02131.013

Figure supplement 3. PIN1 recycling in mitotic cells.

DOI: 10.7554/eLife.02131.014

Figure supplement 4. Highly schematic model of secretory and recycling trafficking pathways in interphase and cytokinesis.

DOI: 10.7554/eLife.02131.015

Although trafficking to the plane of cell division appears to override recycling of endocytosed proteins to the plasma membrane, we noticed one clear exception—auxin-efflux carrier PIN1, which accumulates polarly at the plasma membrane in interphase and during cell division when both BFA-resistant BIG3 and engineered BFA-resistant GNOM were expressed. Rather than substituting for BIG1-4 in traffic to the plane of cell division, recycling ARF-GEF GNOM appeared to counteract that process by promoting PIN1 recycling to the basal plasma membrane. Of course, the critical question is whether both processes occur at the same time or whether GNOM-dependent PIN1 recycling only sets in after trafficking to the cell plate has come to an end. Although there are no time-course studies, which would be difficult to perform because the process is very fast, detailed analysis of dividing cells at different mitotic stages revealed that polar recycling mediated by BFA-resistant GNOM occurs throughout mitosis and cytokinesis. Furthermore, only in the absence of both BFA-resistant BIG3 and BFA-resistant GNOM is PIN1 trapped in BFA compartments. If then BFA-resistant GNOM is expressed PIN1 is not delivered to the plane of division but rather polarly recycled to the plasma membrane, again suggesting that the latter pathway is a direct route bypassing the cell plate. PIN1 might be exceptional because continuous recycling of PIN1 is required for maintaining the polar transport of auxin across tissues (***Geldner et al., 2003***). If PIN1 recycling were shut down during cytokinesis this would disrupt the polar auxin transport required in specific developmental situations such as forming lateral root primordia when essentially all cells proliferate (***Geldner et al., 2004***). Another problem in auxin flow arises from cell division when the partitioning membrane has physically separated the two daughter cells: one daughter suddenly has PIN1 located at opposite ends. Obviously, PIN1 has to be removed from the wrong end in order to sustain polar auxin transport. This seems to be a fast process and has been studied for the related auxin-efflux carrier PIN2 in detail (***Men et al., 2008***).

Animal and plant cytokinesis differ in the way the partitioning membrane is laid down. In animals, secretory and recycling pathways contribute to the ingrowth of the plasma membrane mediated by a contractile actomyosin ring and to the subsequent abscission of the daughter cells (***Schiel and Prekeris, 2013***). In plants, a massive flow of membrane vesicles from TGN/early endosome to the plane of cell division sustains, by fusion, the rapid formation and outward expansion of the partitioning cell plate (***Samuels et al., 1995***). This process is orchestrated by a specialised cytoskeletal array termed phragmoplast that delivers those membrane vesicles to the division plane. Phragmoplast-assisted trafficking might be required for completing the partitioning membrane on time, in the absence of a cytokinesis-interphase checkpoint, and would thus effectively rule out recycling of endocytosed proteins to the plasma membrane. However, our results make clear that this is not the case because recycling to the plasma membrane is not switched off during cytokinesis. Rather, endocytosed proteins enter the late-secretory pathway to reach the division plane at the expense of being recycled to the plasma membrane, which requires the late-secretory ARF-GEFs BIG1-4. In conclusion, our results raise the possibility that in general, different ARF-GEFs have different specificity of action during vesicle formation such that the same cargo protein can be delivered to different destinations.

Materials and methods

Plant material and growth conditions

Plants were grown on soil or agar plates in growth chambers under continuous light conditions at 23°C. *big* mutant lines: *big1* (GK-452B06) and *big2* (GK-074F08) T-DNA lines were from GABI-KAT (http://www.gabi-kat.de), *big3* (SALK_044617) and *big4* (SALK_069870) T-DNA lines from the SALK collection (http://signal.salk.edu/cgi-bin/tdnaexpress). *big3* mutant lines were selected on MS plates using kanamycin.

The following transgenic marker lines were used: H4::RFP-PEN1 (**Reichardt et al., 2011**) (expressed from *HISTONE4* (*H4*) promoter during S phase), KN::Myc-SYP132 (**Reichardt et al., 2011**) (expressed during lateG2/M phase), HS::secGFP (**Viotti et al., 2010**) (expressed from heat shock promoter), GFP-KN (**Reichardt et al., 2007**), BOR1-GFP (**Takano et al., 2005**), DR5::NLS-3xGFP (**Weijers et al., 2006**), VHA-a1-RFP (**Viotti et al., 2010**), AP1M2-3xHA (**Park et al., 2013**).

T-DNA genotyping of *big* mutant lines

Primers used to test for *big1* heterozygosity:
5′GCAAGATCAGGGAAGACG 3′ and 5′ACCAGAGGAAGGTGCTTCTTC 3′
Primers used to test for *big1* homozygosity:
5′TCGTCCCATCTTCTTCATTTG 3′ and 5′ACCAGAGGAAGGTGCTTCTTC 3
Primers used to test for *big2* heterozygosity:
5′GCAAGATCAGGGAAGACG 3′ and 5′TTGAGGGGTTCATATGACAGC 3′
Primers used to test for *big2* homozygosity:
5′TTTCCCACTTTTTCCACTGTG 3′ and 5′TTGAGGGGTTCATATGACAGC 3′
Primers used to test for *big3* heterozygosity:
5′AAACTCTCCACTGGCTAAGCC 3′ and 5′ATTTTGCCGATTTCGGAAC 3′
Primers used to test for *big3* homozygosity:
5′AAACTCTCCACTGGCTAAGCC 3′ and 5′GCAAGTTTTCTTGCGCAATAC 3′
Primers used to test for *big4* heterozygosity:
5′ATTTTGCCGATTTCGGAAC 3′ and 5′CTATCTTGCGCTGGAGACAAC 3′
Primers used to test for *big4* homozygosity:
5′TCCTCTTCAAACTCGTCAACG 3′ and 5′CTATCTTGCGCTGGAGACAAC 3′

Generating transgenic plants

Genomic BIG4 was amplified and introduced into pDONR221 (Invitrogen, Darmstadt, Germany) and afterwards into *UBQ10::YFP* destination vector (**Grefen et al., 2010**). For generation of BFA-resistant *UBQ10::BIG4^{R}-YFP*, methionine at position 695 was exchanged with leucine by site-directed mutagenesis. *BIG3* promoter was amplified and introduced into pUC57L4 via *Kpn*I and *Sma*I restriction sites. Multistep gateway cloning was performed using pUC57L4-*BIG3*-promoter, pEntry221-*BIG4* and R4pGWB553 (**Nakagawa et al., 2008**) yielding *BIG3::BIG4-RFP*. Cloning the CDS from *BIG3* into pGREENII via *Apa*I and *Sma*I restriction sites generated pGII-*BIG3*. The 1 kb *BIG3* promoter was amplified and introduced into pGII-*BIG3* via *Apa*I. 1 kb of 3′UTR was amplified and introduced into pGII-*BIG3::BIG3* via *Sma*I and *Spe*I. C-terminal YFP was inserted via *Sma*I and *Spe*I. *AFVY-RFP* was amplified from *35S::AFVY-RFP* (**Scheuring et al., 2011**) and introduced into pDONR221 (Invitrogen) generating a pEntry clone. Afterwards, LR reaction was performed introducing *AFVY-RFP* into the estradiol-inducible destination vector pMDC7 (**Curtis and Grossniklaus, 2003**). *PIN1* cDNA was cloned into pGem-T (Promega, Mannheim, Germany). *RFP* was inserted in *PIN1* via the *Xho*I site. *PIN1-RFP* was amplified and introduced first into pDONR221 and then into pMDC7. *YFP-SYP132* was amplified and introduced into pDONR221 and then into pMDC7.

All constructs were transformed into *big3* mutants and BFA-resistant GN (GN^{R}) in *big3* mutant background. T1 plants of *UBQ10::BIG4-YFP*, *UBQ10::BIG4^{R}-YFP* and *BIG3-YFP* were selected by spraying with Basta. T1 seeds of estradiol-inducible lines and *BIG3::BIG4-RFP* were selected with hygromycin. Experiments were performed using T2 or T3 seedlings. At least three independent lines were analysed.

Immunofluorescence localization and live imaging in seedling roots

5 days old seedlings were incubated in 1 ml liquid growth medium (0.5x MS medium, 1% sucrose, pH 5.8) containing 50 μM BFA (Invitrogen, Molecular Probes) for 1 hr or 3 hr at room temperature in 24-well

cell-culture plates. Seedlings treated with 50 μM BFA for (a) 1 hr or (b) 3 hr, respectively, were used for the following immunolocalisation studies: (a) AP1M2 vs γCOP, AP1M2 vs SYP61, PIN1; (b) KNOLLE vs Tubulin, KNOLLE vs PIN1, H4::RFP-PEN1 vs GFP-KN and KN::Myc-SYP132 vs KN. Incubation was stopped by fixation with 4% paraformaldehyde in MTSB. Immunofluorescence staining was performed as described (***Lauber et al., 1997***) or with an InsituPro machine (Intavis, Cologne, Germany) (***Müller et al., 1998***).

Antibodies used: mouse anti-MYC (Santa Cruz Biotechnology, Heidelberg, Germany) 1:600, mouse anti-HA 1:1000 (BAbCO, Richmond, CA, USA), rat anti-tubulin 1:600 (Abcam, Cambridge, UK), rabbit anti-PIN1 1:1000 (***Geldner et al., 2001***), rabbit anti-γCOP 1:1000 (Agrisera, Vännäs, Sweden), rabbit anti-KNOLLE 1:2000 (***Reichardt et al., 2007***) and rabbit anti-SYP61 1:700 (***Park et al., 2013***). Alexa-488 or Cy3-conjugated secondary antibodies (Dianova, Hamburg, Germany) were diluted 1:600.

Live-cell imaging was performed with 2 μM FM4-64 or FM1-43 (Invitrogen, Molecular Probes) or propidium iodide (10 μg/ml).

Estradiol induction was performed using 10 or 20 μM estradiol. BFA incubation (25 μM) was done together with estradiol for 6 hr.

Heat-shock inducible secGFP (HS::secGFP) lines were first incubated for 30 min at 37°C in MS at pH8.1. BFA treatment (50 μM) in MS at pH8.1 followed for 4 hr at plant room conditions.

Analysis of BOR1 degradation was performed according to ***Takano et al. (2005)*** . In addition, we treated the seedlings with BFA, 5 μM, for 1 hr together with boron.

Electron microscopy

For ultrastructural analysis, root tips were high-pressure frozen (Bal-Tec HPM010; Balzers) in hexadecene (Merck Sharp and Dohme, Haar, Germany), freeze-substituted in acetone containing 2.5% osmium tetroxide, washed at 0°C with acetone, and embedded in Epon. For immunogold labeling of ultrathin thawed cryosections, root tips were fixed with 8% formaldehyde (2 hr), embedded in gelatin, and infiltrated with 2.1 M sucrose in PBS as previously described (***Dettmer et al., 2006***). Thawed ultrathin sections were labeled with rabbit anti-GFP antibodies (1:300; Abcam) and silver-enhanced (HQ Silver, 8 min; Nanoprobes, Yaphank, NY, USA) goat anti-rabbit IgG coupled to Nanogold (no. 2004; Nanoprobes). Antibodies and markers were diluted in blocking buffer (PBS supplemented with 0.5% BSA and 1% milk powder).

Acquisition and processing of fluorescence images

Fluorescence images were acquired at 512 × 512 or 512 × 256 pixels with the confocal laser scanning microscope TCS-SP2 or TCS-SP8 from Leica, using the 63x water-immersion objective and Leica software. All images were processed with Adobe Photoshop CS3 only for adjustment of contrast and brightness. Intensity line profile was performed with Leica software.

Pollen germination

Pollen medium was prepared as described (***Boavida and McCormick, 2007***). Pollen germinated over night or for 5 hr before microscopic analysis.

Physiological tests

To investigate primary root growth, 5–6 days old seedlings were transferred to plates with 10 μM BFA and analysed after 5–7 additional days using ImageJ. DR5::NLS-GFP expressing seedlings analysed for lateral root formation were treated with 5 μM NAA or 5 μM NAA plus 10 μM BFA over night. Roots were cleared according to ***Geldner et al. (2004)***. Gravitropic response was investigated by transferring 5 days old seedlings, expressing DR5::NLS-GFP, to BFA plates (5 μM). Seedlings were grown vertically for 1 hr on BFA plates before rotated by 135° for 4 hr.

For analysis of seed germination, seeds were sown out on MS medium containing 5 μM BFA. Images were taken after 5 days of growth.

Phylogenetic tree

Full-length protein sequence of BIG3 was used to search for related sequences from different plant species with sequenced genomes that are available at the phytozome homepage (http://www.phytozome.net/). ARF-GEFs from different species were aligned by ClustalW (www.ebi.ac.uk/clustalw) and the phylogenetic tree was drawn with Dendroscope (***Huson et al., 2007***).

Acknowledgements

We thank Lukas Sonnenberg and Marlene Ballbach for technical assistance, Toru Fujiwara, Niko Geldner, Christopher Grefen, Ueli Grossniklaus, Sumie Ishiguru, Peter Pimpl, Masao H. Sato and Karin Schumacher for sharing published materials, Joop Vermeer (Univ. Lausanne) for cloning vector pUC57L4, and NASC for T-DNA insertion lines. We also thank Martin Bayer, Niko Geldner, Christopher Grefen, Michael Hothorn and Steffen Lau for critical reading of the manuscript.

Additional information

Funding

Funder	Grant reference number	Author
German Research Foundation (DFG)	SFB446/TP A9	Gerd Jürgens
German Research Foundation (DFG)	JU 179/18-1	Gerd Jürgens
Carlsberg Foundation	2011_01_0789	Mads Eggert Nielsen

The funders had no role in study design, data collection and interpretation, or the decision to submit the work for publication.

Author contributions

SR, Conception and design, Acquisition of data, Analysis and interpretation of data, Drafting or revising the article; MK, MEN, MP, RG, CK, UV, HB, UM, Y-DS, Acquisition of data, Analysis and interpretation of data; SB, Analysis and interpretation of data, Drafting or revising the article; GJ, Conception and design, Analysis and interpretation of data, Drafting or revising the article

Additional files

Supplementary files

• Supplementary file 1. Localization of vesicle trafficking markers. This table summarizes the localization of different vesicle trafficking markers without BFA (1th column) and with BFA in wild-type (Col; 2th column), *big3* (3th column), BFA-resistant GNOM (GN^R; 4th column) and BFA-resistant GNOM in *big3* mutant background (GN^R *big3*; 5th column). Abbreviations: PM, plasma membrane; CP, cell plate; BFA-comp., BFA-compartment.

DOI: 10.7554/eLife.02131.016

References

Boavida LC, McCormick S. 2007. Temperature as a determinant factor for increased and reproducible in vitro pollen germination in *Arabidopsis thaliana*. *Plant Journal* **52**:570–582. doi: 10.1111/j.1365-313X.2007.03248.x.

Casanova JE. 2007. Regulation of Arf activation: the Sec7 family of guanine nucleotide exchange factors. *Traffic* **8**:1476–1485. doi: 10.1111/j.1600-0854.2007.00634.x.

Collins NC, Thordal-Christensen H, Lipka V, Bau S, Kombrink E, Qiu JL, Hückelhoven R, Stein M, Freialdenhoven A, Somerville SC, Schulze-Lefert P. 2003. SNARE-protein-mediated disease resistance at the plant cell wall. *Nature* **425**:973–977. doi: 10.1038/nature02076.

Cox R, Mason-Gamer RJ, Jackson CL, Segev N. 2004. Phylogenetic analysis of Sec7-domain-containing Arf nucleotide exchangers. *Molecular Biology of the Cell* **15**:1487–1505. doi: 10.1091/mbc.E03-06-0443.

Curtis MD, Grossniklaus U. 2003. A gateway cloning vector set for high-throughput functional analysis of genes in planta. *Plant Physiology* **133**:462–469. doi: 10.1104/pp.103.027979.

Dettmer J, Hong-Hermesdorf A, Stierhof YD, Schumacher K. 2006. Vacuolar H^+-ATPase activity is required for endocytic and secretory trafficking in Arabidopsis. *Plant Cell* **18**:715–730. doi: 10.1105/tpc.105.037978.

Geldner N, Anders N, Wolters H, Keicher J, Kornberger W, Muller P, Delbarre A, Ueda T, Nakano A, Jürgens G. 2003. The Arabidopsis GNOM ARF-GEF mediates endosomal recycling, auxin transport, and auxin-dependent plant growth. *Cell* **112**:219–230. doi: 10.1016/S0092-8674(03)00003-5.

Geldner N, Dénervaud-Tendon V, Hyman DL, Mayer U, Stierhof YD, Chory J. 2009. Rapid, combinatorial analysis of membrane compartments in intact plants with a multicolor marker set. *Plant Journal* **59**:169–178. doi: 10.1111/j.1365-313X.2009.03851.x.

Geldner N, Friml J, Stierhof YD, Jürgens G, Palme K. 2001. Auxin transport inhibitors block PIN1 cycling and vesicle trafficking. *Nature* **413**:425–428. doi: 10.1038/35096571.

Geldner N, Richter S, Vieten A, Marquardt S, Torres-Ruiz RA, Mayer U, Jürgens G. 2004. Partial loss-of-function alleles reveal a role for GNOM in auxin transport-related, post-embryonic development of Arabidopsis. *Development* **131**:389–400. doi: 10.1242/dev.00926.

Grefen C, Donald N, Hashimoto K, Kudla J, Schumacher K, Blatt MR. 2010. A ubiquitin-10 promoter-based vector set for fluorescent protein tagging facilitates temporal stability and native protein distribution in transient and stable expression studies. *Plant Journal* **64**:355–365. doi: 10.1111/j.1365-313X.2010.04322.x.

Huson DH, Richter DC, Rausch C, Dezulian T, Franz M, Rupp R. 2007. Dendroscope: an interactive viewer for large phylogenetic trees. *BMC Bioinformatics* **8**:460. doi: 10.1186/1471-2105-8-460.

Lauber MH, Waizenegger I, Steinmann T, Schwarz H, Mayer U, Hwang I, Lukowitz W, Jürgens G. 1997. The Arabidopsis KNOLLE protein is a cytokinesis-specific syntaxin. *Journal of Cell Biology* **139**:1485–1493. doi: 10.1083/jcb.139.6.1485.

Men S, Boutté Y, Ikeda Y, Li X, Palme K, Stierhof YD, Hartmann MA, Moritz T, Grebe M. 2008. Sterol-dependent endocytosis mediates post-cytokinetic acquisition of PIN2 auxin efflux carrier polarity. *Nature Cell Biology* **10**:237–244. doi: 10.1038/ncb1686.

Movafeghi A, Happel N, Pimpl P, Tai GH, Robinson DG. 1999. Arabidopsis Sec21p and Sec23p homologs. Probable coat proteins of plant COP-coated vesicles. *Plant Physiol* **119**:1437–1446. doi: 10.1104/pp.119.4.1437.

Müller A, Guan C, Gälweiler L, Tänzler P, Huijser P, Marchant A, Parry G, Bennett M, Wisman E, Palme K. 1998. AtPIN2 defines a locus of Arabidopsis for root gravitropism control. *The EMBO Journal* **17**:6903–6911. doi: 10.1093/emboj/17.23.6903.

Nakagawa T, Nakamura S, Tanaka K, Kawamukai M, Suzuki T, Nakamura K, Kimura T, Ishiguro S. 2008. Development of R4 gateway binary vectors (R4pGWB) enabling high-throughput promoter swapping for plant research. *Bioscience Biotechnology and Biochemistry* **72**:624–629. doi: 10.1271/bbb.70678.

Nielsen M, Albrethsen J, Larsen F, Skriver K. 2006. The Arabidopsis ADP-ribosylation factor (ARF) and ARF-like (ARL) system and its regulation by BIG2, a large ARF-GEF. *Plant Science* **171**:707–717. doi: 10.1016/j.plantsci.2006.07.002.

Nielsen ME, Feechan A, Bohlenius H, Ueda T, Thordal-Christensen H. 2012. Arabidopsis ARF-GTP exchange factor, GNOM, mediates transport required for innate immunity and focal accumulation of syntaxin PEN1. *Proceedings of the National Academy of Sciences of the United States of America* **109**:11443–11448. doi: 10.1073/pnas.1117596109.

Nomura K, Debroy S, Lee YH, Pumplin N, Jones J, He SY. 2006. A bacterial virulence protein suppresses host innate immunity to cause plant disease. *Science* **313**:220–223. doi: 10.1126/science.1129523.

Nomura K, Mecey C, Lee YN, Imboden LA, Chang JH, He SY. 2011. Effector-triggered immunity blocks pathogen degradation of an immunity-associated vesicle traffic regulator in Arabidopsis. *Proceedings of the National Academy of Sciences of the United States of America* **108**:10774–10779. doi: 10.1073/pnas.1103338108.

Park M, Song K, Reichardt I, Kim H, Mayer U, Stierhof YD, Hwang I, Jürgens G. 2013. Arabidopsis mu-adaptin subunit AP1M of adaptor protein complex 1 mediates late secretory and vacuolar traffic and is required for growth. *Proceedings of the National Academy of Sciences of the United States of America* **110**:10318–10323. doi: 10.1073/pnas.1300460110.

Reichardt I, Slane D, El Kasmi F, Knöll C, Fuchs R, Mayer U, Lipka V, Jürgens G. 2011. Mechanisms of functional specificity among plasma-membrane syntaxins in Arabidopsis. *Traffic* **12**:1269–1280. doi: 10.1111/j.1600-0854.2011.01222.x.

Reichardt I, Stierhof YD, Mayer U, Richter S, Schwarz H, Schumacher K, Jürgens G. 2007. Plant cytokinesis requires de novo secretory trafficking but not endocytosis. *Current Biology* **17**:2047–2053. doi: 10.1016/j.cub.2007.10.040.

Reyes FC, Buono R, Otegui MS. 2011. Plant endosomal trafficking pathways. *Current Opinion In Cell Biology* **14**:666–673. doi: 10.1016/j.pbi.2011.07.009.

Richter S, Geldner N, Schrader J, Wolters H, Stierhof YD, Rios G, Koncz C, Robinson DG, Jürgens G. 2007. Functional diversification of closely related ARF-GEFs in protein secretion and recycling. *Nature* **448**:488–492. doi: 10.1038/nature05967.

Richter S, Müller LM, Stierhof YD, Mayer U, Takada N, Kost B, Vieten A, Geldner N, Koncz C, Jürgens G. 2012. Polarized cell growth in Arabidopsis requires endosomal recycling mediated by GBF1-related ARF exchange factors. *Nature Cell Biology* **14**:80–86. doi: 10.1038/ncb2389.

Robinson MS. 2004. Adaptable adaptors for coated vesicles. *Trends in Cell Biology* **14**:167–174. doi: 10.1016/j.tcb.2004.02.002.

Samuels AL, Giddings TH Jnr, Staehelin LA. 1995. Cytokinesis in tobacco BY-2 and root tip cells: a new model of cell plate formation in higher plants. *Journal of Cell Biology* **130**:1345–1357. doi: 10.1083/jcb.130.6.1345.

Scheuring D, Viotti C, Krüger F, Künzl F, Sturm S, Bubeck J, Hillmer S, Frigerio L, Robinson DG, Pimpl P, Schumacher K. 2011. Multivesicular bodies mature from the trans-Golgi network/early endosome in Arabidopsis. *Plant Cell* **23**:3463–3481. doi: 10.1105/tpc.111.086918.

Schiel JA, Prekeris R. 2013. Membrane dynamics during cytokinesis. *Current Opinion In Cell Biology* **25**:92–98. doi: 10.1016/j.ceb.2012.10.012.

Schmid M, Davison TS, Henz SR, Pape UJ, Demar M, Vingron M, Schölkopf B, Weigel D, Lohmann JU. 2005. A gene expression map of *Arabidopsis thaliana* development. *Nature Genetics* **37**:501–506. doi: 10.1038/ng1543.

Stierhof YD, El Kasmi F. 2010. Strategies to improve the antigenicity, ultrastructure preservation and visibility of trafficking compartments in Arabidopsis tissue. *European Journal of Cell Biology* **89**:285–297. doi: 10.1016/j.ejcb.2009.12.003.

Surpin M, Raikhel N. 2004. Traffic jams affect plant development and signal transduction. *Nature Reviews Molecular Cell Biology* **5**:100–109. doi: 10.1038/nrm1311.

Tanaka H, Kitakura S, De Rycke R, De Groodt R, Friml J. 2009. Fluorescence imaging-based screen identifies ARF GEF component of early endosomal trafficking. *Current Biology* **19**:391–397. doi: 10.1016/j.cub.2009.01.057.

Tanaka H, Kitakura S, Rakusová H, Uemura T, Feraru MI, De Rycke R, Robert S, Kakimoto T, Friml J. 2013. Cell polarity and patterning by PIN trafficking through early endosomal compartments in *Arabidopsis thaliana*. *PLOS Genetics* **9**:e1003540. doi: 10.1371/journal.pgen.1003540.

Takano J, Miwa K, Yuan L, von Wiren N, Fujiwara T. 2005. Endocytosis and degradation of BOR1, a boron transporter of *Arabidopsis thaliana*, regulated by boron availability. *Proceedings of the National Academy of Sciences of the United States of America* **102**:12276–12281. doi: 10.1073/pnas.0502060102.

Teh OK, Moore I. 2007. An ARF-GEF acting at the Golgi and in selective endocytosis in polarized plant cells. *Nature* **448**:493–496. doi: 10.1038/nature06023.

Teh OK, Shimono Y, Shirakawa M, Fukao Y, Tamura K, Shimada T, Hara-Nishimura I. 2013. The AP-1 mu adaptin is required for KNOLLE localization at the cell plate to mediate cytokinesis in Arabidopsis. *Plant and Cell Physiology* **54**:838–847. doi: 10.1093/pcp/pct048.

Ueda T, Yamaguchi M, Uchimiya H, Nakano A. 2001. Ara6, a plant-unique novel type Rab GTPase, functions in the endocytic pathway of *Arabidopsis thaliana*. *The EMBO Journal* **20**:4730–4741. doi: 10.1093/emboj/20.17.4730.

Viotti C, Bubeck J, Stierhof YD, Krebs M, Langhans M, van den Berg W, van Dongen W, Richter S, Geldner N, Takano J, Jürgens G, de Vries SC, Robinson DG, Schumacher K. 2010. Endocytic and secretory traffic in Arabidopsis merge in the trans-Golgi network/early endosome, an independent and highly dynamic organelle. *Plant Cell* **22**:1344–1357. doi: 10.1105/tpc.109.072637.

Wang JG, Li S, Zhao XY, Zhou LZ, Huang GQ, Feng C, Zhang Y. 2013. HAPLESS13, the Arabidopsis mu1 adaptin, is essential for protein sorting at the trans-Golgi Network/early endosome. *Plant Physiology* **162**:1897–1910. doi: 10.1104/pp.113.221051.

Weijers D, Schlereth A, Ehrismann JS, Schwank G, Kientz M, Jürgens G. 2006. Auxin triggers transient local signaling for cell specification in *Arabidopsis embryogenesis*. *Developmental Cell* **10**:265–270. doi: 10.1016/j.devcel.2005.12.001.

Marker	- BFA	Col + BFA	*big3* + BFA	GN^R + BFA	GN^R *big3* + BFA
HS::secGFP	apoplast (Viotti et al., 2010)	apoplast	intracellular aggregate	-	-
Est>>YFP-SYP132	PM (this study)	PM	intracellular aggregate	-	-
Est>>AFVY-RFP	vacuole (this study)	vacuole	intracellular aggregate	-	-
BOR1-GFP	PM (Takano et al., 2005)	PM + BFA-comp.	intracellular aggregate	-	-
AP1M2-3xHA	TGN (Park et al., 2013)	BFA-comp.	cytosolic	-	-
γCOP	Golgi (Richter at al., 2007)	Golgi	Golgi	-	-
PIN1 (interphase)	basal PM (Geldner at al., 2001)	PM + BFA-comp.	PM + BFA-comp.	basal PM	basal PM
PIN1 (cytokinesis)	basal PM+CP (Geldner at al., 2001)	PM + CP+BFA-comp.	PM+intracellular aggegate	PM + CP+BFA-comp.	PM+intracellular aggegate
Est>>PIN1-RFP	basal PM (this study)	PM + BFA-comp.	intracellular aggregate	basal PM	intracellular aggregate
KNOLLE	CP (Lauber at al., 1997)	CP + BFA-comp.	intracellular aggregate	CP + BFA-comp.	intracellular aggregate
H4::RFP-PEN1	PM+CP (Reichardt et al., 2011)	PM+CP+BFA-comp.	PM+intracellular aggegate	-	-
KN::MYC-SYP132	PM+CP (Reichardt et al., 2011)	PM+CP	PM+intracellular aggegate	-	-

Supplementary Table 1. Localization of vesicle trafficking markers.
This table summarizes the localization of different vesicle trafficking markers without BFA (1th column) and with BFA in wild-type (Col; 2th column), *big3* (3th column), BFA-resistant GNOM (GN^R; 4th column) and BFA-resistant GNOM in *big3* mutant background (GN^R *big3*; 5th column). Abbreviations: PM, plasma membrane; CP, cell plate; BFA-comp., BFA-compartment.

5.2 Singh et al., 2014

Protein Delivery to Vacuole Requires SAND Protein-Dependent Rab GTPase Conversion for MVB-Vacuole Fusion

Manoj K. Singh, Falco Krüger, Hauke Beckmann, Sabine Brumm, Joop E.M. Vermeer, Teun Munnik, Ulrike Mayer, York-Dieter Stierhof, Christopher Grefen, Karin Schumacher, Gerd Jürgens

Current Biology Volume 24, Issue 12, 16 June 2014, Pages 1383–1389

Current Biology 24, 1383–1389, June 16, 2014 ©2014 Elsevier Ltd All rights reserved http://dx.doi.org/10.1016/j.cub.2014.05.005

Report

Protein Delivery to Vacuole Requires SAND Protein-Dependent Rab GTPase Conversion for MVB-Vacuole Fusion

Manoj K. Singh,[1] Falco Krüger,[2] Hauke Beckmann,[1] Sabine Brumm,[1] Joop E.M. Vermeer,[3,5] Teun Munnik,[3] Ulrike Mayer,[4] York-Dieter Stierhof,[4] Christopher Grefen,[1] Karin Schumacher,[2] and Gerd Jürgens[1,*]

[1]Center for Plant Molecular Biology (ZMBP), Developmental Genetics, University of Tübingen, Auf der Morgenstelle 32, 72076 Tübingen, Germany

[2]Center for Organismal Studies (COS), University of Heidelberg, 69120 Heidelberg, Germany

[3]Section Plant Physiology, University of Amsterdam, Swammerdam Institute for Life Sciences, 1098 SM, Amsterdam, the Netherlands

[4]Center for Plant Molecular Biology (ZMBP), Microscopy, University of Tübingen, 72076 Tübingen, Germany

Summary

Plasma-membrane proteins such as ligand-binding receptor kinases, ion channels, or nutrient transporters are turned over by targeting to a lytic compartment—lysosome or vacuole—for degradation. After their internalization, these proteins arrive at an early endosome, which then matures into a late endosome with intraluminal vesicles (multivesicular body, MVB) before fusing with the lysosome/vacuole in animals or yeast [1, 2]. The endosomal maturation step involves a SAND family protein mediating Rab5-to-Rab7 GTPase conversion [3]. Vacuolar trafficking is much less well understood in plants [4–6]. Here we analyze the role of the single-copy *SAND* gene of *Arabidopsis*. In contrast to its animal or yeast counterpart, *Arabidopsis* SAND protein is not required for early-to-late endosomal maturation, although its role in mediating Rab5-to-Rab7 conversion is conserved. Instead, *Arabidopsis* SAND protein is essential for the subsequent fusion of MVBs with the vacuole. The inability of *sand* mutant to mediate MVB-vacuole fusion is not caused by the continued Rab5 activity but rather reflects the failure to activate Rab7. In conclusion, regarding the endosomal passage of cargo proteins for degradation, a major difference between plants and nonplant organisms might result from the relative timing of endosomal maturation and SAND-dependent Rab GTPase conversion as a prerequisite for the fusion of late endosomes/MVBs with the lysosome/vacuole.

Results and Discussion

Endocytosis is crucial in controlling the plasma-membrane protein repertoire in all eukaryotic cells. Membrane proteins such as cell-surface receptors are delivered to the lumen of the lytic compartment (lysosome or vacuole) for degradation. On their way, proteins endocytosed from the plasma membrane successively pass through the early endosome (EE) and the late endosome (LE) before reaching the lytic compartment (vacuole/lysosome). Recent evidence suggests that early endosomes mature into late endosomes containing intraluminal vesicles—so-called multivesicular bodies (MVBs)—through a process of Rab GTPase conversion [7]. This process involves Mon1/SAND protein, which together with CCZ1 acts as a guanine-nucleotide exchange factor (GEF) on Rab7-type GTPases that also inactivates Rab5-type GTPases [1, 3, 8, 9].

The lack of an independent early endosome (EE) is a distinguishing feature of the plant endomembrane system [10, 11]. In plants, the trans-Golgi network (TGN) is the first compartment reached by endocytic cargo and is thus at the crossroads of the secretory and endocytic routes [12]. Importantly, Rab5-like GTPases as well as phosphatidylinositol-3-phosphate (PI3P), hallmarks of yeast and animal early endosomes, are largely absent from the plant TGN/EE [13, 14]. Nevertheless, it has recently been proposed that MVBs mature from the TGN/EE [15] and we have thus investigated whether the single-copy *Arabidopsis SAND* gene is involved in TGN/EE-to-MVB maturation and/or whether it plays a role in mediating Rab5-to-Rab7 conversion.

Endosomal maturation from TGN/EE to MVB was examined in *Arabidopsis* seedling root cells, via pairwise colabeling of three marker proteins: TGN/EE-localized subunit a1 of V-ATPase (VHA-a1) [10], Rab5-like GTPase ARA7 (aka RABF2b) [13], and the fluorescent PI3P sensor YFP-2xFYVE [14]. In line with previous findings, colocalization between VHA-a1 and ARA7 was generally low as ARA7 mostly accumulated at the MVB [10, 16]. However, ARA7 also marked a subdomain of the VHA-a1-positive TGN/EE (Figure 1A). The dual localization of ARA7 to TGN/EE and MVB has also been observed in EM images of immunolabeled cryosections [13]. In contrast, 2xFYVE was separate from, but often abutted, the TGN/EE (Figure 1B). ARA7 was mostly colocalized with 2xFYVE, which labeled an additional subpopulation of endosomes devoid of ARA7 (Figure 1C). Upon BFA treatment, which causes aggregation of TGN/EEs into "BFA compartments" that do not include MVBs [16], some ARA7 colocalized with VHA-a1 in BFA compartments although the majority of the ARA7 signal still gave a distinct punctate pattern (Figure 1D). In contrast, the 2xFYVE signal was not altered such that the BFA compartments were exclusively ARA7 positive in double-labeled root cells (Figure 1E). Taken together, these results suggest that endosomal maturation in *Arabidopsis* appears to originate in a subdomain of the TGN/EE that recruits Rab5-like ARA7 and subsequently matures into an MVB, and this transition is accompanied by the accumulation of PI3P (Figure 1F). This conclusion is supported by ultrastructural studies indicating MVB formation on Golgi-associated tubular-vesicular structures, the local presence of ESCRT proteins on TGN/EE, and the strong reduction in the number of MVBs observed after inhibition of the V-ATPase in the TGN/EE [15].

The *Arabidopsis* genome harbors a single-copy *SAND* gene encoding a member of the eukaryotic SAND/Mon1 protein family and this gene appears to be expressed at moderate level throughout development (Figures S1A and S1B available online). Two mutant alleles, *sand-1* and *sand-2*, caused by T-DNA insertional gene inactivation (Figures S1C and S1D), impaired seed germination, seedling root growth, and plant growth but had almost no adverse effect on gametophyte

[5]Present address: Department of Plant Molecular Biology (DBMV), University of Lausanne, UNIL-Sorge, 1015 Lausanne, Switzerland

*Correspondence: gerd.juergens@zmbp.uni-tuebingen.de

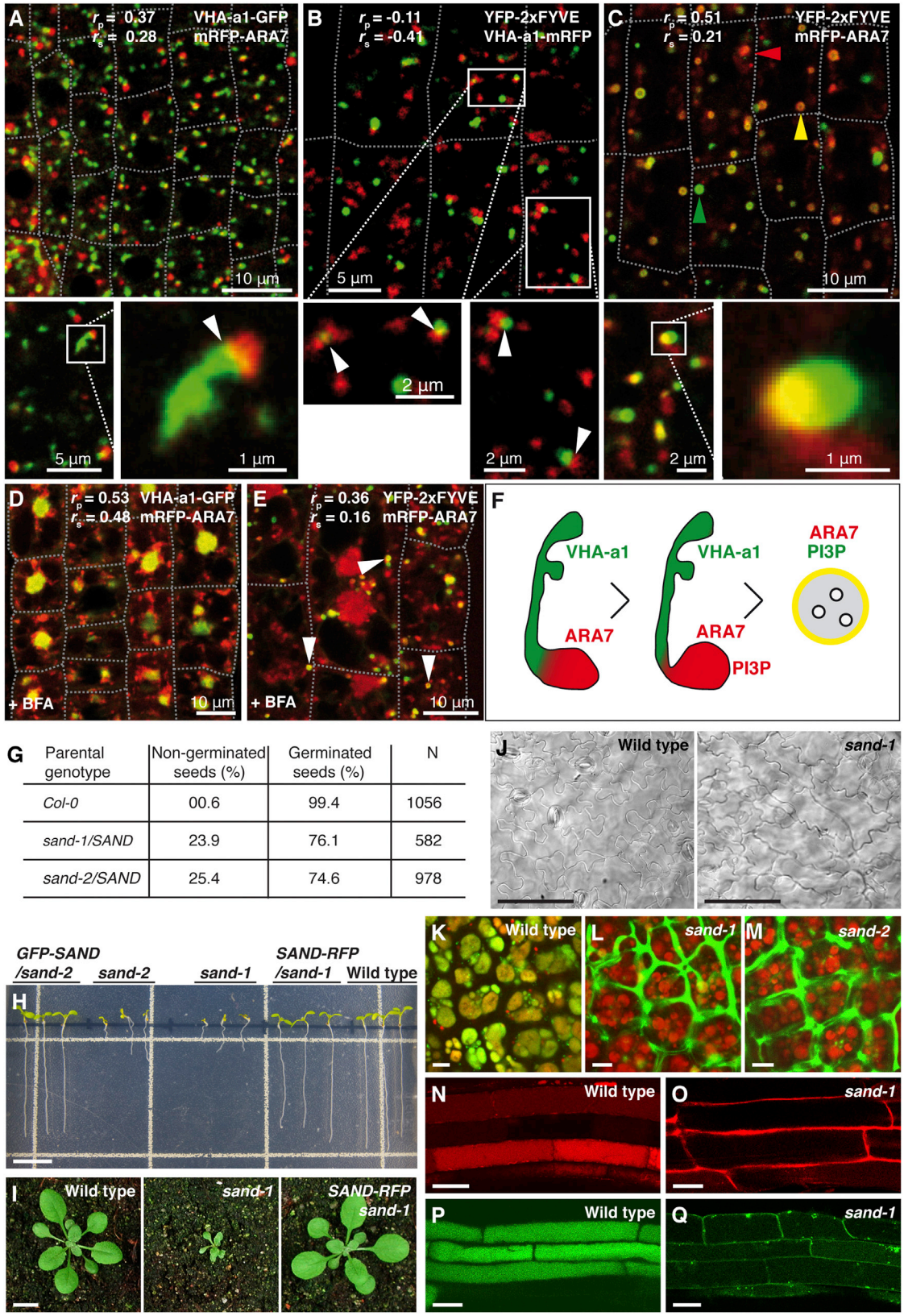

Figure 1. Spatial Relationship of TGN and MVB Markers, *sand* Mutant Phenotype, and Membrane Trafficking Defects

(A) Localization of VHA-a1-GFP and mRFP-ARA7. The lower panels show both proteins at a higher magnification, revealing a subdomain of mRFP-ARA7 at the VHA-a1-GFP-labeled TGN. Fluorescence in lower panel was recorded with a pinhole diameter of 0.37 AU.

(B) Localization of YFP-2xFYVE and VHA-a1-mRFP. The lower panels show corresponding close-up views where small areas of overlap are visible. The images were obtained with a pinhole diameter of 0.37 AU.

(legend continued on next page)

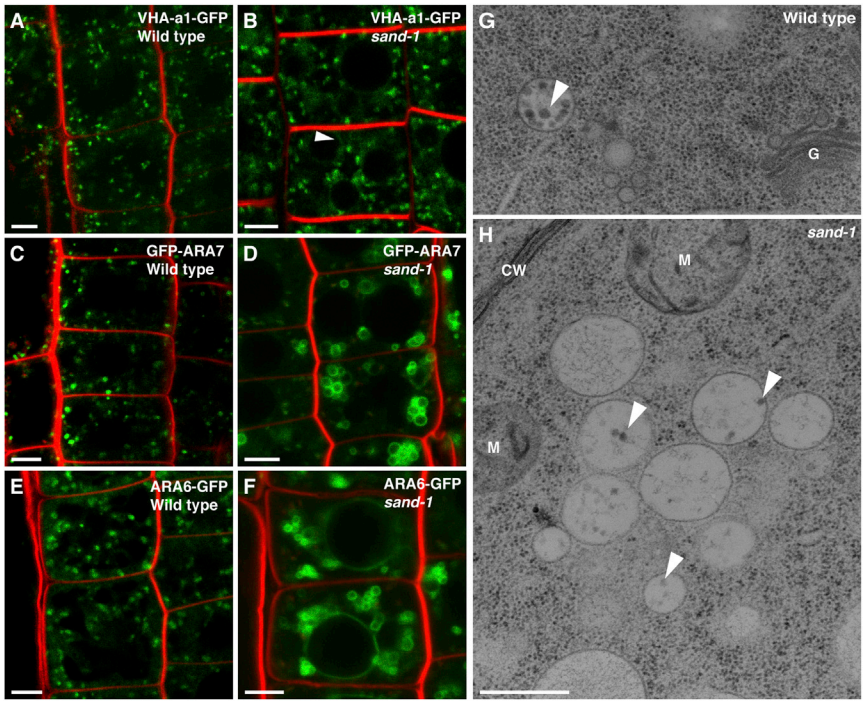

Figure 2. SAND Protein Acts at MVBs

(A and B) Localization of TGN-resident VHA-a1-GFP in wild-type and *sand-1*. Note additional faint labeling of vacuolar membrane in *sand-1* (B; arrowheads).

(C and D) ARA7-positive organelles are enlarged and clustered in *sand-1* (D).

(E and F) ARA6-positive organelles are enlarged and clustered in *sand-1* (F). In addition, ARA6 labeling of vacuolar membrane is also observed (F).

(G and H) Electron micrographs of clusters of enlarged MVBs in *sand-1* (H) as compared to wild-type (G). Note the presence of intraluminal vesicles in MVB clusters in *sand-1* similar to wild-type (arrowheads). CW, cell wall; G, Golgi stack; M, mitochondrion.

Scale bars represent 5 μm (A–F); 500 nm (G, H). See also Figure S2.

development or function (Figures 1G–1I and S1E–S1J). In addition, the pavement cells of the cotyledon epidermis were much less lobed in *sand-1* than in wild-type (Figure 1J). Similarly, cell sizes and cell shapes in the seedling root appeared abnormal (Figure S1G). These defects were abolished by expression of N-terminally GFP-tagged SAND driven by *UBQ10* promoter or C-terminally mRFP-tagged SAND under the control of *RPS5A* promoter, indicating that SAND protein is required in all those developmental contexts (Figures 1H, 1I, and S1).

To identify the trafficking pathway(s) in which SAND acts, we analyzed the subcellular localization of pathway-specific markers (Figures 1K–1Q and S2). Vacuolar marker proteins comprised fluorescent protein fusions of sorting signals from two storage proteins, α′-subunit of β-conglycinin (CT24) [17] and phaseolin (AFVY) [15], and the soluble protease aleurain fused to GFP [18], normally being delivered to the protein storage vacuole or the lytic vacuole, respectively. Rather than being delivered to the vacuole, all three soluble marker proteins for vacuolar trafficking were secreted from the cell (Figures 1K–1Q). These trafficking defects impair storage protein accumulation and vacuolar protein breakdown, limiting nutrients for growth, and might thus explain the developmental defects described above (see Figures 1K–1Q). In contrast, there was no detectable effect on secretory or recycling post-Golgi trafficking pathways. Cytokinesis-specific syntaxin KNOLLE [19] accumulated at the cell plate as in wild-type (Figures S2A and S2B), auxin efflux carrier PIN1 [20] was localized at the basal plasma membrane (Figures S2C and S2D), and PIN2 [21] accumulated at the apical end of epidermal cells (Figures S2E and S2F). The steady-state accumulation of the two PIN proteins at the plasma membrane results from their continuous cycling through endosomes [20, 21]. However, some aberrant endosomal localization of PIN2, but not PIN1, was detected (Figures S2E and S2F), which might suggest that vacuolar trafficking of PIN2 is impaired, consistent with the higher turnover of PIN2 as compared to PIN1 [21]. Thus, late secretory and recycling traffic from the TGN to the plasma membrane or the cell division plane does not require SAND function and SAND appears to be specifically required for protein delivery to the vacuole.

To delineate the site of action of SAND protein, we analyzed the subcellular localization of TGN and MVB markers in both wild-type and *sand-1* mutant seedling roots (Figure 2).

(C) Overview of YFP-2xFYVE and mRFP-ARA7 showing independent green and red signals together with compartments of merged fluorescence, marked with color-coded arrowheads. The close-up views reveal that some of these compartments display a gradual fluorescence distribution.

(D) VHA-a1GFP and mRFP-ARA7 after BFA treatment (50 μM, 30 min).

(E) YFP-2xFYVE and mRFP-ARA7 after BFA treatment (50 μM, 30 min). Note that some ring-like signals of YFP-2xFYVE still colocalize with mRFP-ARA7 on MVB (arrowheads).

(F) Schematic diagram showing spatial relationship between VHA-a1, ARA7, and PI3P. A subdomain of a TGN undergoing maturation becomes enriched with ARA7 and subsequently with PI3-kinases, generating a membrane domain positive for both ARA7 and PI3P. Once an MVB is pinched off from the TGN, its surface is covered with both PI3P and ARA7.

(G) Germination defect in *sand* mutant seeds. Homozygous mutant progeny (25% expected) from *sand-1*/SAND and *sand-2*/*SAND* mother plants often fail to germinate.

(H) Root growth of *sand* mutant seedlings is impaired. The growth of *sand-1* and *sand-2,* complemented by transgene is similar to that of wild-type.

(I) Homozygous *sand-1* showed severe dwarf phenotype on soil. The growth defects of *sand-1* plants expressing SAND-RFP were fully rescued.

(J) Reduced lobing of epidermal pavement cells in *sand-1* cotyledons.

(K–M) Storage vacuole marker GFP-CT24 delivered to the storage vacuole (red) in developing seeds of wild-type (K) but secreted from the cell in *sand-1* (L) and *sand-2* (M).

(N–Q) Phaseolin vacuolar targeting sequence AFVY fused to RFP (N, O) and lytic-vacuole marker aleurain fused to GFP (P, Q) secreted from the cell in *sand-1* (O, Q). Cell boundaries in (A)–(E) are shown with the dotted lines. The values of Pearson (r_p) and Spearman (r_s) correlation coefficients represent the extent of colocalization between the two proteins. The values range between +1, indicating a positive correlation, and −1 for a negative correlation. Scale bars represent 1 cm (H, I); 100 μm (J); 5 μm (K–M); 20 μm (N–Q). See also Figures S1 and S2.

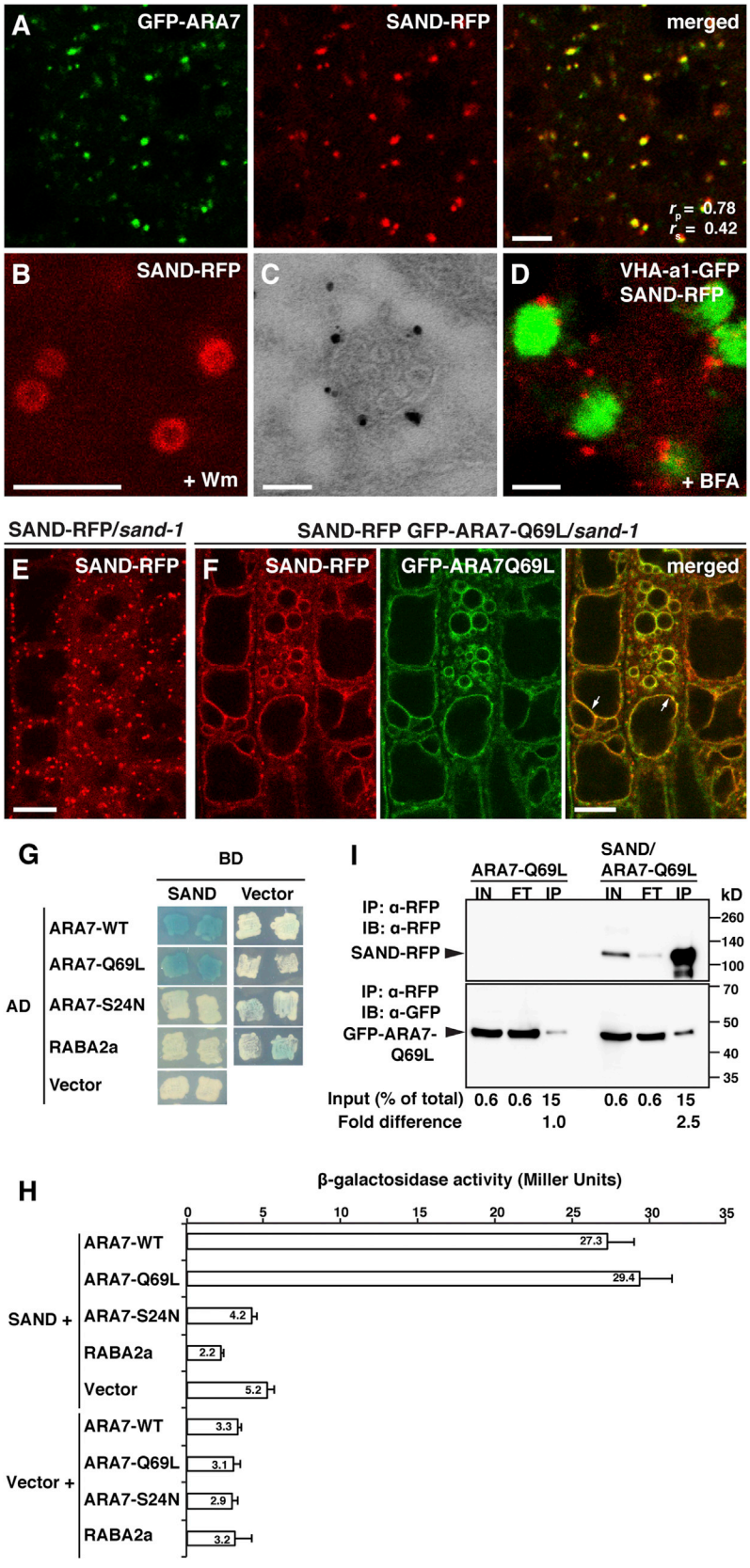

Figure 3. SAND Protein Localization and Interaction with Rab5-like ARA7

(A) Colocalization of SAND-RFP with GFP-ARA7. The values of Pearson (r_p) and Spearman (r_s) correlation coefficients represent the extent of colocalization between the two proteins. The values range between +1, indicating a positive correlation, and −1 for a negative correlation. See also Figure S3A.

(B) Enlarged ring-shaped signals of SAND-RFP in response to wortmannin treatment.

(C) Immuno-gold localization of SAND-RFP on limiting membrane of MVB.

(D) Double-labeling of TGN-localized VHA-a1-GFP and SAND-RFP in BFA-treated root cells. Note the close association of SAND signal (red) with VHA-a1-positive BFA compartment (green).

(E) SAND localization in rescued *sand-1* mutant.

(F) Double labeling of GFP-ARA7-Q69L (GTP-locked form) and SAND in rescued *sand-1* mutant. Note the colocalization of the two proteins in the vacuolar membrane (arrows).

(G) Yeast two-hybrid interaction analysis of SAND with ARA7 wild-type (WT), GTP-locked (Q69L), GDP-locked (S24N) forms, and RABA2a (TGN-localized; contr).

(H) Quantitation of SAND-ARA7 interaction strength in yeast, using β-galactosidase activity. Data shown as means ± SE; n = 5.

(I) Coimmunoprecipitation of ARA7-Q69L with SAND. *Arabidopsis* seedlings stably expressing both SAND-RFP and GFP-ARA7-Q69L, in *sand-1* background, were used for precipitation with anti-RFP antibody-linked agarose beads. Seedlings expressing only GFP-ARA7-Q69L were used as control. Upper half of the membrane was detected with anti-RFP antibody whereas lower half was used for anti-GFP antibody detection. The signal intensity of GFP-ARA7-QL band in IP relative to their respective inputs was used to calculate fold change. IN, input; FL, flow-through; IP, immunoprecipitate; IB, immunoblot; kD, kilodalton. Input (%) represents loading volume relative to the total volume used for IP.

Scale bars represent 5 μm (A, B, D); 100 nm (C); 10 μm (E, F). See also Figures S3 and S4.

TGN-localized VHA-a1 was largely unaffected. However, the vacuolar membrane was faintly labeled in *sand-1*, in addition to the exclusive labeling of the TGN in wild-type (Figures 2A and 2B). In contrast, two Rab5-like GTPases, ARA6 (aka RABF1) [22] and ARA7 (aka RABF2b), labeled clusters of abnormally shaped endosomal structures, which ultrastructural analysis identified as clusters of enlarged MVBs containing intraluminal vesicles (Figures 2C–2H). The mutant MVBs were approximately 60% larger than wild-type MVBs in diameter and had slightly fewer intraluminal vesicles (Figures 2G, 2H, and S2I). Interestingly, ARA6 (RABF1) and YFP-2xFYVE labeled the vacuolar membrane in *sand-1* mutants (Figures 2E, 2F, S2G, and S2H, arrowhead). Thus, SAND appears to act at the MVB.

SAND colocalized with ARA7 (RABF2b) and, like ARA7, was responsive to the PI3-kinase inhibitor wortmannin [23], yielding ring-shaped signals (Figures 3A, 3B, and S3A). Consistent with these findings, SAND localized to the limiting membrane of MVBs by immunogold labeling of ultrastructural sections (Figure 3C). Furthermore, the SAND-positive compartment did not respond to BFA treatment (Figure 3D). SAND also did not colocalize with TGN-resident VHA-a1 but largely colocalized

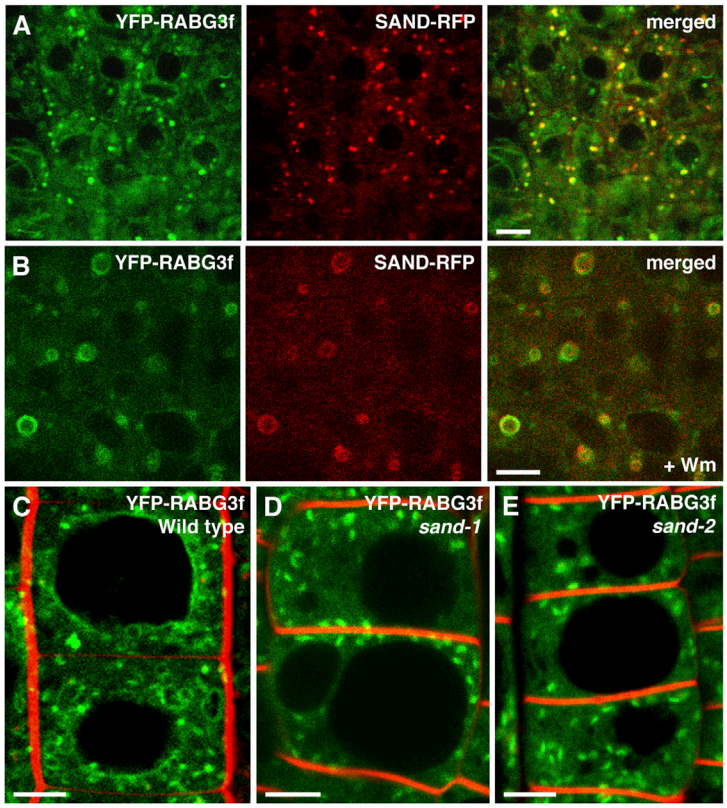

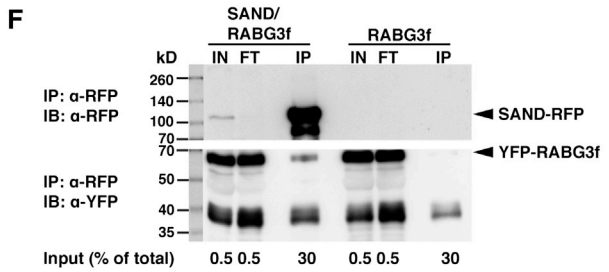

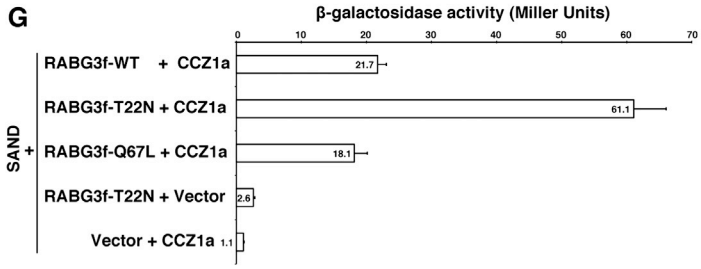

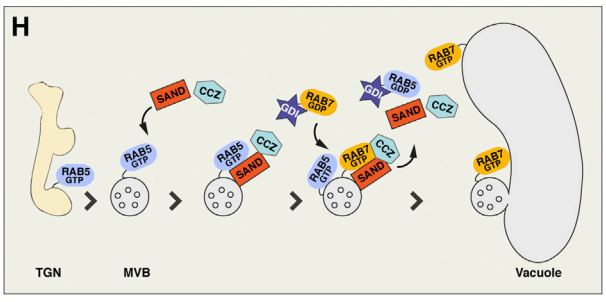

Figure 4. Role of SAND in Localization of Rab7-like RABG3f and Interaction of SAND-CCZ1 with Its GDP-Locked Isoform

(A) Colocalization of SAND-RFP and RabG3f in punctate structures.

(B) Colocalization of SAND-RFP and RabG3f in enlarged ring-shaped structures in wortmannin (Wm)-treated root cells.

(C) RabG3f localized to punctate structures and vacuolar membrane in wild-type.

(D and E) RabG3f localized to punctate structures and in the cytosol but not at the vacuolar membrane in *sand-1* (D) and *sand-2* (E).

(F) Coimmunoprecipitation of RABG3f with SAND. Immunoprecipitation was performed with transgenic line expressing both SAND-RFP and YFP-RABG3f and anti-RFP antibody-linked agarose beads. Seedlings expressing only YFP-RABG3f were used as control. Upper part of the membrane was developed with anti-RFP antibody and lower part was visualized with anti-YFP antibody. IN, input; FL, flow-through; IP, immunoprecipitate; IB, immunoblot; kD, kilodalton. Input (%) represents loading volume relative to the total volume used for IP.

(G) Quantitation of interaction strength between SAND (fused to binding domain) and wild-type (WT), GTP-locked (Q67L), or GDP-locked (T22N) isoforms of RABG3f (fused to activation domain) in presence or absence of CCZ1 protein in yeast three-hybrid assay using β-galactosidase reporter activity. Data shown as means ± SE; n = 5.

(H) Model of SAND protein action in vacuolar trafficking. RAB5 (ARA7) is recruited at the TGN and remains bound to the limiting membrane of newly formed MVB where it recruits SAND protein. Once present on MVB, SAND together with CCZ1 protein leads to the activation of RAB7 (RABG3f) on MVB and its fusion with vacuole.

Scale bars represent 5 μm (A–E). See also Figure S4.

with the PI3P sensor 2xFYVE and Rab5-like ARA6 (Figure S3). Constitutive activity of ARA7-Q69L [24, 25] (GTP-locked form) resulted in its vacuolar membrane localization (Figure 3F). Interestingly, in the presence of constitutively active ARA7, SAND was also detected on the enlarged MVBs and at the vacuolar membrane (Figures 3E and 3F). To examine whether SAND interacts with ARA7 directly, yeast two-hybrid interaction assays were performed. Both the wild-type form of ARA7 and the GTP-locked form (ARA-Q69L) interacted with SAND whereas the GDP-locked form (ARA7-S24N) did not (Figures 3G, 3H, S4A, and S4B). Interaction of SAND-RFP with GFP-tagged ARA7-Q69L was also detected by coimmunoprecipitation in extracts of transgenic *Arabidopsis* seedlings (Figure 3I). Thus, SAND appears to be an effector of GTP-bound ARA7.

In yeast, SAND/Mon1 forms a heterodimer with CCZ1 that acts as a guanine-nucleotide exchange factor (GEF) of late-endosomal/vacuolar Rab7-like Ypt7 [8]. In *Arabidopsis*, there are eight Rab7-like GTPases including RABG3f, which has been localized to MVBs and the vacuole [26, 27]. RABG3f colocalized with SAND protein both in untreated and in wortmannin-treated seedling roots, displaying ring-shaped signals upon wortmannin treatment (Figures 4A and 4B). Furthermore, YFP-tagged RABG3f localized to MVBs and the vacuolar membrane in wild-type roots (Figure 4C). In contrast, no YFP signal was detected on the vacuolar membrane in *sand-1* mutant seedling roots. Instead, RABG3f was present in punctae and in the cytosol (Figures 4D, 4E, and S4E). These punctate structures did not respond to wortmannin in *sand-1*, in contrast to wild-type, suggesting that they are not MVBs (Figure S4E). Thus, SAND is required for the correct localization of

RABG3f including its accumulation on the vacuolar membrane, which is similar to the dependence of Rab7-like Ypt7 on Mon1/SAND in yeast [28]. These data suggested that SAND, directly or indirectly, might interact with RABG3f. Indeed, interaction was detected in coimmunoprecipitation assays via extracts of transgenic plants that expressed SAND-RFP and YFP-tagged RABG3f (Figure 4F). We then employed yeast three-hybrid analysis involving CCZ1 as a bridging protein to characterize the potential interaction between SAND and RABG3f (Figures 4G, S4A, S4C, and S4D). In the presence of CCZ1, SAND interacted much more strongly with the GDP-locked form of RABG3f than with wild-type or the GTP-locked form, which would be consistent with a role for SAND-CCZ1 as RABG3f-GEF (see also the accompanying manuscript by Ebine et al [29]., which demonstrates RabG3f-GEF activity of SAND-CCZ1). Moreover, SAND alone did not interact with the GDP-locked form of RABG3f, suggesting that the coimmunoprecipitation of RABG3f with SAND from plant extracts actually involved the presence of the SAND-CCZ1 heterodimer.

Our results indicate that in plants, as has been described in nonplant organisms, protein trafficking to the vacuole for degradation involves endosomal maturation from early endosome to MVB and subsequent fusion of MVBs with the vacuole (see model in Figure 4H). In addition, the role of SAND protein in Rab5-to-Rab7 conversion appears to be evolutionarily conserved. Surprisingly, however, SAND-mediated Rab conversion is not required for MVB formation in *Arabidopsis*, as revealed by the presence of intraluminal vesicles in *sand* mutant plants, indicating that maturation of late endosomes from early endosomes takes place in the presence of Rab5 and the absence of Rab7. Instead, in plants Rab conversion by SAND is specifically required for the subsequent MVB-vacuole fusion. It is conceivable, though, that SAND-mediated Rab conversion might also play a role in MVB-vacuole/lysosome fusion in nonplant organisms, as suggested by the interaction of Rab7-like Ypt7 with the vacuolar HOPS complex [8]. However, this might not be readily apparent because of the earlier requirement of SAND protein in endosomal maturation such that functional MVBs are not generated in *sand* mutants. The underlying difference between plants and nonplant organisms thus relates to a difference in specific membrane recruitment and/or activation of Rab5-like GTPases, with ARA6 and ARA7 of *Arabidopsis* mainly associating with MVBs/LEs and Rab5 and yeast Vps21p associating with early endosomes [30]. It is tempting to speculate that the difference between plants and nonplant organisms observed in endosomal maturation and Rab conversion might result from the relative timing of two distinct processes: ESCRT-dependent formation of intraluminal vesicles, which transforms early into late endosomes, and Rab5-to-Rab7 conversion, which essentially prepares late endosomes/MVBs for their fusion with the lysosome/vacuole.

Supplemental Information

Supplemental Information includes four figures and Supplemental Experimental Procedures and can be found with this article online at http://dx.doi.org/10.1016/j.cub.2014.05.005.

Acknowledgments

We thank Niko Geldner, Ueli Grossniklaus, and Takashi Ueda for sharing published materials and Sacco de Vries for kindly providing anti-YFP antiserum and NASC for T-DNA insertion lines. This work was funded by DFG grant Ju179/18-1.

Received: February 12, 2014
Revised: April 7, 2014
Accepted: May 2, 2014
Published: May 29, 2014

References

1. Huotari, J., and Helenius, A. (2011). Endosome maturation. EMBO J. *30*, 3481–3500.
2. Henne, W.M., Buchkovich, N.J., and Emr, S.D. (2011). The ESCRT pathway. Dev. Cell *21*, 77–91.
3. Poteryaev, D., Datta, S., Ackema, K., Zerial, M., and Spang, A. (2010). Identification of the switch in early-to-late endosome transition. Cell *141*, 497–508.
4. Otegui, M.S., and Spitzer, C. (2008). Endosomal functions in plants. Traffic *9*, 1589–1598.
5. Richter, S., Voss, U., and Jürgens, G. (2009). Post-Golgi traffic in plants. Traffic *10*, 819–828.
6. Reyes, F.C., Buono, R., and Otegui, M.S. (2011). Plant endosomal trafficking pathways. Curr. Opin. Plant Biol. *14*, 666–673.
7. Rink, J., Ghigo, E., Kalaidzidis, Y., and Zerial, M. (2005). Rab conversion as a mechanism of progression from early to late endosomes. Cell *122*, 735–749.
8. Nordmann, M., Cabrera, M., Perz, A., Bröcker, C., Ostrowicz, C., Engelbrecht-Vandré, S., and Ungermann, C. (2010). The Mon1-Ccz1 complex is the GEF of the late endosomal Rab7 homolog Ypt7. Curr. Biol. *20*, 1654–1659.
9. Kinchen, J.M., and Ravichandran, K.S. (2010). Identification of two evolutionarily conserved genes regulating processing of engulfed apoptotic cells. Nature *464*, 778–782.
10. Dettmer, J., Hong-Hermesdorf, A., Stierhof, Y.D., and Schumacher, K. (2006). Vacuolar H+-ATPase activity is required for endocytic and secretory trafficking in *Arabidopsis*. Plant Cell *18*, 715–730.
11. Contento, A.L., and Bassham, D.C. (2012). Structure and function of endosomes in plant cells. J. Cell Sci. *125*, 3511–3518.
12. Viotti, C., Bubeck, J., Stierhof, Y.D., Krebs, M., Langhans, M., van den Berg, W., van Dongen, W., Richter, S., Geldner, N., Takano, J., et al. (2010). Endocytic and secretory traffic in *Arabidopsis* merge in the trans-Golgi network/early endosome, an independent and highly dynamic organelle. Plant Cell *22*, 1344–1357.
13. Stierhof, Y.D., and El Kasmi, F. (2010). Strategies to improve the antigenicity, ultrastructure preservation and visibility of trafficking compartments in *Arabidopsis* tissue. Eur. J. Cell Biol. *89*, 285–297.
14. Vermeer, J.E., van Leeuwen, W., Tobeña-Santamaria, R., Laxalt, A.M., Jones, D.R., Divecha, N., Gadella, T.W., Jr., and Munnik, T. (2006). Visualization of PtdIns3P dynamics in living plant cells. Plant J. *47*, 687–700.
15. Scheuring, D., Viotti, C., Krüger, F., Künzl, F., Sturm, S., Bubeck, J., Hillmer, S., Frigerio, L., Robinson, D.G., Pimpl, P., and Schumacher, K. (2011). Multivesicular bodies mature from the trans-Golgi network/early endosome in *Arabidopsis*. Plant Cell *23*, 3463–3481.
16. Robinson, D.G., Jiang, L., and Schumacher, K. (2008). The endosomal system of plants: charting new and familiar territories. Plant Physiol. *147*, 1482–1492.
17. Fuji, K., Shimada, T., Takahashi, H., Tamura, K., Koumoto, Y., Utsumi, S., Nishizawa, K., Maruyama, N., and Hara-Nishimura, I. (2007). *Arabidopsis* vacuolar sorting mutants (green fluorescent seed) can be identified efficiently by secretion of vacuole-targeted green fluorescent protein in their seeds. Plant Cell *19*, 597–609.
18. Sohn, E.J., Kim, E.S., Zhao, M., Kim, S.J., Kim, H., Kim, Y.W., Lee, Y.J., Hillmer, S., Sohn, U., Jiang, L., and Hwang, I. (2003). Rha1, an *Arabidopsis* Rab5 homolog, plays a critical role in the vacuolar trafficking of soluble cargo proteins. Plant Cell *15*, 1057–1070.
19. Reichardt, I., Stierhof, Y.D., Mayer, U., Richter, S., Schwarz, H., Schumacher, K., and Jürgens, G. (2007). Plant cytokinesis requires de novo secretory trafficking but not endocytosis. Curr. Biol. *17*, 2047–2053.
20. Geldner, N., Friml, J., Stierhof, Y.D., Jürgens, G., and Palme, K. (2001). Auxin transport inhibitors block PIN1 cycling and vesicle trafficking. Nature *413*, 425–428.

21. Abas, L., Benjamins, R., Malenica, N., Paciorek, T., Wiśniewska, J., Moulinier-Anzola, J.C., Sieberer, T., Friml, J., and Luschnig, C. (2006). Intracellular trafficking and proteolysis of the *Arabidopsis* auxin-efflux facilitator PIN2 are involved in root gravitropism. Nat. Cell Biol. *8*, 249–256.
22. Ebine, K., Fujimoto, M., Okatani, Y., Nishiyama, T., Goh, T., Ito, E., Dainobu, T., Nishitani, A., Uemura, T., Sato, M.H., et al. (2011). A membrane trafficking pathway regulated by the plant-specific RAB GTPase ARA6. Nat. Cell Biol. *13*, 853–859.
23. Takáč, T., Pechan, T., Samajová, O., Ovečka, M., Richter, H., Eck, C., Niehaus, K., and Samaj, J. (2012). Wortmannin treatment induces changes in *Arabidopsis* root proteome and post-Golgi compartments. J. Proteome Res. *11*, 3127–3142.
24. Ueda, T., Yamaguchi, M., Uchimiya, H., and Nakano, A. (2001). Ara6, a plant-unique novel type Rab GTPase, functions in the endocytic pathway of *Arabidopsis thaliana*. EMBO J. *20*, 4730–4741.
25. Jia, T., Gao, C., Cui, Y., Wang, J., Ding, Y., Cai, Y., Ueda, T., Nakano, A., and Jiang, L. (2013). ARA7(Q69L) expression in transgenic *Arabidopsis* cells induces the formation of enlarged multivesicular bodies. J. Exp. Bot. *64*, 2817–2829.
26. Rutherford, S., and Moore, I. (2002). The *Arabidopsis* Rab GTPase family: another enigma variation. Curr. Opin. Plant Biol. *5*, 518–528.
27. Geldner, N., Dénervaud-Tendon, V., Hyman, D.L., Mayer, U., Stierhof, Y.D., and Chory, J. (2009). Rapid, combinatorial analysis of membrane compartments in intact plants with a multicolor marker set. Plant J. *59*, 169–178.
28. Cabrera, M., and Ungermann, C. (2013). Guanine nucleotide exchange factors (GEFs) have a critical but not exclusive role in organelle localization of Rab GTPases. J. Biol. Chem. *288*, 28704–28712.
29. Ebine, K., Inoue, T., Ito, J., Ito, E., Uemura, T., Goh, T., Abe, H., Sato, K., Nakano, A., and Ueda, T. (2014). Plant vacuolar trafficking occurs through distinctly regulated pathways. Curr. Biol. *24*, this issue.
30. Markgraf, D.F., Peplowska, K., and Ungermann, C. (2007). Rab cascades and tethering factors in the endomembrane system. FEBS Lett. *581*, 2125–2130.

Note Added in Proof

An independent analysis of MON1, which is allelic to SAND, was recently reported (Cui et al., *The Plant Cell*, in press). Although Cui and colleagues used a different mutant allele and different trafficking markers, their study yielded essentially the same conclusion.

Current Biology, Volume *24*

Supplemental Information

Protein Delivery to Vacuole Requires SAND Protein-Dependent Rab GTPase Conversion for MVB-Vacuole Fusion

Manoj K. Singh, Falco Krüger, Hauke Beckmann, Sabine Brumm, Joop E.M. Vermeer, Teun Munnik, Ulrike Mayer, York-Dieter Stierhof, Christopher Grefen, Karin Schumacher, and Gerd Jürgens

Figure S1

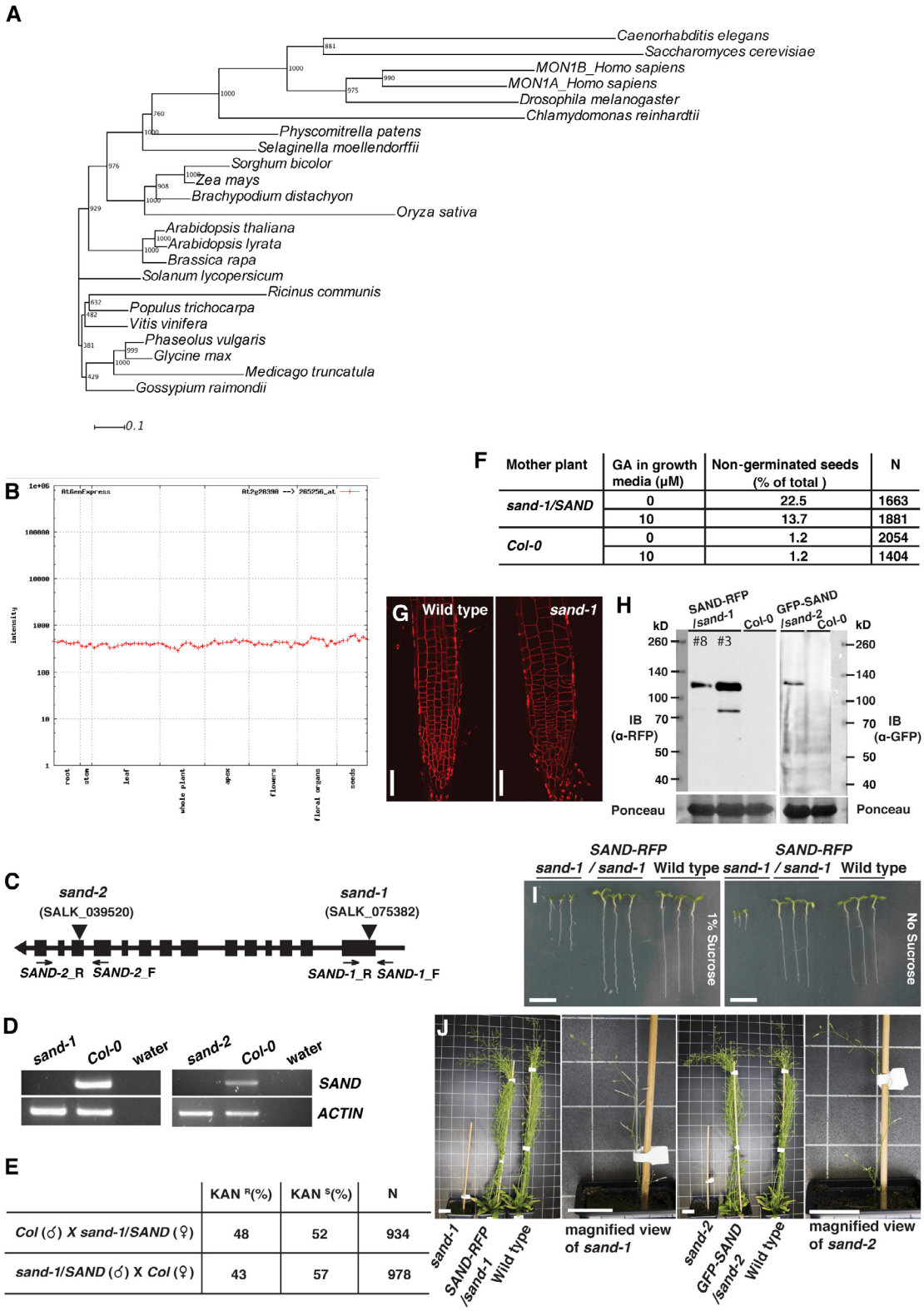

Figure S1, Related to Figure 1. *SAND* gene and mutant phenotypes
(A) Phylogenetic tree of SAND orthologs in various monocot and dicot plants, yeast, algae and animals. Following sequences were used for construction of the tree:

Chlamydomonas reinhardtii (Cre03.g154500.t1.2); *Saccharomyces cerevisiae* (NP_011391.2); *Caenorhabditis elegans* (NP_500791.2); *Homo sapiens* MON1B (NP_055755.1); *Homo sapiens* MON1A (Q86VX9.2); *Drosophila melanogaster* (NP_608868.1); *Physcomitrella patens* (Pp1s452_21V6); *Selaginella moellendorffii* (EFJ23517.1); *Sorghum bicolor* (XP_002459184.1); *Zea mays* (NP_001149118.1); *Brachypodium distachyon* (XP_003567548.1); *Oryza sativa* (Os01g74460.2); *Arabidopsis thaliana* (At2g28390); *Arabidopsis lyrata* (EFH55358.1); *Brassica rapa* (Bra000494); *Solanum lycopersicum* (XP_004235972.1); *Ricinus communis* (EEF27973.1); *Populus trichocarpa* (POPTR_0004s22080); *Vitis vinifera* (XP_002285170.1); *Phaseolus vulgaris* (Phvul.005G134800.1); *Glycine max* (Glyma12g29450.1); *Gossypium raimondii* (Gorai.003G141900.1); *Medicago truncatula* (AES67499.1)
(B) Expression profile of Arabidopsis *SAND* gene (At2g28390). Expression data was obtained using AtGenExpress Visualisation Tool (http://www.weigelworld.org/resources/microarray/AtGenExpress; ref. [S1])
(C) Schematic diagram of *SAND gene* indicating position of T-DNA insertions and primers used for RT PCR analysis. (D) RT-PCR analysis of *sand-1* and *sand-2*. (E) Reciprocal crosses. Loss of *SAND* has no effect on gametophytic transmission. (F) Effect of Gibberellic acid (GA) on germination of *sand-1.* Seeds from *Col-0* and *sand-1/SAND* mother plants were germinated on growth media with or without GA. Data presented is from one representative experiment. (G) Abnormal cell shapes and sizes in *sand-1* seedling root. (H) Western blot showing expression of SAND-RFP and GFP-SAND in complemented *sand-1* and *sand-2* mutants. #3 and #8 are two independent rescued *sand-1* mutant lines expressing different levels of SAND-RFP. Col-0, non-transgenic wild type control; IB, Immunoblot; kD, kilodalton. (I) *sand-1* phenotype is aggravated by growth on medium lacking sucrose. (J) Rescue of *sand-1* and *sand-2* phenotype by expression of SAND-RFP and GFP-SAND, respectively. Scale bar represents 50 μm in (G); 1 cm in (H); 3 cm in (I).

Figure S2

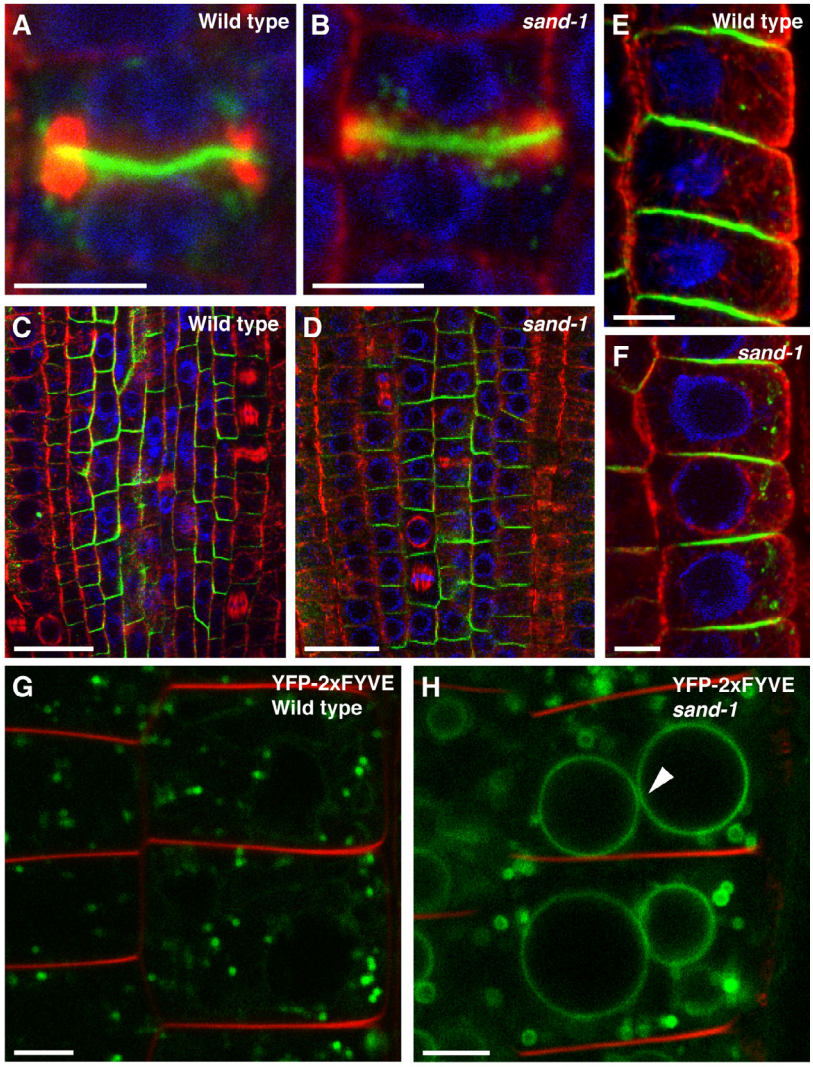

I

Genotype	Average diameter of MVB (in nm)	Average number of intraluminal vesicles (per MVB)	N
Wild type	229.55 ± 68.52	5.45 ± 3.36	29
sand-1	381.13 ± 119.74	3.11 ± 3.62	63

Figure S2, Related to Figure 1 and Figure 2. Secretory pathway and recycling is unaffected in *sand* mutants

(A, B) KNOLLE localisation at the cell plate. (C, D) Polar PIN1 localisation in inner cells. (E, F) Apical localisation of PIN2 in epidermal cells. Note the accumulation of PIN2 in punctate (endosomal) compartments (F). (G, H) YFP-2xFYVE localisation in wild type (G) and *sand-1* (H). Note the strong labeling of vacuolar membrane in *sand-1* (H; arrowhead) compared to wild type (G) where the signal was mainly on MVBs. (I) Quantitation of average MVB size and number of intraluminal vesicles in wild type and *sand-1* mutant. N, total number of MVBs used for analysis. Data shown as means ± SD.

Scale bar represents 5 µm in (A)(B)(E)-(H); 20µm in (C)(D).

Figure S3

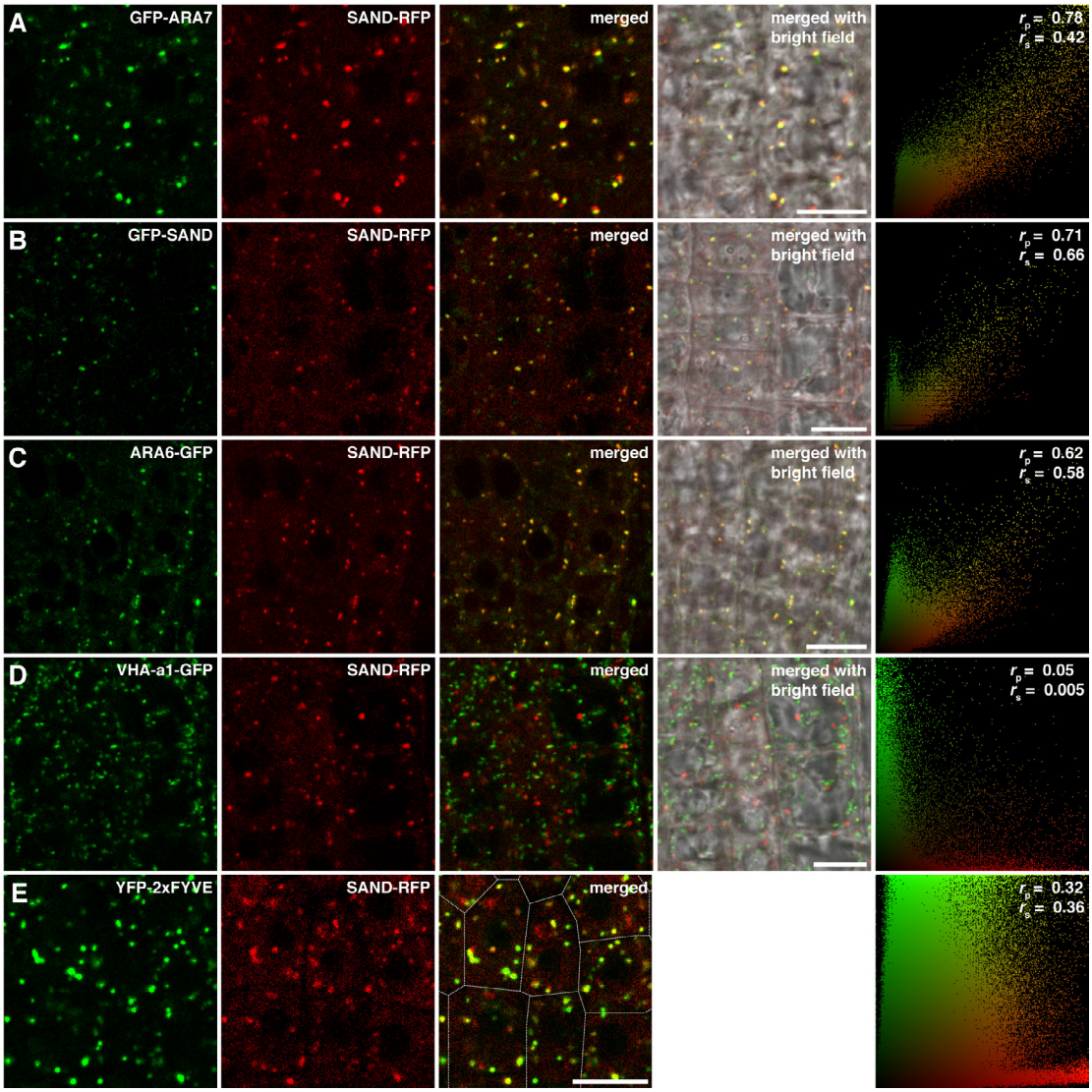

Figure S3, Related to Figure 3. Co-localisation of SAND-RFP with various subcellular markers

(A) GFP-ARA7 and SAND-RFP (same as in Fig. 3A). (B) GFP-SAND and SAND-RFP. (C) MVB marker ARA6-GFP and SAND-RFP. (D) VHA-a1-GFP and SAND-RFP. (E) YFP-2xFYVE and SAND-RFP. Cell boundaries in (E) are shown with dotted lines. Co-localisation analysis was performed using PSC plugin for ImageJ [S19] from a minimum of five independent seedling root images. Pearson (r_p) and Spearman (r_s) correlation coefficients and the scatter plots are shown in the right panels. The extent of co-localisation ranges between +1, indicating a positive correlation, and -1 for a negative correlation. Scale bar, 10 μm.

Figure S4

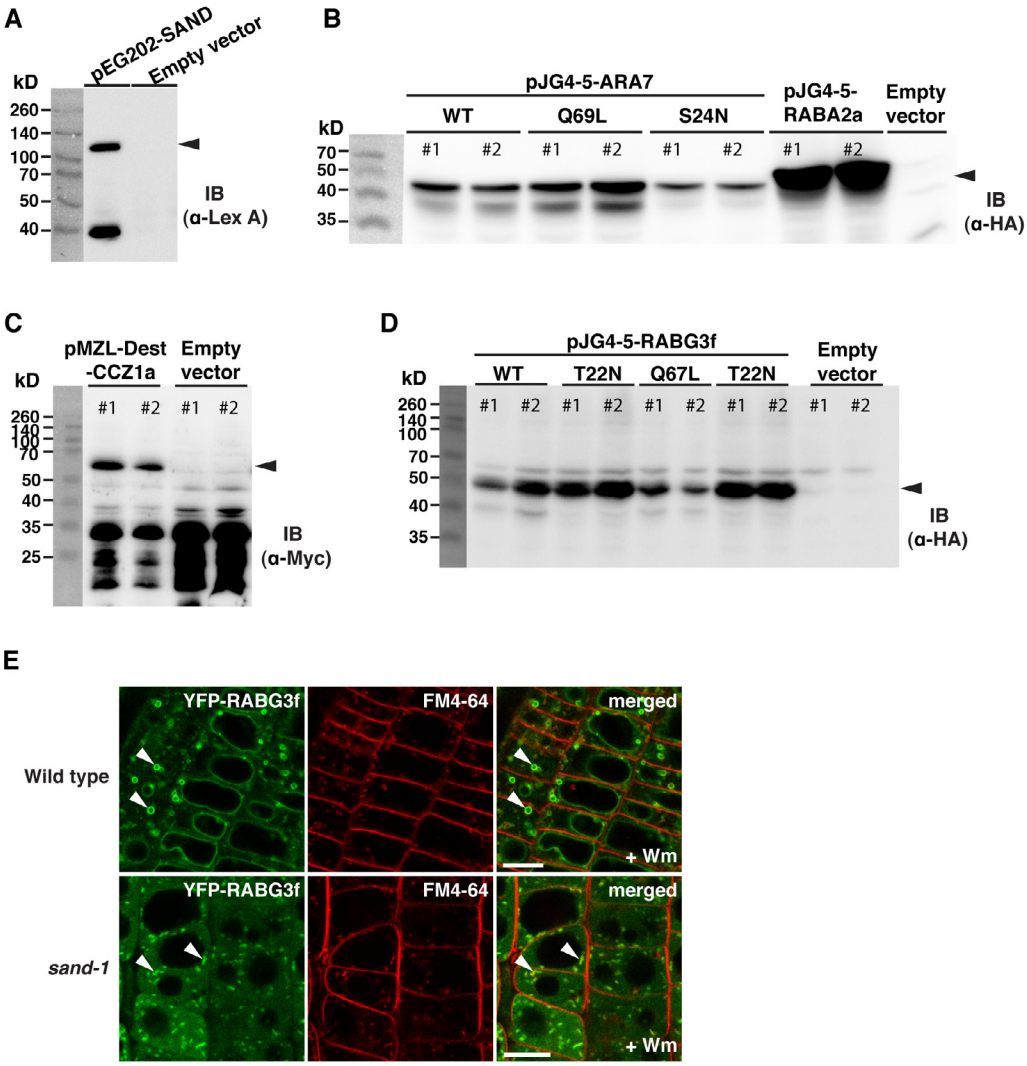

Figure S4, Related to Figure 3 and Figure 4. Yeast two-hybrid and three-hybrid protein expression and differential wortmannin sensitivity of RABG3f in wild type and *sand-1* mutant.

(A-D) Western blots showing expression of different constructs in yeast. Protein bands of LexA-SAND (90kD) in (A), HA-tagged wild type (WT) and mutant forms (Q69L, S24N) of ARA7 (35kD) and RABA2a (36kD) in (B), Myc-CCZ1a (60kD) in (C) and HA-tagged RABG3f isoforms (WT, Q67L and T22N) (35kD) in (D) are marked with arrowheads. #1 and #2 represent two independent yeast colonies. IB, Immunoblot; kD, kilodalton.

(E) Effect of Wortmannin (Wm) treatment on YFP-RABG3f in wild type and *sand-1* background. Note that punctate signals (arrowheads) do not form ring-shaped structures in *sand-1*, in contrast to wild type (arrowheads). Scale bar, 10 μm.

Supplemental Experimental Procedures

Plant Material and growth conditions

Arabidopsis thaliana wild type (ecotype Col-0) and transgenic lines, after surface sterilisation, were grown on Murashige and Skoog (MS) medium containing 1%(w/v) sucrose (if not stated otherwise) and 0.8% (w/v) agar in continuous light at 24^0C.

For seed germination in presence of gibberellic acid (GA), MS medium was supplemented with 10μM GA (GA_{4+7}, Sigma). Seedlings were transferred to soil 8-10 days after germination and grown in same conditions.

Seed germination assay

Seeds obtained from wild type and *sand* heterozygous plants were sown on MS medium supplemented with or without GA. After stratification for 3 nights at 4^0C in dark, plates were transferred to growth chamber. Germinated seeds were counted 4-days after transfer to plant growth chamber.

Isolation of *sand* mutants

SALK T-DNA lines carrying insertion in *SAND* gene (in Col-0 ecotype) were purchased from Nottingham Arabidopsis Stock Centre (NASC). The *sand-1* (SALK_075382) and *sand-2* (SALK_039520) insertions are located in the first and 12^{th} exon, respectively. Genotyping of *sand-1* insertion line was performed using SALK_075382_LP (5´-CGGTTTGCCTGAGTTACTCAG-3´), SALK_075382_RP (5´-AAAAGCCCAACAATATGGGTC-3´) and LBb1.3 (5´-ATTTTGCCGATTTCGGAAC-3´) primers. The *sand-2* insertion line was genotyped using SALK_039520_LP (5´-CAACCAACTCTCGTCTCCATC-3)´, SALK_039520_RP (5´-ATGCGTTCCATCATCTCAAAG-3´) and LBb1.3 primers. *SAND* transcript in mutants was analysed using following primers: *SAND1_F* (5´-ACACGTCTTGCCATTAGAGGA-3), *SAND1_R* (5´-CTTCACCTGCTTCCATTTCC-3), *SAND2_F* (5´-TGGACTTTGGCATTTCATGT-3´), *SAND2_R* (5´-CTTTTACCCTTTGGCACACC-3´).

RNA isolation, cloning and transgenic plants

Total RNA was isolated from seedlings using Trizol® (Invitrogen). After DNAse I (Fermentas) digestion, cDNA was synthesised using RevertAid H Minus First Strand cDNA Synthesis Kit (Thermo scientific).

For generation of transgenic lines expressing SAND-RFP, coding sequence (CDS) of *SAND* was amplified from a cDNA library derived from *Col-0*, cloned upstream of *mRFP* into pGrIIKRPS5a-tNOS vector [S2] and transformed into *sand-1*/*SAND* plants. To generate *GFP-SAND* lines, *SAND* CDS was cloned downstream of *GFP* in pUGT2Kan vector and transformed in *sand-2/SAND* plants. AFVY-RFP and Aleurain (Aleu)-GFP were amplified from existing templates [S3, S4] and cloned, using GATEWAY® (Life Technologies) method, in pMDC7 [S5] vector for generation of estradiol inducible Arabidopsis lines. UBQ10::YFP-2X FYVE was generated by cloning 2xFYVE [S6] into pUNI51 and recombined into pNIGEL07 using the CRE/lox system as described [S7]. Transgenic marker lines expressing YFP-RABG3f [S7], ARA6-GFP [S8], GFP-ARA7Q69L [S8], GFP-ARA7 [S9], mRFP-ARA7 [S10], GFP-CT24 [S11], VHA-a1-mRFP [S12] and VHA-a1-GFP [S12] were described earlier.

Yeast hybrid-protein interaction analysis

For yeast two-hybrid analysis, yeast (EGY48 strain) was transformed with following plasmids: pSH18-34, pEG202-SAND and pJG4-5 carrying either RABA2a or ARA7 isoforms (wild type, Q69L and S24N). The interaction assay was performed as reported previously [S13, S14].

For yeast three-hybrid assay, SAND and RABG3f isoforms (wild type, Q67L and T22N) were expressed using pEG202 and pJG4-5 vector, respectively. CCZ1a (At1g16020) was expressed under ADH promoter and with addition of an N-terminal Myc-tag using the Gateway-compatible yeast expression vector pMZL-Dest. This vector derives from vector pMZU-Dest [S15], the URA3 auxotrophy marker being replaced with LEU2 (sequence information available upon request). The assay was performed similar to two-hybrid assay.

Immunoprecipitation

Arabidopsis seedlings (3.0-3.5g) were ground thoroughly in liquid nitrogen and suspended in lysis buffer (50mM Tris pH 7.5, 150mM NaCl) containing 1%(v/v) Triton X-100 and protease inhibitor cocktail (cOmplete EDTA-free®, Roche). After 30 min incubation on ice, cell debris was removed by centrifugation at 10,000 x g for 30 min at 4^0C. The supernatant was filtered through Miracloth (Calbiochem) and incubated with anti-RFP beads (RFP-Trap®, Chromotek) for 4 hour with end-to-end rotation in the cold room. Beads were washed twice with lysis buffer containing 0.1% Triton, followed by 3 washes with buffer lacking Triton (for SAND-RABG3f coIP studies) or once with lysis buffer containing 0.5% Triton, twice with buffer containing 0.1% Triton followed by two washes using buffer without Triton (for SAND-ARA7Q69L coIP studies). After the last wash, beads were boiled in 2x Laemmli buffer.

Western blotting

Proteins were resolved on SDS-PAGE and immuno-detected using one of the following antibodies: anti-RFP (rat, 1:1,000, chromotek), anti-GFP (mouse 1:1,000, Roche), anti-YFP (rabbit, 1:1,000, a gift from S. de Vries), anti-LexA (mouse, 1: 1000, Santa Cruz Biotechnology), POD-conjugated anti-HA (1:1000, Roche).

Immunofluorescence and microscopy

5-day-old *Arabidopsis* seedlings were fixed in MTSB solution containing 4% paraformaldehyde. The immunostaining was performed as previously reported [S16]. The following antibodies were used for immunolocalisation in this study: rabbit anti-KNOLLE, 1:3,000 [S16]; rabbit anti-PIN1, 1:200 [S17]; rabbit anti-PIN2, 1:500 [S18] and rat anti-Tubulin 1:600 (abcam). Secondary antibodies conjugated with Alexa-488® (Invitrogen) and Cy3 (Dianova) were used at 1:600 dilution.

Live-cell imaging was performed using 4 to 5-day-old seedlings in liquid MS medium. FM4-64 was used at 2 µM final concentration. For induction of AFVY-RFP expression, seedlings were transferred to liquid MS medium (pH 5.8) containing 10 µM β-Estradiol (Sigma) and

kept in dark for 48 hr at 24^0C. Aleurain-GFP induction was, similarly, carried out in liquid MS medium of pH 8.1. For Wortmannin treatments, a final concentration of 33 μM was used for for 1 hr. BFA treatment was performed at a final concentration of 50 μM for 1 hr, unless indicated otherwise. Confocal images were obtained using Leica TCS SP8 microscope. For co-localisation studies, images were acquired using sequential scan mode.

For light microscopy of cotyledon pavement cells, cells were cleared using chloral hydrate (Sigma) solution and images were taken using Zeiss Axiophot microscope.

Immunogold labeling and ultra structural analysis

Immunogold labeling and ultra structural analyses were performed as reported previously [S9].

Co-localisation analysis

Confocal laser scanning microscope (CLSM) images from five independent seedling root images, showing a minimum of 8 cells in each image, were obtained using hybrid detectors (HyDs) of Leica TCS SP8 microscope and processed uniformly using smooth tool of ImageJ. Co-localisation analysis was done by calculating Pearson and Spearman correlation coefficients using PSC colocalization plugin of ImageJ according to the instructions of French et al. [S19] with a background level setting of 3.

Phylogenetic analysis

Full length SAND protein sequences from different organisms were aligned using CLC DNA Workbench 6 and a phylogenetic tree was generated using neighbor-joining algorithm with a bootstrap of 100 replicates. The tree was optimised using Dendroscope (version 2.5) program.

Softwares

CLC DNA Workbench 6 was used for DNA sequences analysis. Signal intensity of bands in western blot was quantified using ImageJ (NIH). For image processing Adobe Photoshop CS3 and Adobe Illustrator CS3 were used.

Supplemental References

S1. Schmid, M., Davison, T.S., Henz, S.R., Pape, U.J., Demar, M., Vingron, M., Scholkopf, B., Weigel, D., and Lohmann, J.U. (2005). A gene expression map of Arabidopsis thaliana development. Nat Genet *37*, 501-506.

S2. Weijers, D., Van Hamburg, J.P., Van Rijn, E., Hooykaas, P.J., and Offringa, R. (2003). Diphtheria toxin-mediated cell ablation reveals interregional communication during Arabidopsis seed development. Plant Physiol *133*, 1882-1892.

S3. Scheuring, D., Viotti, C., Krüger, F., Künzl, F., Sturm, S., Bubeck, J., Hillmer, S., Frigerio, L., Robinson, D.G., Pimpl, P., et al. (2011). Multivesicular bodies mature from the trans-Golgi network/early endosome in Arabidopsis. Plant Cell *23*, 3463-3481.

S4. Sohn, E.J., Kim, E.S., Zhao, M., Kim, S.J., Kim, H., Kim, Y.W., Lee, Y.J., Hillmer, S., Sohn, U., Jiang, L., et al. (2003). Rha1, an Arabidopsis Rab5 homolog, plays a critical role in the vacuolar trafficking of soluble cargo proteins. Plant Cell *15*, 1057-1070.

S5. Curtis, M.D., and Grossniklaus, U. (2003). A gateway cloning vector set for high-throughput functional analysis of genes in planta. Plant Physiol *133*, 462-469.

S6. Vermeer, J.E., van Leeuwen, W., Tobena-Santamaria, R., Laxalt, A.M., Jones, D.R., Divecha, N., Gadella, T.W., Jr., and Munnik, T. (2006). Visualization of PtdIns3P dynamics in living plant cells. Plant J *47*, 687-700.

S7. Geldner, N., Denervaud-Tendon, V., Hyman, D.L., Mayer, U., Stierhof, Y.D., and Chory, J. (2009). Rapid, combinatorial analysis of membrane compartments in intact plants with a multicolor marker set. Plant J *59*, 169-178.

S8. Ebine, K., Fujimoto, M., Okatani, Y., Nishiyama, T., Goh, T., Ito, E., Dainobu, T., Nishitani, A., Uemura, T., Sato, M.H., et al. (2011). A membrane trafficking pathway regulated by the plant-specific RAB GTPase ARA6. Nat Cell Biol *13*, 853-859.

S9. Richter, S., Geldner, N., Schrader, J., Wolters, H., Stierhof, Y.D., Rios, G., Koncz, C., Robinson, D.G., and Jürgens, G. (2007). Functional diversification of closely related ARF-GEFs in protein secretion and recycling. Nature *448*, 488-492.

S10. Beck, M., Zhou, J., Faulkner, C., MacLean, D., and Robatzek, S. (2012). Spatio-temporal cellular dynamics of the Arabidopsis flagellin receptor reveal activation status-dependent endosomal sorting. Plant Cell *24*, 4205-4219.

S11. Fuji, K., Shimada, T., Takahashi, H., Tamura, K., Koumoto, Y., Utsumi, S., Nishizawa, K., Maruyama, N., and Hara-Nishimura, I. (2007). Arabidopsis vacuolar sorting mutants (green fluorescent seed) can be identified efficiently by secretion of vacuole-targeted green fluorescent protein in their seeds. Plant Cell *19*, 597-609.

S12. Dettmer, J., Hong-Hermesdorf, A., Stierhof, Y.D., and Schumacher, K. (2006). Vacuolar H+-ATPase activity is required for endocytic and secretory trafficking in Arabidopsis. Plant Cell *18*, 715-730.

S13. Anders, N., Nielsen, M., Keicher, J., Stierhof, Y.D., Furutani, M., Tasaka, M., Skriver, K., and Jürgens, G. (2008). Membrane association of the Arabidopsis ARF exchange factor GNOM involves interaction of conserved domains. Plant Cell *20*, 142-151.

S14. Park, M., Touihri, S., Muller, I., Mayer, U., and Jürgens, G. (2012). Sec1/Munc18 protein stabilizes fusion-competent syntaxin for membrane fusion in Arabidopsis cytokinesis. Dev Cell *22*, 989-1000.

S15. Grefen, C., and Blatt, M.R. (2012). Do calcineurin B-like proteins interact independently of the serine threonine kinase CIPK23 with the K+ channel AKT1? Lessons learned from a menage a trois. Plant Physiol *159*, 915-919.

S16. Lauber, M.H., Waizenegger, I., Steinmann, T., Schwarz, H., Mayer, U., Hwang, I., Lukowitz, W., and Jürgens, G. (1997). The Arabidopsis KNOLLE protein is a cytokinesis-specific syntaxin. J Cell Biol *139*, 1485-1493.

S17. Vieten, A., Vanneste, S., Wisniewska, J., Benkova, E., Benjamins, R., Beeckman, T., Luschnig, C., and Friml, J. (2005). Functional redundancy of PIN proteins is

accompanied by auxindependent cross-regulation of PIN expression. Development *132*, 4521-4531.

S18. Abas, L., Benjamins, R., Malenica, N., Paciorek, T., Wisniewska, J., Moulinier-Anzola, J.C., Sieberer, T., Friml, J., and Luschnig, C. (2006). Intracellular trafficking and proteolysis of the Arabidopsis auxin-efflux facilitator PIN2 are involved in root gravitropism. Nat Cell Biol *8*, 249-256.

S19. French, A.P., Mills, S., Swarup, R., Bennett, M.J., and Pridmore, T.P. (2008). Colocalization of fluorescent markers in confocal microscope images of plant cells. Nature protocols *3*, 619-628.

5.3 Beckmann et al., 2015

Function of protein domains in large ARF-GEF regulation

Hauke Beckmann, Manoj K. Singh, Nadine Anders, Gerd Jürgens

Manuscript to be submitted

Function of protein domains in large ARF-GEF regulation

Hauke Beckmann[1], Manoj K. Singh[1], Nadine Anders[1,2] and Gerd Jürgens[1]*

[1] ZMBP, Entwicklungsgenetik, Auf der Morgenstelle 32, 72076 Tübingen, Germany

[2] Current address: Department of Biochemistry, University of Cambridge, Cambridge CB2 1QW, United Kingdom

* Author for correspondence:

e-mail: gerd.juergens@zmbp.uni-tuebingen.de

ABSTRACT

Coordinated activation of ARF GTPases by ARF guanine nucleotide exchange factors (ARF-GEFs) is essential for vesicle trafficking. In addition to the catalytic SEC7 domain, large ARF-GEFs contain several non-catalytic domains which contribute to the regulation of ARF activation through specific inter- and intramolecular interactions. In this study, we assess the relevance of the SEC7 domain for ARF-GEF membrane and substrate specificity. Exchanging the SEC7 domains between two differently localized ARF-GEFs had no significant influence on their functionality, indicating that specificity is conferred by the non-catalytic domains. These have been demonstrated to interact with each other, providing conformational regulation of ARF-GEF activity. In particular, the N-terminal DCB domain folds back onto the rest of the protein. Our analysis now reveals that the C-terminal HDS2 and HDS3 domains are not involved in this intramolecular interaction, in contrast to a sequence motif present in the HDS1 domain. We propose that interaction of neighboring domains forms a cover over the SEC7 domain and thereby controls the conditions of ARF-GEF activity.

INTRODUCTION

Vesicle trafficking provides for the dynamic distribution of lipids, proteins and other macromolecules among eukaryotic cell compartments, thereby maintaining integrity of these organelles and permitting adaptive processes in the context of development and response to environmental cues. Key regulators of vesicle formation are small GTPases of the ARF subclass, which in turn are activated by ARF guanine nucleotide exchange factors (ARF-GEFs) (Casanova 2007). Large ARF-GEFs are the only ARF-GEF family found in all eukaryotes and subdivide into two classes based on their relation to either human cis-Golgi localized GBF1 or human trans-Golgi network (TGN) localized BIG1. Their domain architecture is conserved, featuring the central catalytic SEC7 domain, the N-terminal DCB domain, one homology upstream of SEC7 (HUS) domain, and three to four homology downstream of SEC7 (HDS) domains (Figure 1, (Mouratou et al. 2005). The non-catalytic domains regulate ARF-GEF activity through conformational changes or interaction with upstream factors, mainly influencing membrane recruitment.

Figure 1. Domain structure of large ARF-GEFs (modified after Mouratou et al. 2005).

The DCB domain mediates homodimerization (Grebe et al. 2000) and, in addition, is part of a multi-domain interaction mechanism regulating membrane association of the GBF1-related *Arabidopsis* ARF-GEF GNOM. Mutation of conserved regions in the HUS and SEC7 domains disturbs the intramolecular interaction with the DCB domain, rendering the protein unable to attach to membranes (Anders et al. 2008).

Apart from being substrates of ARF-GEFs in their GDP-bound form, GTP-bound ARF GTPases have recently been shown to affect TGN localization of members of the BIG1 class of large ARF-GEFs. An N-terminal fragment of *Drosophila* SEC71 comprising the DCB and HUS domains is recruited to the TGN by the ARF-like GTPase ARL1 (Christis and Munro 2012). In yeast, the HDS1 domain mediates membrane recruitment of SEC7p by ARF1-GTP (Richardson et al. 2012).

As demonstrated in the case of SEC7p, the C-terminal HDS domains also display an autoinhibitory effect on the GDP-GTP exchange activity. HDS1 autoinhibition is overcome by interaction with ARF1-GTP (Richardson et al. 2012), whereas binding of active RAB-GTPases Ypt1 and Ypt31/32 to the HDS2 or HDS3 domain alleviates HDS4 auto-inhibition and stimulates exchange activity on ARF1 in vitro (McDonold and Fromme 2014).

The factors responsible for cis-Golgi recruitment of GBF1-related large ARF-GEFs are less well understood. Also, it is unknown whether the SEC7 domain plays a role in determining localization through interaction with the GDP-bound ARF substrate or other mechanisms. In this study, we address this question by means of SEC7 domain swaps between the cis-Golgi localized GNOM-LIKE 1 (GNL1) and TGN localized BIG3. A second set of experiments focuses on intramolecular domain interactions in GNOM. Despite numerous efforts, a crystal structure of full-length large ARF-GEFs so far remains elusive. As an alternative, the study of intramolecular domain interactions provides insight into the conformational requirements for ARF-GEF

function. Our results identify an additional regulatory function of the HDS1 domain and enhance the current model of regulation of ARF-GEF activity and membrane association.

RESULTS

BIG3 SEC7 domain does not affect GNL1 membrane and substrate specificity

Arabidopsis thaliana seeds harboring a T-DNA knockout mutation of *GNL1* are not able to successfully germinate when sown on medium containing Brefeldin A (BFA), a fungal toxin inhibiting activity of sensitive ARF-GEFs (Peyroche et al. 1999; Sata et al. 1999). In *Arabidopsis*, Golgi-ER retrograde vesicle traffic is jointly regulated by BFA-sensitive GNOM and BFA-resistant GNL1 (Richter et al. 2007). In *gnl1* seeds, GNOM function is eliminated by BFA without GNL1 being able to compensate. The resulting block of secretory traffic inhibits germination. In order to test the relevance of the SEC7 domain in regard to substrate and membrane specificity, we introduced a chimeric *GNL1* construct, where its SEC7 domain is replaced by the (also BFA-resistant) BIG3 SEC7 domain ($GNL1^{BIG3\text{-}SEC7}$), into *gnl1* plants and assessed its ability to rescue the germination phenotype. In two independent transgenic lines (1G and 2G), the germination ratio in the presence of 7µM BFA was restored to wild type levels (Figure 2A).

In addition to the severe BFA-induced phenotype, *gnl1* plants display general growth retardation. Although GNOM is available to coordinate Golgi-ER traffic, absence of GNL1 entails a reduced ARF-GEF dose negatively affecting secretory traffic. This becomes manifest in stunted growth and reduced fertility. Introduction of $GNL1^{BIG3\text{-}SEC7}$ rescued this phenotype (Figure 2B).

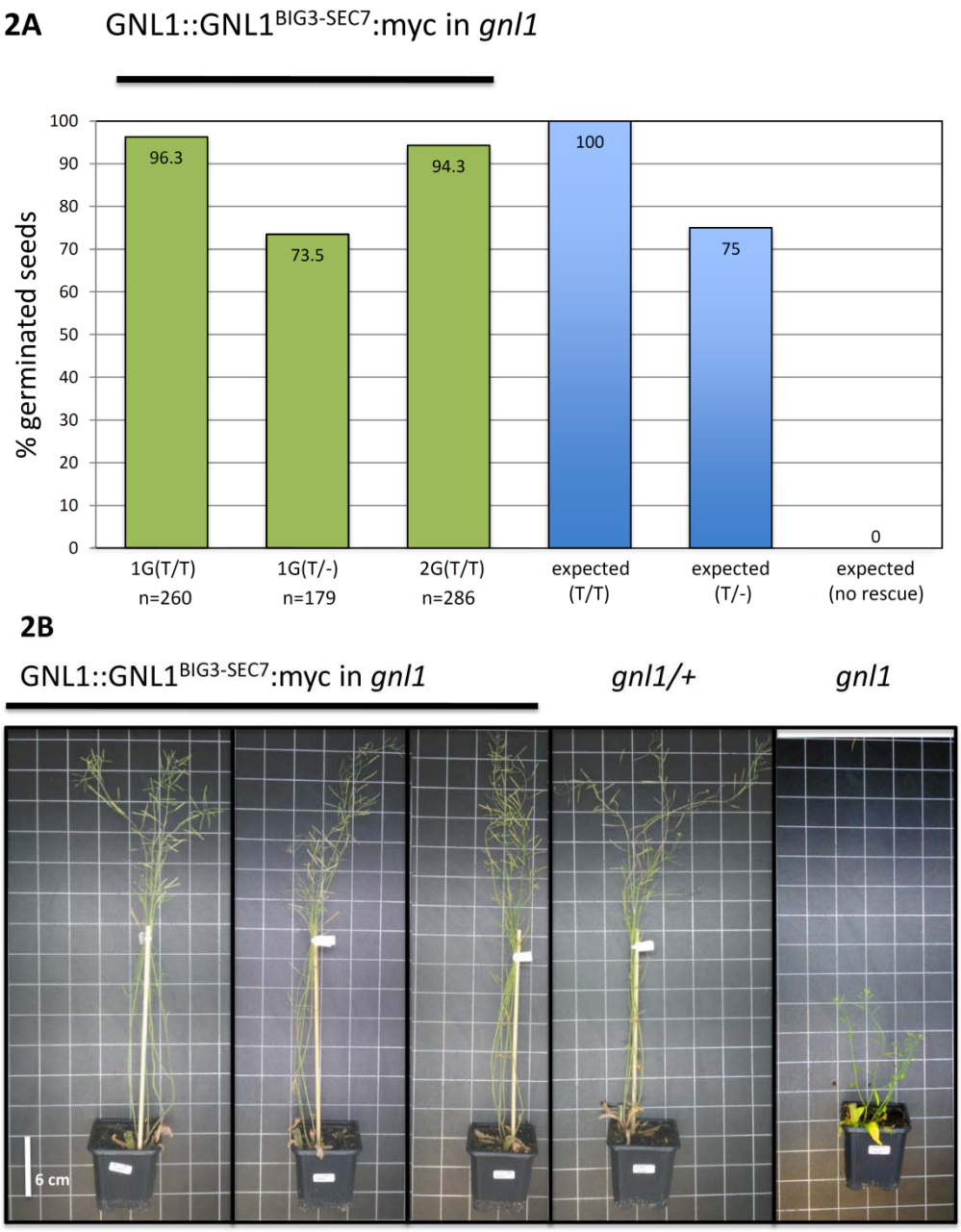

Figure 2. Rescue of *gnl1* by GNL1$^{BIG3\text{-}SEC7}$.

A *gnl1* BFA-induced germination deficiency rescued by GNL1$^{BIG3\text{-}SEC7}$. The germination ratio is restored to 94-96 percent in lines that are homozygous for the transgene (T/T) and to 74 percent in the heterozygous line (T/-). 7µM BFA; 6d. **B** *gnl1* stunted growth phenotype rescued by GNL1$^{BIG3\text{-}SEC7}$. Wild type represented by *gnl1*/+ heterozygous plant.

.

GNL1 SEC7 domain in BIG3: partial rescue of *big3* germination phenotype

In *Arabidopsis*, BIG1-4 redundantly regulate post-Golgi secretory traffic (Richter et al. 2014). BIG3 is resistant to BFA, whereas BIG1, 2 and 4 are sensitive. As in the case of GNOM and GNL1, knockout of the resistant ARF-GEF renders this specific step of secretory traffic vulnerable to inhibition by BFA. Consequently, *big3* mutant seeds display germination deficiency similar to *gnl1* when treated with BFA. We introduced a $BIG3^{GNL1\text{-}SEC7}$ swap construct into *big3* plants and tested it for rescue of the germination phenotype. In three independent transgenic lines, seeds were able to germinate in the presence of 5µM BFA (Figure 3A). However, the majority of seedlings exhibited stunted growth with short roots and small cotyledons compared to wild type, possibly reflecting insufficient expression or stability of the chimeric protein (Figure 3B).

3A

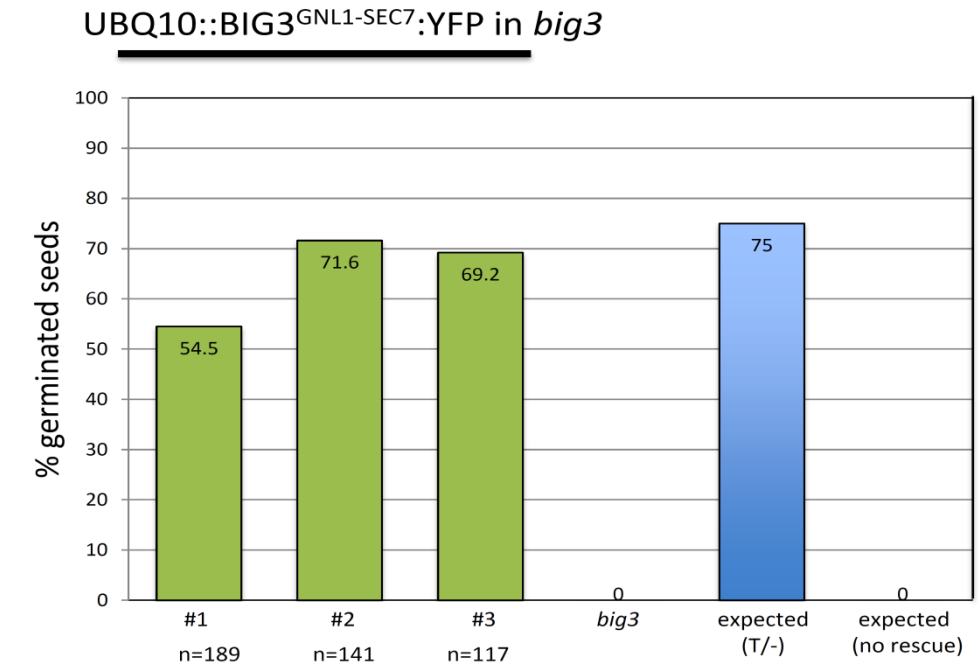

3B

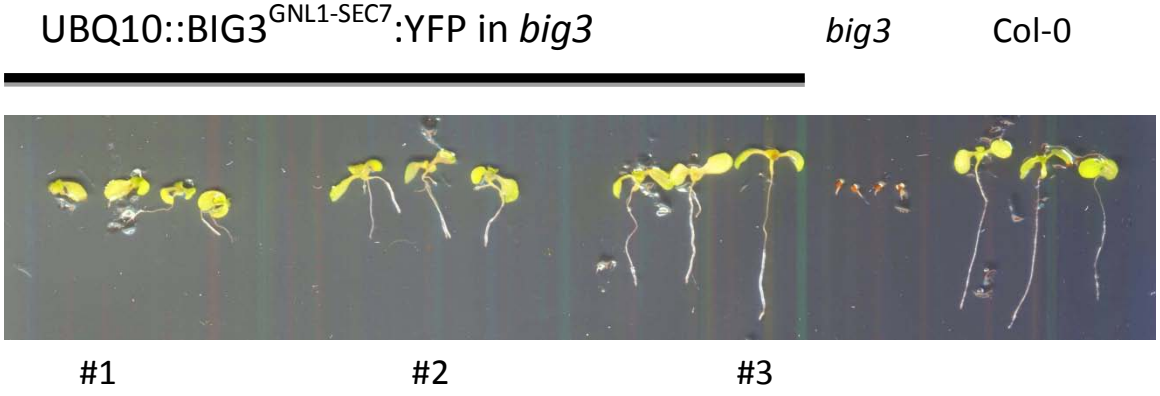

Figure 3. Rescue of big3 by BIG3$^{GNL1\text{-}SEC7}$.

A *big3* BFA-induced germination deficiency rescued by BIG3$^{GNL1\text{-}SEC7}$. Transgenic lines are heterozygous for the chimera construct (T/-). Germination ratios are restored to values slightly below the expected 75 percent in lines 2 and 3 and to a lower extent in line 1. 5µM BFA; 8d. **B** Partial rescue of *big3:* germinated seedlings are smaller and have shorter roots than wild type. 5µM BFA; 8d.

GNOM DCB domain strongly interacts with a C-terminal fragment of the protein

The N-terminal DCB domain of GNOM mediates homodimerization by homotypic interaction with other DCB domains (Grebe et al. 2000). A detailed study by Anders et al. (2008) revealed an additional interaction of the DCB domain with truncated GNOM lacking the DCB domain (GNOM-ΔDCB). Point mutations in conserved regions in the HUS (D486G, also "HUS-Box" mutation) and SEC7 (G579R) domains abolished this heterotypic interaction. These mutant alleles severely impair plant viability and compromise membrane association of GNOM. Thus, large ARF-GEF function may be regulated through cyclic conformational changes: a cytosolic form with its DCB domain folded back onto the HUS and SEC7 domains is competent for membrane tethering, whereas an open form is membrane-attached and catalytically active (Anders et al. 2008). In order to quantify the effects of these point mutations on the heterotypic DCB interactions, we performed a yeast-two-hybrid β-galactosidase activity assay comparing the relative interaction strength of the DCB domain with GNOM-ΔDCB, GNOM-ΔDCB^{G579R}, and GNOM-ΔDCB$^{HUS\text{-}BOX}$. Additionally, we included a fragment of GNOM lacking both the DCB and HUS domains (GNOM-SEC7-HDS) to further elucidate the backfolding mechanism. The experiment revealed a strong interaction of the DCB domain with GNOM-ΔDCB, but not with GNOM-ΔDCB^{G579R} and GNOM-ΔDCB$^{HUS\text{-}BOX}$, confirming the observations of Anders et al (2008). No interaction was detected for GNOM-SEC7-HDS, suggesting that the HUS domain is essential for the heterotypic interaction (Figure 4A).

GNL1 DCB domain also interacts with GNOM-ΔDCB

As mentioned above, GNL1 and GNOM are functionally interchangeable in the coordination of retrograde Golgi-ER traffic (Richter et al. 2007). However, GNOM has an additional regulatory function in endosomal recycling, particularly in polar plasma membrane distribution of the auxin efflux carrier PIN1. This is critical to establish the apical-basal polarity axis during *Arabidopsis* embryonic development (Steinmann et al. 1999; Geldner et al. 2001; Geldner et al. 2003). This endosomal function of GNOM cannot be compensated for by GNL1 (Richter et al. 2007). Also, heterodimers of GNOM and GNL1 could not be detected in co-immuno precipitation experiments (Singh, personal communication). Thus, despite their amino acid sequence similarity and joint action at the Golgi, there appear to be specific differences between GNOM and GNL1. To address the question of whether these are reflected in DCB

backfolding behavior, we tested the GNL1 DCB domain for interaction with GNOM fragments in a β-galactosidase activity assay. The results show that the GNL1 DCB domain can interact with GNOM-ΔDCB, although slightly weaker than GNOM DCB. Furthermore, this interaction is also inhibited by the HUS-Box and G579R mutations and dependent on the HUS domain (Figure 4B), suggesting that differences in specificity for membranes and / or substrates are achieved through other means.

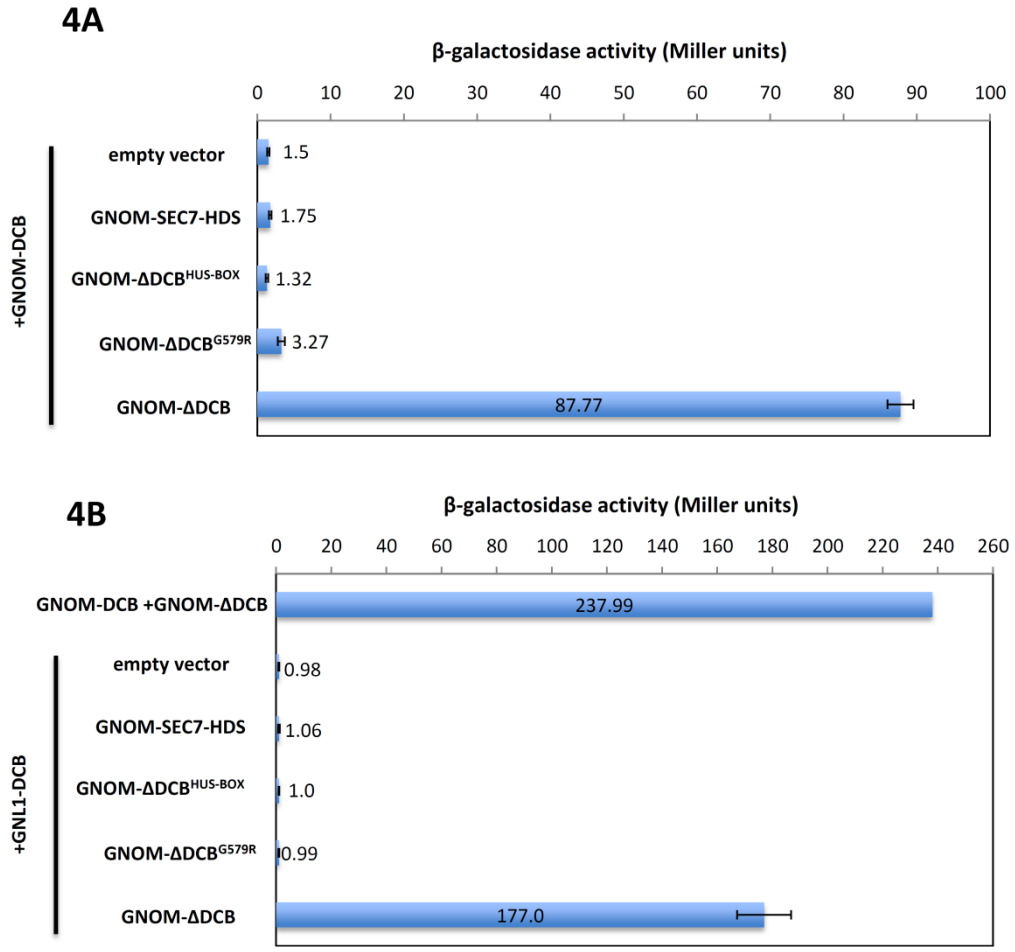

Figure 4. Quantitation of interaction strength between GNOM/GNL1 DCB domains and C-terminal fragments and alleles of GNOM by yeast two-hybrid β-galactosidase activity assay.

A Interaction of GNOM DCB with GNOM-ΔDCB, GNOM-ΔDCB^{G579R}, GNOM-ΔDCB$^{HUS-BOX}$ and GNOM-SEC7-HDS. Data shown as means ± SE; n=4. **B** Interaction of GNL1 DCB with GNOM-ΔDCB, GNOM-ΔDCB^{G579R}, GNOM-ΔDCB$^{HUS-BOX}$ and GNOM-SEC7-HDS. GNOM-DCB + GNOM-ΔDCB used as control. Data shown as means ± SE; n=4 (except GNOM-DCB + GNOM-ΔDCB: n=1).

The HDS1 domain is part of the backfolding interface

The previous experiments established that the HUS domain, and particularly the conserved HUS-Box motif, is an essential target for backfolding of the DCB domain. In order to identify additional domains that might be involved in this regulatory mechanism, we created fragments of GNOM-ΔDCB truncated after the SEC7 domain: One fragment consisting only of the HUS and SEC7 domains (HUS-SEC7), and two versions of HUS-SEC7-HDS1 (HUS-SEC7-HDS1_a and b) based on different domain annotations. These fragments were tested in a yeast two-hybrid X-Gal assay for interaction with the DCB domain. Interestingly, only HUS-SEC7-HDS1_b interacted with the DCB domain (Figure 5A). This fragment is 77aa longer than HUS-SEC7-HDS1_a, suggesting, since both constructs are stably expressed, the presence of a motif influencing the DCB interaction in this region. This is supported by the finding that HUS-SEC7 alone is not sufficient to bind the DCB domain.

Another question that we tried to address is whether a physical connection between certain domains is required for backfolding. In other words, where can you place the cut when you create fragments so that they are still able to interact? We cut GNOM between the HUS and SEC7 domain and tested a DCB-HUS fragment for interaction with SEC7-HDS and, originally thought to be a positive control, with DCB alone (Figure 5B). Surprisingly, DCB-HUS did not interact with DCB. Since the DCB domain interacts with the HUS domain, a possible explanation for this was an overly tight binding between the two domains in the DCB-HUS fragment, preventing the homotypic DCB-DCB interaction. To adjust for this possibility, we introduced the HUS-BOX mutation into the fragment, which would in theory alleviate the internal DCB-HUS binding. However, no interaction of DCB-HUS$^{HUS\text{-}BOX}$ with DCB could be observed (data not shown), suggesting an abnormal structure of the fragment. Accordingly, DCB-HUS did not interact with SEC7-HDS as well.

5A

GNOM Fragment	Amino acid range	Interaction with DCB	Expression GNOM fragment	Expression DCB
GNΔDCB	233-1451			
HUS-SEC7	227-775		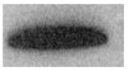	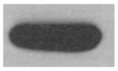
HUS-SEC7-HDS1_a	303-853		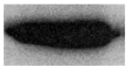	
HUS-SEC7-HDS1_b	303-930		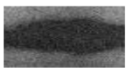	

5B

GNOM Fragment	Amino acid range	Interaction with DCB	Expression DCB-HUS	Expression DCB
DCB-HUS	1-561		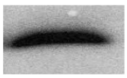	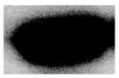
		Interaction with SEC7-HDS	Expression DCB-HUS	Expression SEC7-HDS
DCB-HUS	1-561		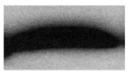	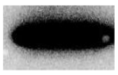

Figure 5. Analysis of interaction of intramolecular domain interactions in GNOM by yeast two-hybrid interaction assay.

A HUS-SEC7 and HUS-SEC7-HDS1 tested for interaction with DCB. Two representative yeast colonies are shown for each combination. Expression of fragments was confirmed via Western blot. Picture of GN+GNΔDCB taken from Anders et al., 2008 and included for clearness. **B** No interaction of DCB-HUS with DCB and SEC7-HDS. Two representative yeast colonies are shown for each combination. Expression of fragments was confirmed via Western blot.

A conserved motif in the HDS1 domain is essential for DCB backfolding

The observation that the HUS-SEC7-HDS1_b fragment, but not the 77aa shorter HUS-SEC7-HDS1_a fragment, can interact with the DCB domain (Figure 5A), pointed towards the presence of a DCB-binding motif in this 77aa region of the HDS1 domain. In their analysis of yeast SEC7p membrane recruitment by ARF1-GTP, Richardson et al. characterized several patches of conserved residues in the HDS1 domain in regard to their relevance for SEC7p function (Richardson et al. 2012). When mutated, one of these sequence patterns (ExxxKN1154), caused mislocalization of SEC7p to the cytoplasm, whereas a direct involvement in ARF1-GTP-mediated membrane recruitment could not be determined. Thus, it might play a role in DCB backfolding-dependent membrane association. The orthologous motif in GNOM (DExxxxxxxDxK857) is situated in the 77aa region of interest, making it a candidate for a DCB domain-binding motif (Figure 6A). We introduced triple and single alanine substitutions (D857A/E858A/K868A) into HUS-SEC7-HDS1_b, and additionally cloned a “minimal” version ending directly after the putative motif (aa303-869) in order to rule out that the remaining C-terminal part of the 77aa stretch is responsible for DCB binding. These fragments were then tested for interaction with the DCB domain in a yeast two-hybrid X-Gal assay (Figure 6B). Triple mutation of the pattern abolished the DCB interaction, whereas the single alanine substitution D857A had no negative effect. The E858A and K868A constructs could so far not be stably expressed in yeast. The minimal construct did not interact, raising the suspicion that the not-included conserved positively charged residue at position 870 (R870) might be required for DCB binding, although with present data we cannot rule out an involvement of the C-terminal part of the 77aa stretch. In any case, the DExxxxxxxDxK857 motif clearly participates in the DCB backfolding interface.

6A

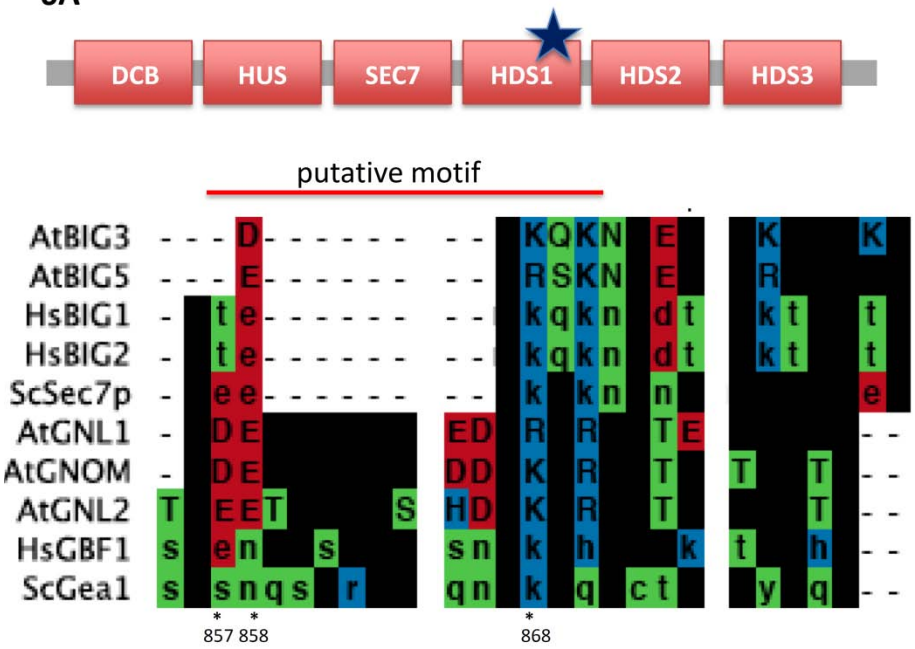

6B

HUS-SEC7-HDS1_b version	Amino acid range	Interaction with DCB	Expression HUS-SEC7-HDS1_b	Expression DCB
D857A/E858A/K868A	303-930			
D857A	303-930			
E858A	303-930			
K868A	303-930			
minimal	303-869		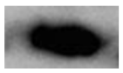	

Figure 6. Characterization of the “HDS1-Box” motif and its role in DCB backfolding.

A The motif of interest is situated at the C-terminal end of the HDS1 domain. Alignment of amino acid sequences of large ARF-GEFs from human, yeast and *Arabidopsis* shows the conservation of possibly critical residues. Note the central expansion of the motif in GBF1 class ARF-GEFs compared to the BIG1 class. Positions of residues analyzed in this study are depicted by asterisks. Polarity colors. **B** Test for interaction of mutated versions of HUS-SEC7-HDS1_b with DCB by yeast two-hybrid X-Gal assay. Two representative yeast colonies shown for each combination. Expression was confirmed via Western blot.

DISCUSSION

In this study, we analyzed potential involvement of different domains of large ARF-GEFs in the regulation of membrane association and substrate specificity.

In the case of cis-Golgi-localized GNL1 and TGN-localized BIG3, swapping the SEC7 domains did not eliminate functionality of the respective ARF-GEF, suggesting that neither membrane nor substrate specificity is conferred by the SEC7 domain. However, recent observations indicate that GNL1 and BIG3 both use ARF1 as substrate (Singh, personal communication), which is consistent with ARF1 localizing at both Golgi and TGN (Stierhof and El Kasmi 2010). In light of this fact, an adverse effect of the domain swap on substrate activation is not to be expected. Nonetheless, it cannot be ruled out that the varying extents of rescue ability displayed by GNL1$^{BIG3\text{-}SEC7}$ (full rescue) and BIG3$^{GNL1\text{-}SEC7}$ (partial rescue) are due to a more complex scenario: Proper regulation of post-Golgi trafficking by BIG3 might depend on activation of an additional ARF GTPase that cannot interact with the GNL1 SEC7 domain, resulting in only partial rescue of *big3* by BIG3$^{GNL1\text{-}SEC7}$. The same is conceivable for membrane specificity: TGN localization of BIG3$^{GNL1\text{-}SEC7}$ might be reduced or unstable. However, low levels of the chimeric protein are more likely the cause of the suboptimal rescue, as use of BIG3-based constructs often entails protein stability problems. Analysis of expression and subcellular localization of the chimeras will resolve these issues.

As revealed by the yeast two-hybrid interaction experiments, the DCB domain of GNOM heterotypically interacts with a fragment comprising the HUS, SEC7, and HDS1 domains. Neither SEC7-HDS1-3 nor HUS-SEC7 was sufficient to interact with DCB, contrary to reports for mammalian GBF1, where a weak interaction between DCB and HUS-SEC7 was observed in a semi-quantitative yeast two-hybrid leucine growth assay (Ramaen et al. 2007). Our qualitative blue / white assay might not be sensitive enough to discover such a small-scale interaction. Use of a quantitative β-galactosidase activity assay will clarify whether this is true, or whether there are differences between plants and animals in regard to heterotypical domain interactions of large ARF-GEFs. In any case, a robust DCB interaction appears to require the presence of both domains flanking the SEC7 domain.

In addition to previously described critical motifs in the HUS and SEC7 domains (Ramaen et al. 2007; Anders et al. 2008), we identified a conserved region at the C-terminal end of the HDS1 domain that is essential for DCB backfolding. While triple alanine substitutions in this motif abolished the DCB interaction, the role of individual amino acid residues is not yet clear. Anders et al. proposed a model of conformational regulation of large ARF-GEF function through cyclic changes between a closed cytosolic form that is competent for membrane tethering, and a catalytically active membrane-associated form. This mechanism would allow for reversible membrane recruitment of large ARF-GEFs, and thus for control of their activity in space and time. In the cytosolic form, the DCB folds back onto the HUS and SEC7 domains. With our findings, this model is enhanced by the added involvement of the HDS1 domain, suggesting a conformation where the catalytic SEC7 domain is shielded by the surrounding domains (Figure 7). This would prevent inadvertent interaction with other proteins in the cytosol, such as ARF substrates, thereby restricting ARF-GEF activity to membranes.

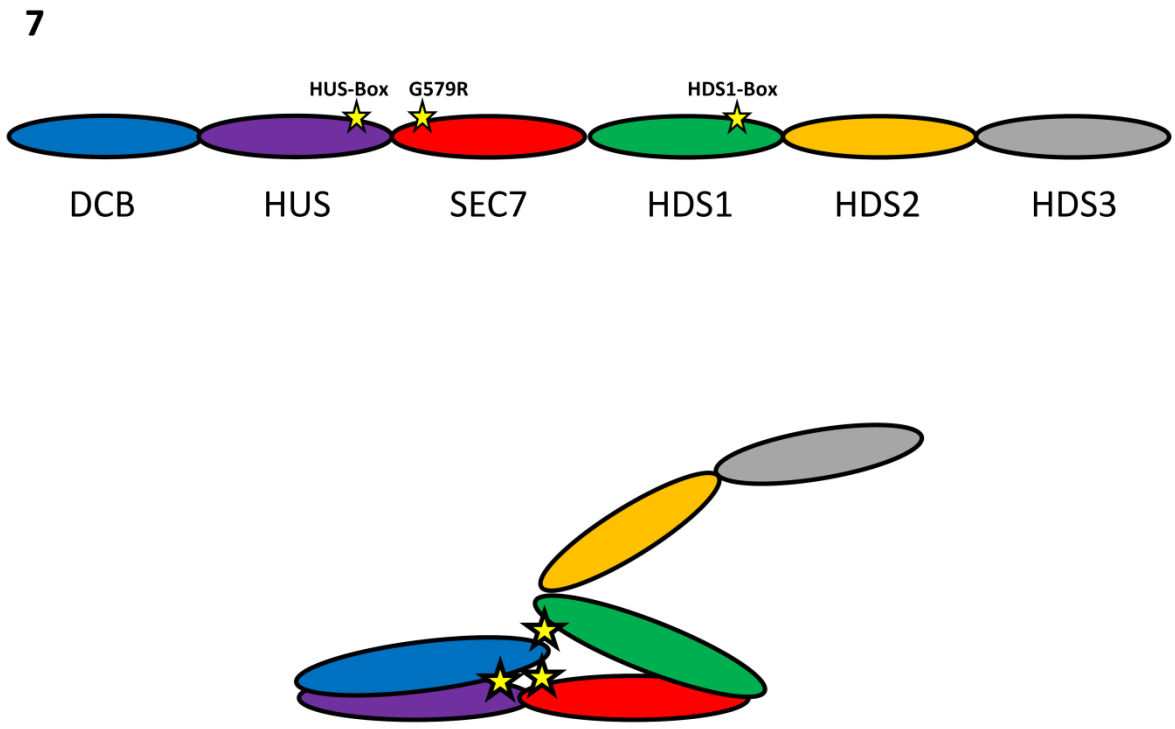

Figure 7. Closed cytosolic form of large ARF-GEFs, inspired by Anders et al., 2008. The DCB, HUS, and HDS1 domains form a cover over the catalytic center of the SEC7 domain. Stars depict motifs in the HUS, SEC7 and HDS1 domains involved in DCB backfolding.

However, whether the critical motifs are actually part of the interaction interface or rather passively influence the conformation is debatable. The mutations introduced into the HDS1 motif (D857A, E858A, and K868A) and the HUS-Box (D486G), substitute charged amino acid residues for uncharged residues. Charged amino acids often interact with each other through the formation of salt bridges, conferring stability to energetically unfavorable folded conformations of proteins. The G579R mutation situated in the SEC7 domain exchanges glycine for a charged arginine residue. Glycine is known to provide structural flexibility to protein regions. Therefore, in this case the substitution does not cause loss of charged amino acid interaction, but might lead to a structural disturbance passively hindering DCB backfolding.

Nonetheless, the findings of the yeast two-hybrid experiments need to be followed up *in planta*. An HDS1-Box mutant of GNOM or another ARF-GEF should be tested for loss of functionality, particularly for deficient membrane recruitment, since DCB backfolding is a prerequisite for membrane association. A further interesting implication is that the first four domains might be sufficient for large ARF-GEF function. All known alleles of *GNOM* with mutations in the HDS domains cause only weak phenotypes and are based on premature stop codons in the HDS2 or 3. The resulting truncated gene products are less stable than wild type protein, suggesting that the weak phenotype is caused by low protein levels rather than loss of functionality. One of these alleles, $gnom^{SIT4}$, produces a protein truncated in the HDS2 domain after amino acid 983, and the $gnom^{R5}$ product lacks a short part of the HDS3 domain (Geldner et al. 2004). Truncation of the HDS3 domain in a mutant allele of *GNL1 (gnl1-3)* also leads to a mild phenotype (Teh and Moore 2007). In summary, the HDS2 and 3 domains affect protein stability and attenuate the catalytic activity by autoinhibition (Richardson et al. 2012; McDonold and Fromme 2014), but they do not seem to have an essential function. In our yeast two-hybrid experiments, the HUS-SEC7-HDS1 fragment ending at amino acid 930 was stably expressed and sufficient to accomplish DCB backfolding. Although it is 53 amino acids shorter than $GNOM^{SIT4}$, a DCB-HUS-SEC7-HDS1 fragment might be stable when introduced into plants. Assessment of the performance of the fragment will help to confine essential large ARF-GEF abilities like membrane association and substrate specificity to specific domains. The reduced size of the fragment (provided that it is functional) might also facilitate obtaining a crystal structure, which could provide further insight into conformational regulation of large ARF-GEFs.

MATERIALS AND METHODS

Plant Material and growth conditions

Arabidopsis thaliana wild type (ecotype Col-0), mutant and transgenic lines, after surface sterilisation, were grown on Murashige and Skoog (MS) medium containing 1% (w/v) sucrose and 0.8% (w/v) agar in continuous light at 23°C. After stratification for 2 nights at 4°C in the dark, plates were transferred to growth chamber. Seedlings were transferred to soil 8-10 days after germination and grown in same conditions.

Seed germination assay

For the germination analysis of GNL1$^{BIG3\text{-}SEC7}$, seeds from plants heterozygous or homozygous for the transgene and homozygous for the *gnl1* T-DNA insertion, and seeds from *gnl1* homozygous and wild type plants were sown on MS medium containing 5 µM BFA and stratified for 2 days at 4°C in the dark before transfer to growth chamber. Germinated seeds were counted 6 days after transfer.

For the germination analysis of BIG3$^{GNL1\text{-}SEC7}$, seeds from plants heterozygous or homozygous for the transgene and homozygous for the *big3* T-DNA insertion, and seeds from *big3* homozygous and wild type plants were sown on MS medium containing 7 µM BFA and stratified for 2 days at 4°C in the dark before transfer to growth chamber. Germinated seeds were counted 8 days after transfer.

Yeast two-hybrid-protein interaction analysis

For yeast two-hybrid analysis, yeast (EGY48 strain) was transformed with the reporter plasmid psH18-34, and the bait and prey constructs based on pEG202 and pJG4-5. The interaction assay was performed as reported previously (Anders et al. 2008; Park et al. 2012).

Western blotting

Proteins were resolved on SDS-PAGE and immuno-detected using one of the following antibodies: anti-LexA (mouse, 1: 1000, Santa Cruz Biotechnology), POD-conjugated anti-HA (1:1000, Roche).

Softwares

CLC DNA Workbench 6 was used for DNA sequences analysis. For image processing Adobe Photoshop CS3 and Adobe Illustrator CS3 were used.

REFERENCES

Anders, N., M. Nielsen, et al. (2008). "Membrane association of the Arabidopsis ARF exchange factor GNOM involves interaction of conserved domains." Plant Cell **20**(1): 142-151.

Casanova, J. E. (2007). "Regulation of Arf activation: the Sec7 family of guanine nucleotide exchange factors." Traffic **8**(11): 1476-1485.

Christis, C. and S. Munro (2012). "The small G protein Arl1 directs the trans-Golgi-specific targeting of the Arf1 exchange factors BIG1 and BIG2." J Cell Biol **196**(3): 327-335.

Geldner, N., N. Anders, et al. (2003). "The Arabidopsis GNOM ARF-GEF mediates endosomal recycling, auxin transport, and auxin-dependent plant growth." Cell **112**(2): 219-230.

Geldner, N., J. Friml, et al. (2001). "Auxin transport inhibitors block PIN1 cycling and vesicle trafficking." Nature **413**(6854): 425-428.

Geldner, N., S. Richter, et al. (2004). "Partial loss-of-function alleles reveal a role for GNOM in auxin transport-related, post-embryonic development of Arabidopsis." Development **131**(2): 389-400.

Grebe, M., J. Gadea, et al. (2000). "A conserved domain of the arabidopsis GNOM protein mediates subunit interaction and cyclophilin 5 binding." Plant Cell **12**(3): 343-356.

McDonold, C. M. and J. C. Fromme (2014). "Four GTPases differentially regulate the Sec7 Arf-GEF to direct traffic at the trans-golgi network." Dev Cell **30**(6): 759-767.

Mouratou, B., V. Biou, et al. (2005). "The domain architecture of large guanine nucleotide exchange factors for the small GTP-binding protein Arf." BMC Genomics **6**: 20.

Park, M., S. Touihri, et al. (2012). "Sec1/Munc18 protein stabilizes fusion-competent syntaxin for membrane fusion in Arabidopsis cytokinesis." Dev Cell **22**(5): 989-1000.

Peyroche, A., B. Antonny, et al. (1999). "Brefeldin A acts to stabilize an abortive ARF-GDP-Sec7 domain protein complex: involvement of specific residues of the Sec7 domain." Mol Cell **3**(3): 275-285.

Ramaen, O., A. Joubert, et al. (2007). "Interactions between conserved domains within homodimers in the BIG1, BIG2, and GBF1 Arf guanine nucleotide exchange factors." J Biol Chem **282**(39): 28834-28842.

Richardson, B. C., C. M. McDonold, et al. (2012). "The Sec7 Arf-GEF is recruited to the trans-Golgi network by positive feedback." Dev Cell **22**(4): 799-810.

Richter, S., N. Geldner, et al. (2007). "Functional diversification of closely related ARF-GEFs in protein secretion and recycling." Nature **448**(7152): 488-492.

Richter, S., M. Kientz, et al. (2014). "Delivery of endocytosed proteins to the cell-division plane requires change of pathway from recycling to secretion." Elife **3**: e02131.

Sata, M., J. Moss, et al. (1999). "Structural basis for the inhibitory effect of brefeldin A on guanine nucleotide-exchange proteins for ADP-ribosylation factors." Proc Natl Acad Sci U S A **96**(6): 2752-2757.

Steinmann, T., N. Geldner, et al. (1999). "Coordinated polar localization of auxin efflux carrier PIN1 by GNOM ARF GEF." Science **286**(5438): 316-318.

Stierhof, Y. D. and F. El Kasmi (2010). "Strategies to improve the antigenicity, ultrastructure preservation and visibility of trafficking compartments in Arabidopsis tissue." Eur J Cell Biol **89**(2-3): 285-297.

Teh, O. K. and I. Moore (2007). "An ARF-GEF acting at the Golgi and in selective endocytosis in polarized plant cells." Nature **448**(7152): 493-496.

6 Diskussion

Eine Besonderheit pflanzlicher Zellen ist die Eigenschaft des TGN als frühes Endosom (EE) (Dettmer et al. 2006; Viotti et al. 2010), was dieses Kompartiment mehr als in nichtpflanzlichen Organismen zum Schnittpunkt bedeutender intrazellulärer Transportwege macht und gleichzeitig deren Analyse erschwert. Unsere Ergebnisse legen nahe, dass der auf Reifung des frühen zum späten Endosom basierende Proteintransport vom TGN zur lytischen Vakuole (Scheuring et al. 2011) in Pflanzen und anderen Organismen zeitlich unterschiedlich reguliert wird, während die grundlegenden Prozesse konserviert sind: Einerseits müssen die für die späten Endosomen (LEs / MVBs) typischen intraluminalen Vesikel (ILVs) gebildet werden, die die spätere Freisetzung membrangebundener Proteine in das Innere der Vakuole ermöglichen. Dies wird durch die Komponenten der ESCRT-Maschinerie bewerkstelligt: ESCRT-0 sammelt ubiquitinierte Cargoproteine, ESCRT-I und II leiten die Bildung der Vesikelknospe ein und ESCRT-III die Abtrennung des Vesikels (Hurley und Hanson 2010). Zweitens muss sich die Membrankomposition des Endosoms ändern, um die Kompetenz für die Fusion mit der Vakuole herzustellen. Hierfür spielt der von dem heterodimeren RAB-GEF SAND/CCZ1 vermittelte Austausch von RAB 5/F durch RAB 7/G an der Membran eine wichtige Rolle (Rink et al. 2005; Poteryaev et al. 2010). Diese RAB-Konversion ist bei Säugetieren und Hefen essentiell für die Entstehung des LE. Wie wir zeigen konnten, bildet sich in Pflanzenzellen das LE/MVB auch in funktionslosen *sand*-Mutanten und bei konstitutiver Aktivität von RAB 5/F. Das Fehlen von RAB7/G an der MVB-Membran in *sand* scheint jedoch die Fusion mit der Vakuole zu verhindern. Während also in tierischen Zellen ILV-Bildung und RAB-Konversion mehr oder weniger simultan ablaufen und für das Hervorgehen des späten Endosoms aus dem frühen voraussetzend sind, sind sie bei Pflanzen entkoppelt und in unterschiedlichen endosomalen Reifungsstadien von Bedeutung. Diese regulatorischen Besonderheiten reflektieren vermutlich die Unterschiede in Bezug auf das Endomembransystem bei Tieren und Pflanzen: Während das pflanzliche LE/MVB aus einer größeren Struktur, dem TGN, abknospt, geht das tierische LE aus einer Umwandlung eines separaten EE hervor. Bestimmte chemische Parameter, die bei der endosomalen Reifung ein Rolle spielen, wie zum Beispiel eine Senkung des pH-Werts oder eine Änderung der Ca^{2+}-Konzentration zwischen LE und EE (Martinez-Munoz und Kane 2008; Shen et al. 2013), lassen sich in Pflanzenzellen

möglicherweise erst nach der Abspaltung des MVBs einstellen, so dass die Kompetenz für die Fusion mit der Vakuole hier erst dann erzeugt wird. Damit in Einklang stehen Hinweise auf die Existenz eines zusätzlichen, zwischen MVB und Vakuole stehenden Endosoms in *Nicotiana* (Foresti et al. 2010). Dieses könnte eine spätere Reifungsphase repräsentieren.

Dem auf endosomaler Reifung beruhenden Proteintransport steht der klassische Vesikeltransport gegenüber. Ein entscheidender regulatorischer Schritt bei der Bildung von Vesikeln ist die Aktivierung von ARF-GTPasen (ARFs) durch große ARF-GEFs (Casanova 2007). Aktivierte ARFs rekrutieren Hüllproteine zum Ort der Vesikelknospung, die Cargo selektieren und die Donormembran modifizieren. In dieser Arbeit konnte gezeigt werden, dass die ARF-GEFs BIG1-4 essentiell für die sekretorischen (PM-gerichteten) und vakuolären Routen des post-Golgi-Transports sind. Davon abzugrenzen ist die Rezyklierung von endocytierten Proteinen zur PM, die – zumindest teilweise - durch den ARF-GEF GNOM vermittelt wird. Die durch Funktionsverlust von BIG1-4 verursachte cytosolische Fehllokalisation der Untereinheit AP1M2 des Adaptorkomplexes AP-1 legt nahe, dass BIG1-4 die Bildung von Clathrin-umhüllten Vesikeln (CCVs) regulieren. Für deren Beteiligung am vakuolären Proteintransport gibt es Pro- und Kontra-Argumente (Song et al. 2006; Scheuring et al. 2011; Park et al. 2013; Sauer et al. 2013). Ein abschließendes Urteil ist zu diesem Zeitpunkt nicht möglich. Unsere Beobachtung, dass BIG1-4 notwendig für die Lieferung von sowohl löslichen Proteinen als auch endocytierten PM-Proteinen zur Vakuole sind, wirft die Frage auf, wie der Transport entlang dieser Route im Detail abläuft. Eine Möglichkeit ist, dass es mehrere Wege vom TGN zur Vakuole gibt: Neben der MVB-Reifung könnte es auch Vesikeltransport vom TGN zur Vakuole und / oder zum MVB geben, was auch die Abhängigkeit von Clathrin-Adaptorkomplexen erklären würde (Song et al. 2006; Park et al. 2013; Sauer et al. 2013). Ein anderes Szenario, das die fehlende kompetitive Hemmung des vakuolären Transport durch eine inaktive Clathrin-Käfig-Komponente einbezieht (Scheuring et al. 2011), beinhaltet, dass zwischen den einzelnen Subdomänen des TGNs gerichteter Vesikeltransport stattfindet. Ein Funktionsverlust von BIG1-4 würde diesen und damit die strukturelle Integrität des TGNs zusammenbrechen lassen, was in der Folge auch die Entstehung von MVBs verhindern würde. Weitere Analysen sind notwendig, um hier Licht ins Dunkel zu bringen.

In jedem Fall scheint es aber mehrere CCV-getragene, BIG1-4-abhängige Vesikeltransportwege am TGN zu geben. Wie wird unterschieden zwischen PM-gerichteten CCVs und solchen, die an der vakuolären Route beteiligt sind? Als Spezifität verleihende Faktoren kommen vor allem die Komponenten der Vesikelbildungsmaschinerie in Frage, also ARF-GEFs, ARF-GTPasen und Hüllproteine. Neben dem aus je drei schweren und leichten Proteinketten bestehenden Clathrin-Triskelion enthält eine Clathrinhülle spezifische heterotetramere Adaptorprotein (AP)-Komplexe. AP-1 und AP-3 sind im vakuolären Transport involviert, und AP-1 zusätzlich im PM-Transport (Feraru et al. 2010; Zwiewka et al. 2011; Park et al. 2013). AP-Komplexe werden von aktivierten ARFs rekrutiert und interagieren außerdem mit Cargo-Molekülen. Beide könnten also die Zusammensetzung der Vesikelhülle beeinflussen und damit Spezifität für bestimmte Transportrouten erzeugen. Eine mögliche Präferenz von ARF-GEFs für bestimmte ARF-Substrate wurde bis jetzt nicht demonstriert. ARF1 wurde jedoch sowohl am cis-Golgi als auch am TGN nachgewiesen (Stierhof und El Kasmi 2010), und Co-Immunopräzipitationsexperimente legen eine Aktivierung von ARF1 durch sowohl GNOM als auch BIG1-4 nahe (Singh, persönliche Mitteilung), was gegen eine Substratspezifität der ARF-GEFs spricht. Auch unsere Untersuchungen an chimären ARF-GEFs, bei denen die katalytische SEC7-Domäne zwischen an unterschiedlichen Vesikeltransportwegen beteiligten ARF-GEFs ausgetauscht wurde (GNL1$^{BIG3\text{-}SEC7}$ und BIG3$^{GNL1\text{-}SEC7}$), ergaben keine starken Hinweise in diese Richtung. Allerdings läßt sich bei der jetzigen Datenlage eine Beteiligung eines weiteren ARFs zumindest bei der BIG1-4-vermittelten Vesikelbildung nicht ausschließen, da BIG3$^{GNL1\text{-}SEC7}$ den Funktionsverlust von BIG1-4 nur partiell kompensieren konnte. Rein theoretisch könnten also durch ARF1 und eine unbekannte ARF-GTPase nach ihrer Aktivierung durch BIG1-4 am TGN jeweils andere Adaptorproteine rekrutiert werden und damit unterschiedliche Clathrin-umhüllte Vesikel gebildet werden. In *Saccharomyces* wurde eine Bindung von ARF1 und AP-1 an das Phospholipid Phosphatidylinositol-4-Phosphat (PI4P) nachgewiesen, das in TGN-Membranen angereichert ist (Wang et al. 2003). Es ist vorstellbar, dass einzelne Subdomänen des TGN eine unterschiedliche Membrankomposition aufweisen, die die Rekrutierung von spezifischen, die Vesikelbildung regulierenden Faktoren vermittelt. Die steigende mikroskopische Auflösung wird in Zukunft eine Charakterisierung der Subdomänen, für deren Existenz es bis jetzt nur indireke Hinweise gibt, ermöglichen; und weitere

Interaktionsstudien und Analysen von chimären Proteinen sowie die Charakterisierung der Phänotypen von *arf*-Mutanten werden klären, ob möglicherweise alle (großen) ARF-GEFs ARF1 aktivieren und welche Rolle die anderen ARF-Untergruppen im intrazellulären Vesikeltransport spielen.

Während die katalytische SEC7-Domäne der großen ARF-GEFs möglicherweise keine Rolle bei der Erzeugung von Spezifität spielt, gibt es Hinweise darauf, dass die nicht-katalytischen Domänen Einfluss auf die Konditionen der ARF-Aktivierung nehmen. Die N-terminalen Domänen DCB und HUS vermitteln durch Interaktion mit der ARF-ähnlichen GTPase ARL1 die TGN-Rekrutierung von *Drosophila*-SEC71 (Christis und Munro 2012); und aktiviertes ARF1 rekrutiert in *Saccharomyces* durch Bindung in der HDS1-Domäne den ARF-GEF SEC7p an die TGN-Membran (Richardson et al. 2012). Die DCB-Domäne vermittelt zudem die Homodimerisierung des ARF-GEFs GNOM (Grebe et al. 2000) und interagiert außerdem mit dem Rest des Proteins. Diese Rückfaltung der DCB-Domäne ist notwendig für die Membranassoziation von GNOM (Anders et al. 2008). Bereiche in den HUS- und SEC7-Domänen beeinflussen die Rückfaltung. GNOM scheint demzufolge eine spezielle geschlossene cytosolische Konformation anzunehmen, an der die DCB-, HUS- und SEC7-Domänen beteiligt sind (Anders et al. 2008). Im Rahmen dieser Arbeit konnten wir zeigen, dass hierbei auch die C-terminal der SEC7-Domäne gelegene HDS1-Domäne involviert ist, während die folgenden HDS2- und HDS3-Domänen keine Rolle spielen. Der biologische Zweck dieser Konformation könnte darin liegen, dass die katalytische SEC7-Domäne im Cytosol durch ihre Nachbardomänen bedeckt und dadurch gegen eine Interaktion mit ARF-Substraten abgeschirmt wird. Strukturelle Daten legen nahe, dass der von ARF-GEFs vermittelte Austausch des ARF-gebundenen GDPs durch GTP nur an der Membran erfolgen kann (Cherfils und Melancon 2005). Trotzdem könnte die bei einer offenen cytosolischen Konformation des ARF-GEFS mögliche vorzeitige Interaktion mit ARF nachteilig für die Zelle sein, umso mehr, wenn die SEC7-Domäne selbst keine Selektion von Substraten leisten kann. Es erscheint also sinnvoll, dass die nicht-katalytischen Domänen die Bindung an spezifische Membranen und Substrate vermitteln und erst dann die SEC7-Domäne für die katalytische Reaktion freigeben. Außerdem könnte durch den Wechsel zwischen zwei Konformationen eine reversible Membranassoziation des ARF-GEFs ermöglicht werden, und damit eine weitere Option für die Feinabstimmung der Austauschaktivität. Die zitierten und die von uns

erzielten Ergebnisse in Bezug auf die intramolekularen Interaktionen von ARF-GEF-Domänen beruhen auf Studien an GNOM, einem Mitglied der GBF1-verwandten Unterfamilie der großen ARF-GEFs. Interessant wäre die Überprüfung eines ähnlichen Rückfaltungsmechanismus bei den BIG1-verwandten Austauschfaktoren. Bei menschlichem BIG1 wurde eine Interaktion der DCB-Domäne mit verschiedenen anderen Domänen gezeigt (Ramaen et al. 2007); die jedoch nicht in jedem Detail der Rückfaltung bei GNOM entspricht. Weitere Analysen der heterotypischen Interaktionen und die Untersuchung mutanter ARF-GEFs *in planta* werden die mögliche allgemeine Bedeutung dieser Konformation in der Regulation der Aktivität von großen ARF-GEFs klären.

7 Eigenanteil an den Publikationen

Publikation Richter et al., 2014

Delivery of endocytosed proteins to the cell-division plane requires change of pathway from recycling to secretion

Eigenanteil: Herstellung des BIG3::BIG3-YFP-Konstrukts.

Publikation Singh et al., 2014

Protein delivery to vacuole requires SAND protein-dependent Rab GTPase conversion for MVB-vacuole fusion.

Eigenanteil: Herstellung der CCZ1- und ARA7-QL-Konstrukte für die Yeast Two- und Three-Hybrid-Interaktionsexperimente sowie deren Durchführung und Auswertung. Bearbeitung von Teilen des Manuskripts.

Manuskript Beckmann et al., 2015

Function of protein domains in large ARF-GEF regulation

Eigenanteil: Mit Ausnahme der GN-DCB-, GN-ΔDCB (mutant und wildtypisch)- und SEC7-HDS-Konstrukte wurden alle Konstrukte von mir hergestellt. Alle Experimente, die Interpretation der Egebnisse und das Verfassen des Manuskripts wurden von mir durchgeführt.

8 Literaturverzeichnis

Anders, N. and G. Jürgens (2008). "Large ARF guanine nucleotide exchange factors in membrane trafficking." Cell Mol Life Sci **65**(21): 3433-3445.

Anders, N., M. Nielsen, J. Keicher, Y. D. Stierhof, M. Furutani, M. Tasaka, K. Skriver and G. Jurgens (2008). "Membrane association of the Arabidopsis ARF exchange factor GNOM involves interaction of conserved domains." Plant Cell **20**(1): 142-151.

Antonny, B., S. Beraud-Dufour, P. Chardin and M. Chabre (1997). "N-terminal hydrophobic residues of the G-protein ADP-ribosylation factor-1 insert into membrane phospholipids upon GDP to GTP exchange." Biochemistry **36**(15): 4675-4684.

Bassham, D. C. and M. R. Blatt (2008). "SNAREs: cogs and coordinators in signaling and development." Plant Physiol **147**(4): 1504-1515.

Blomberg, N., E. Baraldi, M. Nilges and M. Saraste (1999). "The PH superfold: a structural scaffold for multiple functions." Trends Biochem Sci **24**(11): 441-445.

Bonifacino, J. S. (2004). "The GGA proteins: adaptors on the move." Nat Rev Mol Cell Biol **5**(1): 23-32.

Braulke, T. and J. S. Bonifacino (2009). "Sorting of lysosomal proteins." Biochim Biophys Acta **1793**(4): 605-614.

Bucci, C., R. G. Parton, I. H. Mather, H. Stunnenberg, K. Simons, B. Hoflack and M. Zerial (1992). "The small GTPase rab5 functions as a regulatory factor in the early endocytic pathway." Cell **70**(5): 715-728.

Casanova, J. E. (2007). "Regulation of Arf activation: the Sec7 family of guanine nucleotide exchange factors." Traffic **8**(11): 1476-1485.

Charych, E. I., W. Yu, C. P. Miralles, D. R. Serwanski, X. Li, M. Rubio and A. L. De Blas (2004). "The brefeldin A-inhibited GDP/GTP exchange factor 2, a protein involved in vesicular trafficking, interacts with the beta subunits of the GABA receptors." J Neurochem **90**(1): 173-189.

Cherfils, J. and P. Melancon (2005). "On the action of Brefeldin A on Sec7-stimulated membrane-recruitment and GDP/GTP exchange of Arf proteins." Biochem Soc Trans **33**(Pt 4): 635-638.

Christis, C. and S. Munro (2012). "The small G protein Arl1 directs the trans-Golgi-specific targeting of the Arf1 exchange factors BIG1 and BIG2." J Cell Biol **196**(3): 327-335.

Cox, R., R. J. Mason-Gamer, C. L. Jackson and N. Segev (2004). "Phylogenetic analysis of Sec7-domain-containing Arf nucleotide exchangers." Mol Biol Cell **15**(4): 1487-1505.

Dettmer, J., A. Hong-Hermesdorf, et al. (2006). "Vacuolar H+-ATPase activity is required for endocytic and secretory trafficking in Arabidopsis." Plant Cell **18**(3): 715-730.

Desnoyers, L., J. S. Anant and M. C. Seabra (1996). "Geranylgeranylation of Rab proteins." Biochem Soc Trans **24**(3): 699-703.

Duden, R. (2006). Vesicular Traffic. Encyclopedic Reference of Genomics and Proteomics in Molecular Medicine, Springer Berlin Heidelberg**:** 1977-1982.

Ebine, K., M. Fujimoto, Y. Okatani, T. Nishiyama, T. Goh, E. Ito, T. Dainobu, A. Nishitani, T. Uemura, M. H. Sato, H. Thordal-Christensen, N. Tsutsumi, A. Nakano and T. Ueda (2011). "A membrane trafficking pathway regulated by the plant-specific RAB GTPase ARA6." Nat Cell Biol **13**(7): 853-859.

Echard, A., F. Jollivet, O. Martinez, J. J. Lacapere, A. Rousselet, I. Janoueix-Lerosey and B. Goud (1998). "Interaction of a Golgi-associated kinesin-like protein with Rab6." Science **279**(5350): 580-585.

Faini, M., R. Beck, F. T. Wieland and J. A. Briggs (2013). "Vesicle coats: structure, function, and general principles of assembly." Trends Cell Biol **23**(6): 279-288.

Feraru, E., T. Paciorek, et al. (2010). "The AP-3 beta adaptin mediates the biogenesis and function of lytic vacuoles in Arabidopsis." Plant Cell **22**(8): 2812-2824.

Foresti, O., D. C. Gershlick, F. Bottanelli, E. Hummel, C. Hawes and J. Denecke (2010). "A recycling-defective vacuolar sorting receptor reveals an intermediate compartment situated between prevacuoles and vacuoles in tobacco." Plant Cell **22**(12): 3992-4008.

Gebbie, L. K., J. E. Burn, C. H. Hocart and R. E. Williamson (2005). "Genes encoding ADP-ribosylation factors in Arabidopsis thaliana L. Heyn.; genome analysis and antisense suppression." J Exp Bot **56**(414): 1079-1091.

Geldner, N., N. Anders, H. Wolters, J. Keicher, W. Kornberger, P. Muller, A. Delbarre, T. Ueda, A. Nakano and G. Jurgens (2003). "The Arabidopsis GNOM ARF-GEF mediates endosomal recycling, auxin transport, and auxin-dependent plant growth." Cell **112**(2): 219-230.

Geldner, N., J. Friml, Y. D. Stierhof, G. Jurgens and K. Palme (2001). "Auxin transport inhibitors block PIN1 cycling and vesicle trafficking." Nature **413**(6854): 425-428.

Gillingham, A. K. and S. Munro (2007). "The small G proteins of the Arf family and their regulators." Annu Rev Cell Dev Biol **23**: 579-611.

Goldberg, J. (1998). "Structural basis for activation of ARF GTPase: mechanisms of guanine nucleotide exchange and GTP-myristoyl switching." Cell **95**(2): 237-248.

Goldberg, J. (2000). "Decoding of sorting signals by coatomer through a GTPase switch in the COPI coat complex." Cell **100**(6): 671-679.

Gorvel, J. P., P. Chavrier, M. Zerial and J. Gruenberg (1991). "rab5 controls early endosome fusion in vitro." Cell **64**(5): 915-925.

Grebe, M., J. Gadea, et al. (2000). "A conserved domain of the arabidopsis GNOM protein mediates subunit interaction and cyclophilin 5 binding." Plant Cell **12**(3): 343-356.

Grebe, M. (2005). "Plant biology. Enhanced: growth by auxin: when a weed needs acid." Science **310**(5745): 60-61.

Haas, T. J., M. K. Sliwinski, D. E. Martinez, M. Preuss, K. Ebine, T. Ueda, E. Nielsen, G. Odorizzi and M. S. Otegui (2007). "The Arabidopsis AAA ATPase SKD1 is involved in multivesicular endosome function and interacts with its positive regulator LYST-INTERACTING PROTEIN5." Plant Cell **19**(4): 1295-1312.

Hoepfner, S., F. Severin, A. Cabezas, B. Habermann, A. Runge, D. Gillooly, H. Stenmark and M. Zerial (2005). "Modulation of receptor recycling and degradation by the endosomal kinesin KIF16B." Cell **121**(3): 437-450.

Huotari, J. and A. Helenius (2011). "Endosome maturation." EMBO J **30**(17): 3481-3500.

Hurley, J. H. and P. I. Hanson (2010). "Membrane budding and scission by the ESCRT machinery: it's all in the neck." Nat Rev Mol Cell Biol **11**(8): 556-566.

Hwang, I. (2008). "Sorting and anterograde trafficking at the Golgi apparatus." Plant Physiol **148**(2): 673-683.

Jovic, M., M. Sharma, J. Rahajeng and S. Caplan (2010). "The early endosome: a busy sorting station for proteins at the crossroads." Histol Histopathol **25**(1): 99-112.

Jürgens, G. (2004). "Membrane trafficking in plants." Annu Rev Cell Dev Biol **20**: 481-504.

Jürgens, G. and N. Geldner (2002). "Protein secretion in plants: from the trans-Golgi network to the outer space." Traffic **3**(9): 605-613.

Kirchhausen, T. (2000). "Three ways to make a vesicle." Nat Rev Mol Cell Biol **1**(3): 187-198.

Kotzer, A. M., F. Brandizzi, U. Neumann, N. Paris, I. Moore and C. Hawes (2004). "AtRabF2b (Ara7) acts on the vacuolar trafficking pathway in tobacco leaf epidermal cells." J Cell Sci **117**(Pt 26): 6377-6389.

Lee, G. J., E. J. Sohn, M. H. Lee and I. Hwang (2004). "The Arabidopsis rab5 homologs rha1 and ara7 localize to the prevacuolar compartment." Plant Cell Physiol **45**(9): 1211-1220.

Liu, Y., R. A. Kahn and J. H. Prestegard (2010). "Dynamic structure of membrane-anchored Arf*GTP." Nat Struct Mol Biol **17**(7): 876-881.

Lowery, J., T. Szul, M. Styers, Z. Holloway, V. Oorschot, J. Klumperman and E. Sztul (2013). "The Sec7 guanine nucleotide exchange factor GBF1 regulates membrane recruitment of BIG1 and BIG2 guanine nucleotide exchange factors to the trans-Golgi network (TGN)." J Biol Chem **288**(16): 11532-11545.

Luzio, J. P., S. C. Piper, K. Bowers, M. D. Parkinson, P. J. Lehner and N. A. Bright (2009). "ESCRT proteins and the regulation of endocytic delivery to lysosomes." Biochem Soc Trans **37**(Pt 1): 178-180.

Martinez-Munoz, G. A. and P. Kane (2008). "Vacuolar and plasma membrane proton pumps collaborate to achieve cytosolic pH homeostasis in yeast." J Biol Chem **283**(29): 20309-20319.

Matheson, L. A., S. S. Suri, S. L. Hanton, L. Chatre and F. Brandizzi (2008). "Correct targeting of plant ARF GTPases relies on distinct protein domains." Traffic **9**(1): 103-120.

McDonold, C. M. and J. C. Fromme (2014). "Four GTPases differentially regulate the Sec7 Arf-GEF to direct traffic at the trans-golgi network." Dev Cell **30**(6): 759-767.

Moss, J. and M. Vaughan (1998). "Molecules in the ARF orbit." J Biol Chem **273**(34): 21431-21434.

Mossessova, E., R. A. Corpina and J. Goldberg (2003). "Crystal structure of ARF1*Sec7 complexed with Brefeldin A and its implications for the guanine nucleotide exchange mechanism." Mol Cell **12**(6): 1403-1411.

Mouratou, B., V. Biou, A. Joubert, J. Cohen, D. J. Shields, N. Geldner, G. Jurgens, P. Melancon and J. Cherfils (2005). "The domain architecture of large guanine nucleotide exchange factors for the small GTP-binding protein Arf." BMC Genomics **6**: 20.

Nickel, W. and F. T. Wieland (1997). "Biogenesis of COPI-coated transport vesicles." FEBS Lett **413**(3): 395-400.

Nielsen, E., A. Y. Cheung and T. Ueda (2008). "The regulatory RAB and ARF GTPases for vesicular trafficking." Plant Physiol **147**(4): 1516-1526.

Nielsen, E., F. Severin, J. M. Backer, A. A. Hyman and M. Zerial (1999). "Rab5 regulates motility of early endosomes on microtubules." Nat Cell Biol **1**(6): 376-382.

Nordmann, M., M. Cabrera, A. Perz, C. Brocker, C. Ostrowicz, S. Engelbrecht-Vandre and C. Ungermann (2010). "The Mon1-Ccz1 complex is the GEF of the late endosomal Rab7 homolog Ypt7." Curr Biol **20**(18): 1654-1659.

Novick, P. and P. Brennwald (1993). "Friends and family: the role of the Rab GTPases in vesicular traffic." Cell **75**(4): 597-601.

Park, M., K. Song, et al. (2013). "Arabidopsis mu-adaptin subunit AP1M of adaptor protein complex 1 mediates late secretory and vacuolar traffic and is required for growth." Proc Natl Acad Sci U S A **110**(25): 10318-10323.Pereira-Leal, J. B. and M. C. Seabra (2001). "Evolution of the Rab family of small GTP-binding proteins." J Mol Biol **313**(4): 889-901.

Polo, S., S. Sigismund, M. Faretta, M. Guidi, M. R. Capua, G. Bossi, H. Chen, P. De Camilli and P. P. Di Fiore (2002). "A single motif responsible for ubiquitin recognition and monoubiquitination in endocytic proteins." Nature **416**(6879): 451-455.

Poteryaev, D., S. Datta, K. Ackema, M. Zerial and A. Spang (2010). "Identification of the switch in early-to-late endosome transition." Cell **141**(3): 497-508.

Ramaen, O., A. Joubert, et al. (2007). "Interactions between conserved domains within homodimers in the BIG1, BIG2, and GBF1 Arf guanine nucleotide exchange factors." J Biol Chem **282**(39): 28834-28842.

Randazzo, P. A. and D. S. Hirsch (2004). "Arf GAPs: multifunctional proteins that regulate membrane traffic and actin remodelling." Cell Signal **16**(4): 401-413.

Renault, L., B. Guibert and J. Cherfils (2003). "Structural snapshots of the mechanism and inhibition of a guanine nucleotide exchange factor." Nature **426**(6966): 525-530.

Richardson, B. C., C. M. McDonold and J. C. Fromme (2012). "The Sec7 Arf-GEF is recruited to the trans-Golgi network by positive feedback." Dev Cell **22**(4): 799-810.

Richter, S., N. Geldner, J. Schrader, H. Wolters, Y. D. Stierhof, G. Rios, C. Koncz, D. G. Robinson and G. Jurgens (2007). "Functional diversification of closely related ARF-GEFs in protein secretion and recycling." Nature **448**(7152): 488-492.

Richter, S., L. M. Muller, Y. D. Stierhof, U. Mayer, N. Takada, B. Kost, A. Vieten, N. Geldner, C. Koncz and G. Jurgens (2012). "Polarized cell growth in Arabidopsis requires endosomal recycling mediated by GBF1-related ARF exchange factors." Nat Cell Biol **14**(1): 80-86.

Rink, J., E. Ghigo, et al. (2005). "Rab conversion as a mechanism of progression from early to late endosomes." Cell **122**(5): 735-749.

Rothman, J. E. and G. Warren (1994). "Implications of the SNARE hypothesis for intracellular membrane topology and dynamics." Curr Biol **4**(3): 220-233.

Saito, C. and T. Ueda (2009). "Chapter 4: functions of RAB and SNARE proteins in plant life." Int Rev Cell Mol Biol **274**: 183-233.

Saito, C., T. Ueda, H. Abe, Y. Wada, T. Kuroiwa, A. Hisada, M. Furuya and A. Nakano (2002). "A complex and mobile structure forms a distinct subregion within the continuous vacuolar membrane in young cotyledons of Arabidopsis." Plant J **29**(3): 245-255.

Sauer, M., M. O. Delgadillo, et al. (2013). "MTV1 and MTV4 encode plant-specific ENTH and ARF GAP proteins that mediate clathrin-dependent trafficking of vacuolar cargo from the trans-Golgi network." Plant Cell **25**(6): 2217-2235.

Scheuring, D., C. Viotti, F. Kruger, F. Kunzl, S. Sturm, J. Bubeck, S. Hillmer, L. Frigerio, D. G. Robinson, P. Pimpl and K. Schumacher (2011). "Multivesicular bodies mature from the trans-Golgi network/early endosome in Arabidopsis." Plant Cell **23**(9): 3463-3481.

Shen, J., Y. Zeng, et al. (2013). "Organelle pH in the Arabidopsis endomembrane system." Mol Plant **6**(5): 1419-1437.

Sohn, E. J., E. S. Kim, M. Zhao, S. J. Kim, H. Kim, Y. W. Kim, Y. J. Lee, S. Hillmer, U. Sohn, L. Jiang and I. Hwang (2003). "Rha1, an Arabidopsis Rab5 homolog, plays a critical role in the vacuolar trafficking of soluble cargo proteins." Plant Cell **15**(5): 1057-1070.

Song, J., M. H. Lee, et al. (2006). "Arabidopsis EPSIN1 plays an important role in vacuolar trafficking of soluble cargo proteins in plant cells via interactions with clathrin, AP-1, VTI11, and VSR1." Plant Cell **18**(9): 2258-2274.

Springer, S., A. Spang and R. Schekman (1999). "A primer on vesicle budding." Cell **97**(2): 145-148.

Steinmann, T., N. Geldner, M. Grebe, S. Mangold, C. L. Jackson, S. Paris, L. Galweiler, K. Palme and G. Jurgens (1999). "Coordinated polar localization of auxin efflux carrier PIN1 by GNOM ARF GEF." Science **286**(5438): 316-318.

Stierhof, Y. D. and F. El Kasmi (2010). "Strategies to improve the antigenicity, ultrastructure preservation and visibility of trafficking compartments in Arabidopsis tissue." Eur J Cell Biol **89**(2-3): 285-297.

Ueda, T., M. Yamaguchi, H. Uchimiya and A. Nakano (2001). "Ara6, a plant-unique novel type Rab GTPase, functions in the endocytic pathway of Arabidopsis thaliana." EMBO J **20**(17): 4730-4741.

Ullrich, O., H. Stenmark, K. Alexandrov, L. A. Huber, K. Kaibuchi, T. Sasaki, Y. Takai and M. Zerial (1993). "Rab GDP dissociation inhibitor as a general regulator for the membrane association of rab proteins." J Biol Chem **268**(24): 18143-18150.

Van Valkenburgh, H., J. F. Shern, J. D. Sharer, X. Zhu and R. A. Kahn (2001). "ADP-ribosylation factors (ARFs) and ARF-like 1 (ARL1) have both specific and shared effectors: characterizing ARL1-binding proteins." J Biol Chem **276**(25): 22826-22837.

Vernoud, V., A. C. Horton, Z. Yang and E. Nielsen (2003). "Analysis of the small GTPase gene superfamily of Arabidopsis." Plant Physiol **131**(3): 1191-1208.

Viotti, C., J. Bubeck, Y. D. Stierhof, M. Krebs, M. Langhans, W. van den Berg, W. van Dongen, S. Richter, N. Geldner, J. Takano, G. Jurgens, S. C. de Vries, D. G. Robinson and K. Schumacher (2010). "Endocytic and secretory traffic in Arabidopsis merge in the trans-Golgi network/early endosome, an independent and highly dynamic organelle." Plant Cell **22**(4): 1344-1357.

Wang, Y. J., J. Wang, et al. (2003). "Phosphatidylinositol 4 phosphate regulates targeting of clathrin adaptor AP-1 complexes to the Golgi." Cell **114**(3): 299-310.

Wu, S. K., K. Zeng, I. A. Wilson and W. E. Balch (1996). "Structural insights into the function of the Rab GDI superfamily." Trends Biochem Sci **21**(12): 472-476.

Xu, J. and B. Scheres (2005). "Dissection of Arabidopsis ADP-RIBOSYLATION FACTOR 1 function in epidermal cell polarity." Plant Cell **17**(2): 525-536.

Zhao, X., A. Claude, J. Chun, D. J. Shields, J. F. Presley and P. Melancon (2006). "GBF1, a cis-Golgi and VTCs-localized ARF-GEF, is implicated in ER-to-Golgi protein traffic." J Cell Sci **119**(Pt 18): 3743-3753.

Zhao, X., T. K. Lasell and P. Melancon (2002). "Localization of large ADP-ribosylation factor-guanine nucleotide exchange factors to different Golgi compartments: evidence for distinct functions in protein traffic." Mol Biol Cell **13**(1): 119-133.

Zhu, Y., L. M. Traub and S. Kornfeld (1999). "High-affinity binding of the AP-1 adaptor complex to trans-golgi network membranes devoid of mannose 6-phosphate receptors." Mol Biol Cell **10**(3): 537-549.

Zouhar, J., A. Munoz and E. Rojo (2010). "Functional specialization within the vacuolar sorting receptor family: VSR1, VSR3 and VSR4 sort vacuolar storage cargo in seeds and vegetative tissues." Plant J **64**(4): 577-588.

Zwiewka, M., E. Feraru, et al. (2011). "The AP-3 adaptor complex is required for vacuolar function in Arabidopsis." Cell Res **21**(12): 1711-1722.

Lebenslauf

Lebens- und Bildungsgang

Persönliche Daten

Name:	Hauke Beckmann
Geburtsdatum:	26.10.1979
Geburtsort:	Bünde/Westfalen

Schulische Ausbildung

1986-1990	Grundschule Blasheim
1990-1999	Wittekind-Gymnasium, Lübbecke
1999	Zeugnis der allgemeinen Hochschulreife

Grundwehrdienst

1999-2000	Westfalenkaserne, Ahlen

Hochschulbildung

2000-2002	Grundstudium Biologie an der Eberhard-Karls-Universität Tübingen
2002	Vordiplom Biologie
2002-2009	Hauptstudium Biologie an der Eberhard-Karls-Universität Tübingen
2009	Diplom Biologie
2009-2015	Promotion am Zentrum für Molekularbiologie der Pflanzen (ZMBP) in der Abteilung Entwicklungsgenetik unter Leitung von Prof. Dr. Gerd Jürgens